

AD 660820

TRANSIENT CONDUCTIVITY
IN
ORGANIC INSULATORS

John W. Winslow

Northrop Corporate Laboratories
3401 West Broadway
Hawthorne, California 90250

Contract No. AF 19(628)-6047
Project No. 5620
Task No. 4608-01-01

FINAL REPORT

Period Covered
June 1966 to June 1967

Date of Report: September 1967

Contract Monitor: Clarence Turner
Solid State Sciences Laboratory

Prepared
for

AIR FORCE CAMBRIDGE RESEARCH LABORATORIES
OFFICE OF AEROSPACE RESEARCH
UNITED STATES AIR FORCE
BEDFORD, MASSACHUSETTS

DDC
RECEIVED
NOV 13 1967
C

Distribution of this document is unlimited. It may be released to the Clearinghouse, Department of Commerce, for sale to the general public.

119

AFCRL-67-0515

TRANSIENT CONDUCTIVITY
IN
ORGANIC INSULATORS

John W. Winslow

Northrop Corporate Laboratories
3401 West Broadway
Hawthorne, California 90250

Contract No. AF 19(628)-6047

Project No. 5620

Task No. 4608-01-01

FINAL REPORT

Period Covered

June 1966 to June 1967

Date of Report: September 1967

Contract Monitor: Clarence Turner
Solid State Sciences Laboratory

Prepared

for

AIR FORCE CAMBRIDGE RESEARCH LABORATORIES
OFFICE OF AEROSPACE RESEARCH
UNITED STATES AIR FORCE
BEDFORD, MASSACHUSETTS

Distribution of this document is unlimited. It may be released to the Clearinghouse, Department of Commerce, for sale to the general public.

ABSTRACT

A technique for measuring quasi-dc photoconductance in amorphous polymers during steady-state irradiation has been developed. This technique, which involves control of the sample's voltage history for a period of time prior to making measurements, has been applied successfully to 21 polyethylene and 14 polystyrene samples, during exposure to Co^{60} gamma fields with intensities up to some 2×10^5 r/hr. In both cases the conductances observed using this technique were found inversely proportional to sample thickness, thus permitting calculation of the bulk, quasi-dc photoconductivities.

Preliminary observations were made of polyethylene, polystyrene and polyvinylchloride under pulsed irradiation. These observations verified the existence of three components of radiation-induced conductance: momentum transfer, prompt and delayed. Further, these observations suggest:

1. That the prompt components in all three materials exhibit so-called polarization effects;
2. that the technique developed for the steady-state irradiation case appears promising for study of the pulsed-irradiation case;
3. that the three components may well involve three distinct sets of charge carriers; and
4. that the prompt component in the steady-state case was negligible, so that the observations there reflected primarily the behavior of the delayed component.

To date, analyses of the data from these observations indicate the following:

1. that both these materials are essentially ohmic, at least up to applied electric fields on the order of 10% of breakdown;
2. that trace impurities do not play important roles in the conduction mechanisms involved in either material;

3. that structural defects may play such a role, but if they do, they are present in very large concentrations - in polyethylene at least, so large that they must be considered as essential features of the structure, rather than as occasional structural mistakes; and
4. that in both materials, the dependence on radiation intensity is substantially weaker than has been reported by previous observers.

FOREWORD

At the outset of this investigation of transient conductivity in organic insulators, the plan^a envisioned pursuit of four studies: the first, of conductivity induced through Co⁶⁰ gamma irradiation; the second, of electron-induced conductivity; the third, of the temperature dependence of trapping; and the fourth, a comparison of electron and gamma-ray effects. As the investigation proceeded, this plan was altered somewhat, with the result that the work accomplished falls into three categories. Consequently, this report is divided into four principal sections, one presenting the work of each category, the fourth discussing their results and conclusions as a whole.

ACKNOWLEDGEMENTS

Grateful acknowledgments are due to O. L. Curtis for many valuable discussions and suggestions, to W. W. Chang for assistance with certain of the measurements and data reduction, and to R. C. Headley for his painstaking construction of sample assemblies and parts, and of critical portions of the measuring equipment.

TABLE OF CONTENTS

<u>Section</u>	<u>Title</u>	<u>Page</u>
I.	Transient Conduction During Steady-State Gamma Irradiation	1
A.	Introduction	1
	1. Background: The Two-Component Description	1
	2. Steady-State Irradiation Case Phenomenology	3
	3. Experimental Identification of Components	6
B.	Experimental Details	10
	1. Samples	10
	2. Radiation Dosimetry	17
	3. Circuitry	19
	4. Technique	26
C.	Observations	27
	1. Variables	27
	2. Determination of Conductances	28
	3. Thickness Dependence	35
	4. Accumulated Dose Effects	37
	5. Dose Rate Dependence	41
	6. Deferred Observations	41
D.	Discussion	46
II.	Transient Conduction During Pulsed Electron Irradiation	53
A.	Introduction	53
B.	Experimental Details	53
	1. Samples	53
	2. Radiation and Dosimetry	59
	3. Circuitry and Technique	60
C.	Observations	62
	1. Momentum Transfer	63
	2. Voltage-Driven Components	73
	3. Recharging Effect	80

TABLE OF CONTENTS

<u>Section</u>	<u>Title</u>	<u>Page</u>
	D. Discussion	84
	1. The Momentum Component	84
	2. Prompt Current	85
	3. The Delayed Currents	86
	4. A Speculative Model	87
III.	Other Work	89
	A. Dynamic Observations During Pulsed Electron Irradiation	89
	B. Temperature Dependence of Trapping	90
	1. Samples	90
	2. Radiation and Dosimetry	94
	3. Measuring Circuit and Observations	94
	4. Discussion	95
IV.	General Summary of Results and Recommendations.	97
	A. Specific Results of Current Work	96
	B. Current State of the Art	98
	1. Design Problems and Semantic Difficulties	98
	2. Future Outlook	100
	C. Specific Recommendations for Future Work	101
	1. Momentum Currents	101
	2. Prompt Components	102
	3. The Delayed Components	103
	References	106
	Equipment	107

TABLES

<u>Table</u>	<u>Title</u>	<u>Page</u>
I.	Sample Details, Steady-State Irradiation Study	11
II.	Polyethylene Conductivity Data, Steady-State Irradiation Study	33
III.	Polystyrene Conductivity Data, Steady-State Irradiation Study	34
IV.	Polyethylene Intensity Data, Steady-State Irradiation Study	45

TABLES

<u>Table</u>	<u>Title</u>	<u>Page</u>
V.	Sample Details, Pulsed Electron Study	54

LIST OF ILLUSTRATIONS

<u>Figure</u>	<u>Title</u>	<u>Page</u>
1.	PMMA Spacer, Steady-State Irradiation Study	16
2.	Measuring Circuit Details, Steady-State Irradiation Study	20
3.	Total Observed Photocurrent vs. Applied Voltage for Typical Polyethylene Sample, Steady-State Irradiation Study	29
4.	Total Observed Photocurrent vs. Applied Voltage for Typical Polystyrene Sample, Steady-State Irradiation Study	30
5.	Total Observed Photoconductance per Unit Electrode Area vs. Inverse of Sample Thickness, for Polyethylene Samples from Three Fabricators	36
6.	Total Observed Photoconductance per Unit Electrode Area vs. Inverse of Sample Thickness, for Polystyrene Samples from Two Fabricators	38
7.	Total Observed Photoconductance per Unit Electrode Area vs. Inverse of Sample Thickness, for Polyethylene Samples from One Fabricator	39
8.	Total Observed Photoconductance per Unit Electrode Area vs. Inverse of Sample Thickness, for Polyethylene Samples from Three Fabricators	40
9.	Total Observed Photoconductance per Unit Electrode Area vs. Inverse of Sample Thickness, for Polystyrene Samples from One Fabricator	42
10.	Total Observed Photoconductance per Unit Electrode Area vs. Inverse of Sample Thickness, for Polystyrene Samples from Three Fabricators.	43
11.	Total Observed Photoconductivity vs. Absorbed Dose Rate for 10 Polyethylene and 4 Polystyrene Samples. .	44

LIST OF ILLUSTRATIONS

<u>Figure</u>	<u>Title</u>	<u>Page</u>
12.	Percentage Change in Total Observed Photoconductance per Unit Electrode Area vs. Inverse of Sample Thickness	47
13.	Sample Construction Details, Pulsed Electron Study.	56
14.	Measuring Circuit, Pulsed Electron Study.	61
15.	Pulsed Electron Study Raw Data Tracings Displaying Momentum Transfer Component	64
16.	Pulsed Electron Study Raw Data Tracings Displaying Prompt Component, Prompt Component Polarization, and The Turnaround Point	68
17.	Pulsed Electron Study Raw Data Tracing Displaying Double Turnaround	77
18.	Pulsed Electron Study Raw Data Tracing Displaying Balance Between Delayed and Momentum Components	78
19.	Pulsed Electron Study Raw Data Tracing Displaying Relaxation of Prompt Component Polarization	81
20.	Pulsed Electron Study Raw Data Tracing Displaying "Recharging" Effect	83
21.	Dynamic Study Raw Data Tracings Displaying Momentum Component	91
22.	Dynamic Study Raw Data Tracings Displaying Prompt Component Polarization.	92

SECTION I

TRANSIENT CONDUCTION DURING STEADY-STATE GAMMA IRRADIATION

A. INTRODUCTION

1. Background: The Two-Component Description. Previous investigations^{b,c} have shown that, in several organic insulating materials, the electric current generated in response to short, intense bursts of ionizing radiation can be considered as the sum of two distinct components, the PROMPT CURRENT, and the DELAYED CURRENT. These components can be defined operationally in terms of the experimentally available pulsed radiation field, the prompt component being that which follows the radiation pulse shape with no discernable time lag, and the delayed component being that which remains after the pulse has passed, dying away slowly after the radiation field intensity has been reduced to zero.

In general, the prompt component has been found dependent primarily upon pulse intensity, while the delayed component depends upon the total dose delivered by the pulse. Thus the delayed component builds up during the pulse, and the total current observed during the pulse includes an increasing contribution from this source, as well as the prompt component. In most cases the prompt component is much larger than the delayed component increment generated by the pulse, so that the latter is negligible. The decay rate of the delayed component can be quite slow, however, so that for a series of pulses, the accumulated delayed component may be appreciable for the last pulses in the series.

Such behavior can be accounted for by several models, of various levels of complexity. The simplest, and consequently the most favored, is the single-carrier model, which assumes that both components reflect the transport of electrons which have been liberated from valence states by the incident radiation.

This model views the essential sequence of events which determine the observed currents as a multistep process. First, the incident radiation ionizes the material, producing mobile electrons and stationary positive ions at a constant rate. The ions are fixed, and thus do not contribute to the observed current. The electrons, however, are free to move, and thus are responsible for the prompt current.

The insulator is viewed as containing a practically infinite concentration of traps for electrons. Thus the lifetime of the mobile electrons is both constant throughout the pulse, and short, and the prompt current establishes its steady-state value with a response time small compared to the rise time of the radiation pulse, i.e., on the order of nanoseconds or faster.

The delayed component is viewed by this model as resulting from a series of thermal re-excitations of the trapped electrons into conducting states. The slow increase of the delayed component with continued irradiation corresponds to a gradual filling of the "thermally excitable" states by the ionized electrons, while the slow decay after termination of irradiation corresponds to the reduction of the thermally excitable electron population as conduction state electrons occasionally fall into deep traps, or perhaps into the empty valence states generated by the primary interactions with the radiation field.

In this respect this model differs from that generally used to explain photoconduction in semiconductors, according to which the "delayed conduction" is attributable to the untrapped member of the original excited pair. The latter model may be applicable as well to the insulator case, since hole conduction has not been ruled out. However, the one-carrier model currently is receiving more attention from investigators in the field.

Previous observations indicate that if the radiation pulse is of high intensity and short duration, the prompt current is large and the delayed current is small. If intensity is low, however, and pulse length is long, the prompt current is small, and the delayed current eventually may build up to predominant proportions. Thus, investigations of the prompt current should be conducted using short, intense bursts such as are available from flash x-ray machines and linear accelerators, while investigations of the delayed current should be conducted with radiation fields which are relatively low in intensity, but long-lived. Since the latter is the case with the steady-state gamma study*, this section of the report is concerned with the delayed current, and treatment of the prompt current is not given here.

2. Steady-State Irradiation Case Phenomenology.

a. Component Classification. Several schemes might be considered appropriate for classifying the currents found in the steady-state irradiation case. This report relies upon one which is a hybrid of the mechanistic and operational approaches, the classes being distinguished from each other partially on the basis of details of conduction mechanism, and partially on the basis of measurable parameters.

The conduction mechanism factors are two: an excitation step, by which valence state charge carriers are raised into conducting states; and a transport step, by which the excited carriers are driven away from one electrode and toward another. Each of these factors can be related to a controllable, environmental factor. In addition, a third observable parameter, which has not yet been identified clearly with specific conduction mechanisms, has been found necessary.

*See Section III, p 97.

Each factor has two possible cases, which leads to a scheme having eight classes. Two of these, however, are null sets for fundamental reasons, leaving only six cases of interest. In addition, one of the six cases has not yet been observed in practice, so that only five classes are of practical concern.

The first factor is excitation mechanism. In this work there are two cases, viz., that where charge carriers are excited from their valence states by thermal processes, and that where this excitation is provided by interactions between the exposed material and the incident radiation field. In the situation where the radiation field is zero, only the first type of carrier can be found. When the radiation field is non-zero, both are present simultaneously, since the absolute zero of temperature lies beyond the scope of the present discussion.

The second factor is transport mechanism. In the normal case, charge carrier transport is accomplished by direct electrical interaction between the charge carriers and the applied electric field. If high-energy radiation is present, however, other transport mechanisms are possible. We distinguish between the classes where transport is a voltage-driven phenomenon and those where it is a radiation-field-driven process. When both electric field and radiation field are non-zero, both sets of classes can be found simultaneously.

The third parameter is the time derivative of the observed component. As yet the mechanisms responsible for producing various values of this factor are not identified, so the mechanistic counterparts remain unspecified. For the moment we lump those components having non-zero time derivatives together, and consider them as distinct from the case where this parameter is zero.

b. Nomenclature. As yet a standard system of nomenclature has not been established for this rather complicated technological field. Consequently, the potential for semantic confusion is quite large, and special pains must be taken to ensure accurate communication of ideas. For this reason, the nomenclature used in this report is now given in some detail.

Components whose charge carriers are excited from their valance states by thermal processes are called DARK components, while those whose carriers are excited by the radiation field are called PHOTO- components. These designations are in accord with established practice in visible-light photoconduction studies. Those which require a history involving both types of activation, such as those described in the one-carrier model discussed earlier, are called DELAYED components, in agreement with existing practice in pulsed radiation studies.

Because of their hybrid nature, the delayed components are ambiguous with respect to the basic classification scheme used here. We arbitrarily include them in the PHOTO- components, for purposes of classification.

Radiation-driven components require the transfer of momentum, as well as energy, from the radiation field to the charge carriers. Consequently these are called MOMENTUM currents in this report. Those driven by the applied electric field are the usual sort of currents and hence are called NORMAL. In cases where neither of the two words, NORMAL and MOMENTUM, is used, NORMAL is understood.

Components whose time derivatives are non-zero are called TRANSIENT components, while those whose derivatives are zero are called STEADY STATE components. This is in accord with existing engineering practice and should occasion no difficulty.

The list of classes provided by this scheme, then, is as follows:

1. (normal) transient current,
2. (normal) steady-state dark currents,
3. (normal) transient photocurrents,
4. (normal) steady-state photocurrents, and
5. (steady-state) momentum (photo)currents,

where the parts in parentheses are optional, and may be omitted upon occasion. Of the three remaining descriptor combinations, two are impossible, since the definitions of momentum and dark are mutually exclusive. Hence, by definition, transient and steady-state momentum dark currents cannot exist. The third unlisted combination, transient momentum photocurrent, has yet to be observed, and so is omitted from the list.

3. Experimental Identification of Components. When an observation is made during steady-state irradiation, it is possible in general that components of all five classes may be present. Since the discussions of lifetime which outlined the motivation for this study^a refer specifically to the normal steady-state photocurrent, it is highly desirable to be able to separate this component from the total current observed. This is not a particularly easy task when dealing with insulators, and so a certain amount of discussion of this area now becomes appropriate.

First, we consider the dark components. These can be measured directly by making observations under the condition that radiation field intensity is zero. Correcting the total current observed during irradiation for the dark component, however, is not always accomplished by a simple subtraction of the previously observed dark components. Others^d have shown that the dark and photocurrents do not necessarily add linearly to produce the total observed current, but that details of the conducting mechanism(s) must be taken into consideration. Where these details are not known, it is especially important to operate with total currents that are much larger than the dark currents, so that the latter can be ignored with negligible introduction of error.

The momentum current can be measured directly by making observations during irradiation with zero volts applied to the sample, or by making measurements at both positive and negative voltages and interpolating the current-voltage characteristic to the zero volts intercept. Fortunately the conduction mechanisms involved in momentum currents are essentially independent of those corresponding to the normal components, so the momentum component can be removed analytically from the total observed current by a simple subtraction. Alternatively, one can measure the slope of the current-voltage characteristic and determine the conductance corresponding to the voltage-driven portion of the total current (i.e., the normal components), in this fashion.

Given that the dark components and the momentum current are small enough that they can be ignored and removed respectively, without destroying the structure of the remaining data, the next step would be separation of the transient and steady-state photocurrents. At first glance this seems merely to be a matter of outwaiting the transient components and making observations after they all decay to values negligible with respect to the steady-state photocurrent. This, unfortunately, is much more easily said than done.

The chief practical difficulty with this approach is that the popular organic insulators display some transient photocurrents having very long response times. Polyethylene, for example, has been observed after abrupt changes in applied voltage, during steady-state irradiation, and found to exhibit transient components having relaxation times in the neighborhood of 30 seconds, 2 minutes, and 30 minutes^e. (Whether others of longer relaxation times exist is unknown.) Observations made on a set of samples of polyethylene, which included waiting some 20 minutes after any change in electric or radiation fields^f, yielded conductances that were random with respect to sample thickness. These suggest that substantially longer times than this must be used, if the outwaiting technique is to be applied successfully.

With components that change so slowly, very long observation periods are required to establish that the steady-state condition has indeed been achieved. With such long times, problems associated with maintaining constant applied voltages, with instrument drift, and possibly even with thermal or radiation aging, become appreciable, and the effort can become prohibitive.

A second approach would be first to observe the time dependence of the transient photocomponents and then to attempt to fit the resulting curve to an expression of the form of a sum of terms exponential in time, plus a constant. If a successful fit could be achieved, the value of the constant term required to produce the fit then could be taken as the steady-state photocurrent. This approach would require a large quantity of observed data. In addition, the precision required of the input data is quite high for more than one or two transient components, and success is unsure.

The approach used in this study was somewhat different in that it did not try to eliminate the long-lived transient photocomponents. The philosophy of the approach was based upon the assumed applicability of either of two general equivalent circuits. The first of these visualizes the sample as being represented by a parallel combination of capacitors, each having a resistance in series with it, plus a resistance in parallel with the whole array. In this system, the steady-state photocurrent is identified with the parallel resistor, while each transient component is associated with a capacitor branch of the array. The total current then is simply the sum of those in the individual branches.

According to this picture, the component contributed to the total current by the resistive branch, once a voltage V has been applied, would be constant in time, and proportional to V . The contribution of a given capacitive branch, on the other hand, would depend not only upon V , but also upon (a) the voltage on the sample prior to the application of V , (b) the length of time

the previous voltage has been applied, and (c) the time elapsed between the application of V and the observation. If a series of measurements were taken starting with the system in a fixed reference state, say after the steady state corresponding to voltage V_1 had been achieved, the contribution of each capacitive branch would be proportional to ΔV ($\Delta V \cong V - V_1$)

If a measurement technique could be developed such that V were proportional to ΔV , and if the time for which each applied voltage was held on the sample were held fixed so that the proportionality constant between a given capacitive branch component and ΔV were fixed, and finally if observations were made at a fixed time after each change in applied voltage, the total currents observed should consist of components whose ratios are fixed, and a degree of consistency should result. Such a technique would permit measurements to be made at reasonable times after applying a new voltage.

Another view holds forth the possibility that the very long-lived transients observed may correspond to some type of blocking layers at one or both of the sample-electrode interfaces. In terms of an equivalent circuit diagram, this would correspond to the addition of a capacitance in series with the parallel-branch model described above. If this capacitance were large enough, the slow transient could correspond to the charging of this capacitance, and the total current seen at short times would represent the true state of the sample. If the time constants of the individual branches of the portions corresponding to the sample behavior were short enough, it might be possible to make observations at an optimum time, i.e., after the sample had achieved a steady state, but before the limiting effect of the series capacitance became effective. In this case, observations would reflect the behavior of the true steady-state photocurrent.

In either case, decay of the long-lived transient is quite slow, so that measurements in the period between 3 and 10 minutes after application of a new voltage differ from each other only slightly, and hence short-time measurements require no great precision in timing. In the parallel-branch case, attention to control the parameters determining the contributions of the capacitive branches should permit consistent measurements in this time period. In the case of the series blocking layer model, such measurements actually would be preferable to those at very long times, since the former would be the more representative of the behavior of the bulk of the sample, and might even give the desired steady-state photocurrent directly.

B. EXPERIMENTAL DETAILS

1. Samples. A total of 41 samples, (26 polyethylene and 15 polystyrene) was prepared, mounted, and exposed to Co^{60} gamma radiation in the Northrop 5 kC cobalt source. Of these, 21 polyethylene and 14 polystyrene provided useful data. Details of the samples, including base material, fabricator, and dimensions, are given in Table I.

Since organic insulators often are both elastic and plastic at room temperature, measurement of sample thickness requires standardization of the measurement technique. In this work, all thickness measurements were made with a commercial, dead-weight micrometer equipped with standard anvils¹.

Except for the first sample, which was run by itself as a test of the measurement technique, samples were exposed in groups of 10, each group being referred to as a "can". Cans 1 and 2 both utilized cylindrical exterior shells of sheet aluminum, which provided mechanical support for the sample structure, and electrical shielding, as well. In these cases the completed structure resembled a rather squat tin of preserves. In Cans 3 through 5,

TABLE I. SAMPLE DETAILS, STEADY-STATE IRRADIATION STUDY

Sample	Material	Fabricator	Can	Location in Can	Nominal Thickness mils	t m ⁻⁵	A cm ²
U00J01	PE	unknown	1	only	10	—	—
L12D06	PE	Allied Resinous	2	10 (top)	4	9	0
L12D05	↓	↓	↓	9	↓	↓	↓
L12004	↓	↓	↓	8	30	75	102
L12003	↓	↓	↓	7	↓	74	↓
L12J04	↓	↓	↓	6	10	26	↓
L12J03	↓	↓	↓	5	↓	27	↓
L12D04	↓	↓	↓	4	4	9	↓
L12D03	↓	↓	↓	3	↓	9	↓
L12B04	↓	↓	↓	2	2	5	↓
L12B03	↓	↓	↓	1 (bottom)	↓	5	↓
L11R01	PE	Alchem	3	10 (top)	90	234	105
L12R20	↓	Allied Resinous	↓	9	↓	228	↓
L12N55	↓	↓	↓	8	20	52	↓
L12N36	↓	↓	↓	7	↓	1	↓
L11N22	↓	Alchem	↓	6	↓	53	↓
L51053	↓	Ethyl Visqueen	↓	5	30	78	↓
L11020	↓	Alchem	↓	4	↓	79	↓
L12017	↓	Allied Resinous	↓	3	↓	71	↓
L51J07	↓	Ethyl Visqueen	↓	2	10	27	↓
L51M23	↓	↓	↓	1 (bottom)	15	44	↓
Y35N03	PSTY	Monsanto	4	10 (top)	20	55	105
Y13E01	↓	A&E	↓	9	5	13	↓
Y35H07	↓	Monsanto	↓	8	7½	20	↓
Y41N11	↓	Davis	↓	7	20	52	↓
Y35A03	↓	Monsanto	↓	6	1	2	↓
Y41E09	↓	Davis	↓	5	5	12	↓
Y13J09	↓	A&E	↓	4	10	27	↓
Y35B03	↓	Monsanto	↓	3	2	5	↓
Y41J01	↓	Davis	↓	2	10	26	↓
Y35N05	↓	Monsanto	↓	1 (bottom)	20	55	0
Y41E02	↓	Davis	5	10 (top)	5	20	105
L12014	PE	Allied Resinous	↓	9	30	70	↓
L12R13	PE	↓	↓	8	90	232	↓
L12R70	PE	↓	↓	7	↓	236	↓
L12N26	PE	↓	↓	6	20	52	↓
L12N11	PE	↓	↓	5	↓	54	39.3
Y41N06	PSTY	Davis	↓	4	↓	53	105
Y41N01	PSTY	↓	↓	3	↓	52	↓
Y41H02	PSTV	↓	↓	2	7½	20	↓
Y41H11	PSTY	↓	↓	1 (bottom)	↓	19	↓

PE = polyethylene

A = electrode area

PSTY = polystyrene

t = measured thickness

PE* = pile-irradiated PE

PSTY* = pile-irradiated PSTY

A&E = A & E Plastik pak, Los Angeles, Calif.

Alchem = Alchem Inc., La Mirada, Calif.

Allied Resinous = Allied Resinous Products, Conneaut, Ohio

Davis = Joseph Davis Plastic Co., Kearny, N. J.

Ethyl Visqueen = Ethyl Corp. Visqueen Div., Baton Rouge, La

Monsanto = Monsanto Co., St. Louis, Mo.

structural support was provided by an assembly of polymethylmethacrylate (PMMA) spacers, held together with aluminum tie rods, and shielding was provided by a coat of conductive paint. This structure permitted the use of a roughly octagonal cross section for these assemblies, with a consequent reduction in fabrication time and cost.

In all cases, electrodes and guard rings consisted of colloidal graphite, deposited from a commercially available suspension². In the case of the first sample, they were handpainted directly on the sample itself. In the remainder, they were handpainted on the PMMA spacers, and were held in pressure-contact with the samples by aluminum tie rods. Electrode thickness was not controlled, except by visually observing that coverage was complete.

Except for the few cases specified in later discussion, all electrodes were circular and covered as large an area as was permitted by gross design limitations, e.g., the diameter of the well in which the source was located. The gaps between guard ring and electrode were about one-eighth of an inch wide, at the minimum, and in some regions of some samples were as large as three-eighths inch. In Cans 1 and 2 the guard rings were simple annular rings about an eighth of an inch in width, while in Cans 3 through 5 they were more irregular in shape, although still about the same in width. Considerable care was taken to align the electrodes, in all cases so that they had centers on a common, straight axis.

In all cans, ionized gas paths between the electrodes were minimized by potting techniques. In Can 1, a commercially available, silicone potting compound³ was used. For Cans 2 through 5, a biological sectioning paraffin⁴ (MP ca. 63°C) was used. No significant differences in performance were observed between the two materials.

The first sample, occupying Can 1, was clamped in a horizontal plane between two annular PMMA rings of identical dimensions, the rings being held together with steel screws and nuts at several locations around the periphery. Three of the screws extended a couple of inches below the bottom ring, providing stand-off from the can bottom. Matching circular electrodes and annular guard rings, one of each for each face of the sample, were painted opposite each other on the sample faces left exposed inside the PMMA rings.

In this case, electrical contacts to the graphite areas were provided through spring contacts cut from beryllium copper finger stock. These were attached to the PMMA rings, at widely separated locations, with steel screws. Additional graphite was painted over the ends of the contacts, where they touched the graphite areas, as additional assurance of adequate contact.

Electrical connections to the measurement apparatus were brought out of the can by two cables, one triaxial⁵, the other coaxial⁶, both fed through the can top. The center conductor of the coax cable was soldered to a small binding post attached to the spring connector of the bottom electrode, and to a similar post on the connector of the bottom guard ring. The same technique was used to attach the center conductor of the triax to the top electrode, and the triax inner shield to the top guard ring.

The outer shield of the triax was connected to the body of the can. The shield of the coax, however, was left floating at the can end, to avoid possible difficulties from a ground loop. The coax shield terminated well inside the can, in a volume which was filled with silicone during the potting process.

The observations made with the first sample revealed the presence of appreciable transient currents following a typical voltage change. Because of these, the determination of a single current-voltage characteristic required on the order of two hours, most

of which was spent observing redundant information. Consequently, it was decided to conduct the principal experiments of this study observing several samples simultaneously, and the sample mounting arrangement was redesigned accordingly. The design developed for Can 2, which accommodated 10 samples, was found satisfactory, and as a result, Cans 2 through 5 followed essentially the same basic design.

The principal elements of this design included: a stack of 10 samples; a stack of 9 PMMA spacers (design shown in Figure 1); two end spacers, which differed from the other spacers only in having a single electrode and guard ring, rather than two; two PMMA end blocks; and a set of aluminum welding-rod tie bars and mounting legs. Electrodes were painted on the spacers, which then were interleaved between the samples to form a single stack. This stack was compressed between the two end blocks, which were held together by the tie rods.

Electrical connections were carried to the measuring apparatus by a set of eleven triaxial cables^f, one for each spacer. As shown in Figure 1, the center conductor of each cable was connected to both electrodes on its spacer by means of a graphite lead. To accomplish this it was necessary to drill a long hole from the edge of the spacer toward the center, its axis parallel to the electrodes. It was the limitations imposed by this operation that determined the minimum thickness practical for the spacers. Given better control of the drilling process, particularly those factors governing drill drift, a substantial reduction in this dimension should be possible.

As also shown in Figure 1, the inner shield of each triaxial cable is connected to the two guard rings on its spacer by means of a copper channel. This channel was soldered to the inner shield, and glued to the spacer's edge using a commercial adhesive²³. The guard rings then were painted up to and on to the copper channel's lips.

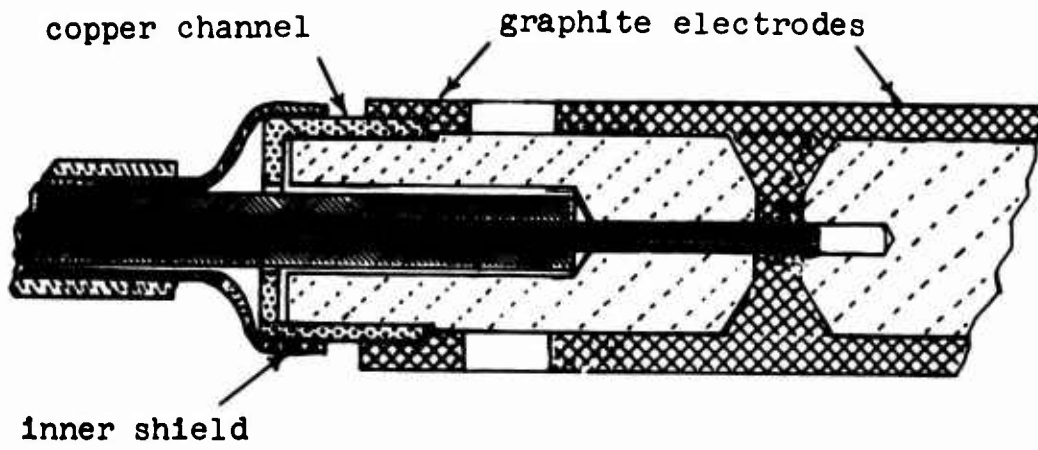
Not shown in Figure 1 is the outer shield of the triaxial cable. In each case this terminated well inside the can's outer surface, i.e., well inside the potting material. Ground was carried to the can through the mechanical supports which held it in place in the cobalt well. Since the cable used was supplied complete with an outer insulating jacket, avoidance of possible ground loops was accomplished simply by maintaining the integrity of this jacket to a point somewhere near the end of the corresponding outer shield, i.e., also well within the potting material.

It will be noted that the tie rods pass through holes cut in the spacers. Matching holes in the stencils used for painting the electrodes provided indexing for alignment of the electrodes. In addition, these holes were deliberately located in a nonsymmetric way, so that matching holes in the outer portions of the samples could be used to provide a nonreversible indexing for ressembly of the structure, should such be desired.

In the case of Can 2, standoff legs similar to those used in Can 1 were attached to the bottom end block and the assembly was placed in the can, the 11 triaxial cables passing through a hole in the top. A homemade clamp was used to hold these cables fixed at this point. A similar set of standoff legs, mounted on the can top, provided attachment to a small, aluminum mounting plate, which in turn provided the means for attaching the entire can to the structure which supported it in the cobalt well.

Potting was done in an air oven, at about 65°C, the molten paraffin being poured in through a hole in the top until full and then being allowed to cool. This process was repeated until the cooled can was essentially full of paraffin. A small cover then was attached in place over the pour hole, and the can was ready for exposure.

The case of Cans 3 through 5 differed from that of 2 in that in the former, bottom standoff legs were not necessary. A similar



NOT TO SCALE

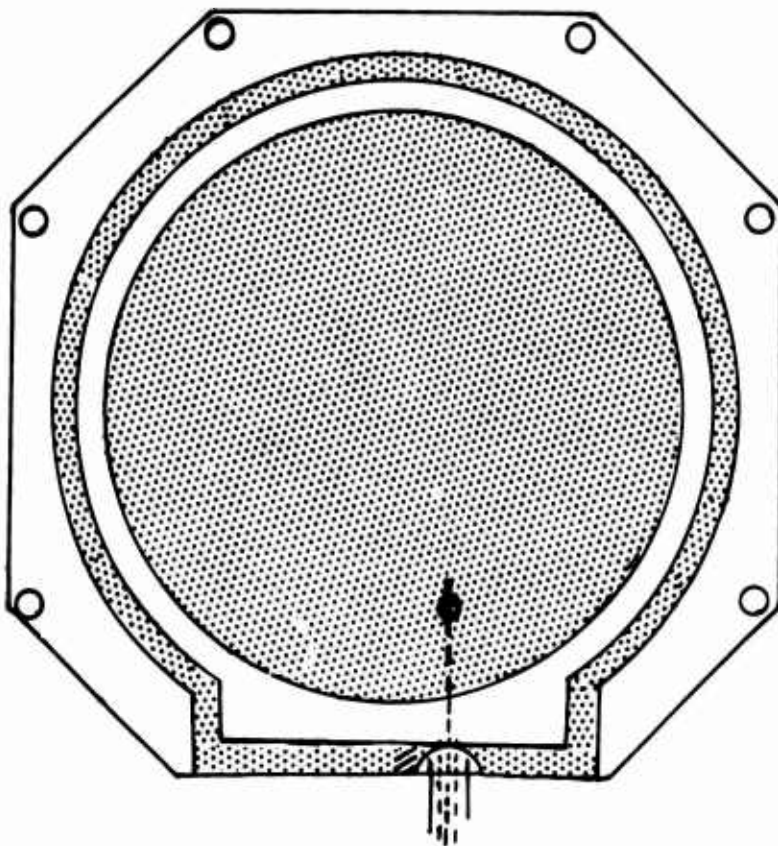


Figure 1. PMMA Spacer, Steady-State Irradiation Study

set of legs was required, of course, to attach the aluminum mounting plate. Here, however, they were attached to the top end block rather than to a can top. The lack of a can top also required slightly different arrangements for clamping the 11 tri-axial cables in place at the top of the structure. In this case, the top end block design was modified to include a suitable clamp at one side as an integral part.

For this case, potting was done by a dipping process similar to that used in candle making. The sample structure was preheated to around 65 to 70°C, dipped into a vat of molten paraffin, and then withdrawn, allowing the adhering paraffin to cool. This process was repeated, without the reheating process of course, until an adequate coat of paraffin was built up. After final cooling, the excess paraffin, and any bits of foreign material adhering to it, was whittled off by hand, and the structure was coated with a commercial silver, conductive paint¹². In this case, the can then was ready for exposure.

2. Radiation and Dosimetry. The radiation used in this study was provided by the Northrop cobalt source, a 5-kC array of Co⁶⁰ rods located in the corporation's reactor facility in Hawthorne, California. The individual cobalt rods, each about 8 inches in length, are mounted with their axes vertical, around the circumference of a horizontal circle about 8 inches in diameter, thus forming a cylindrical cage, open at top and bottom, whose axis also is vertical. This cage is located at the bottom of a circular well about 5 feet deep. Maximum exposure dose rates available at the center of this cage, at the time of this study, were on the order of 2×10^5 roentgen/hr.

Several steel-covered, concrete plugs were available for closing the top of the well. For this study one of these, having a set of copper tubes spiraled down through it to provide passage for electrical leads, was used to provide mechanical support for the

samples. The can in each case (except for Can 1*), was attached to a steel rod by means of the aluminum mounting plate. The rod, in turn was threaded into a hole in the bottom of the plug. The electrical leads from the can were taped to the rod with masking tape, and led through the spiraled tubes. Rod length was chosen so that the center of the can coincided with the center of the cobalt cage when the plug was fully inserted into the well. Can orientation was such that the samples and electrodes were in the horizontal plane, i.e., normal to the cage and rod axes.

A rather low-g geared hoist is available for removing and inserting plugs. This hoist utilizes a single cable, which permits the plug to rotate about its vertical axis. Rough control of this type of motion is achieved with a pair of master-slave manipulators. These are limited in travel, however, so that the angular orientation of the can about its vertical axis is subject to only gross control. Because of this a certain amount of symmetry about the vertical axis was desirable in the samples.

The hoist can be stopped at any point, so that the flux experienced by a sample could be adjusted simply by choosing position along the well's axis. A rough scale, marked with a felt tip pen on the steel lining of the plug, provided a measure of this position. The lip of the well, approximately at ground level, was used as the index. Where the plug bottom was below ground level, height could be measured directly. For positions where the plug bottom was above ground level, its height above the lip was measured with a meter stick held in a manipulator.

Routine determinations of radiation field intensity inside the cobalt cage were made periodically by reactor facility personnel using Fricke chemical dosimeters.

* Can 1 was exposed inside an existing, open-topped aluminum bucket, which had been used for prior work. The can was packed in the bucket with styrofoam blocks, which prevented use of the plug and support rod for electrical purposes. Otherwise, the remarks of this section are valid for Can 1 as well.

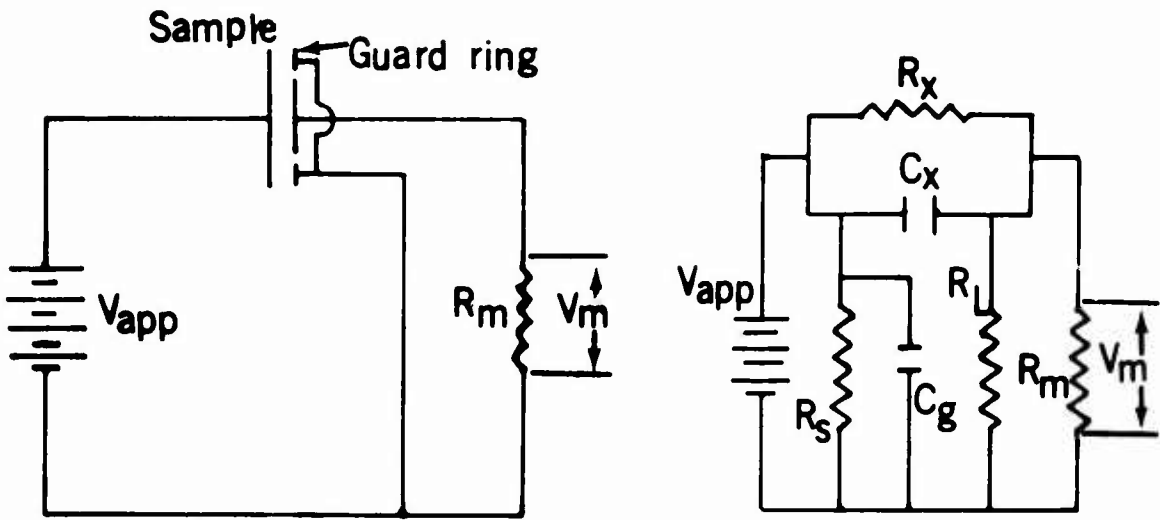
Accumulated measurements of this type have shown the field intensity in the space occupied by the samples, within the cage, to vary less than 10% in the horizontal plane, and less than 5% in the vertical.

In addition, for this study it was necessary to determine intensity as a function of distance along the well axis. This was done using a set of about 40 dosimeters of the LiF Thermoluminescent type. No statistical study of the dosimetry technique has been made, but it is estimated that the accuracy of this determination was on the order of $\pm 10\%$, and the precision, with respect to the intensity at the cage center, was about $\pm 4\%$.

Several samples were exposed to reactor bombardment prior to examination in this study. This exposure was accomplished in air, at room temperature, in the dry exposure room of the Northrop reactor, also located in Hawthorne, California. Samples were tied together in bundles about an inch thick with masking tape, each bundle being taped to a wood support rod for positioning. The samples selected for later examination occupied interior positions within the bundles, so that access to air was somewhat limited, except around the edges.

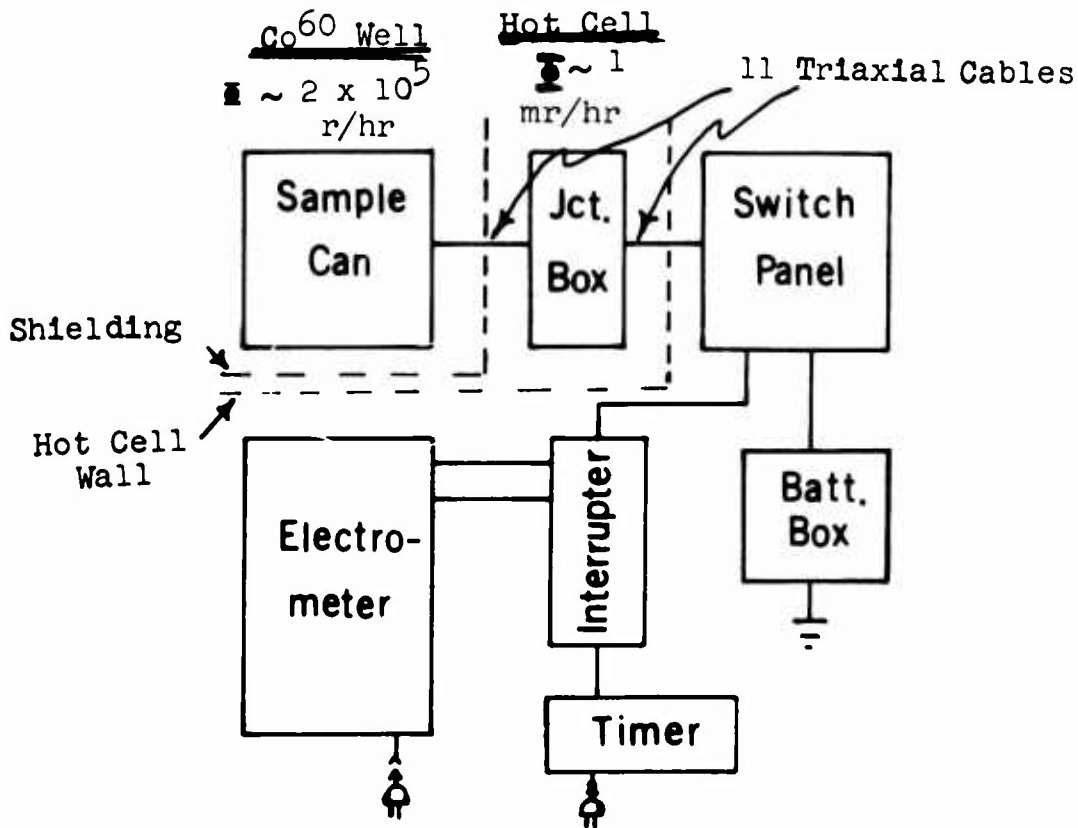
3. Circuitry. It will be noted (Figure 2a) that the circuitry of this study is extremely simple in concept. A battery applies a voltage, V_{APP} , across a plane parallel plate capacitor whose dielectric is the material of interest. The resulting current, I , is measured via the IR drop, V_M , across the measuring resistor, R_M . Surface currents are intercepted by a guard electrode and shunted past R_M , so that only those currents dependent upon transport processes occurring in the volume between the electrodes are observed.

So long as R_M is small compared to the leakage resistance, R_L , which shunts it, and to the parallel equivalent resistance, R_X ,



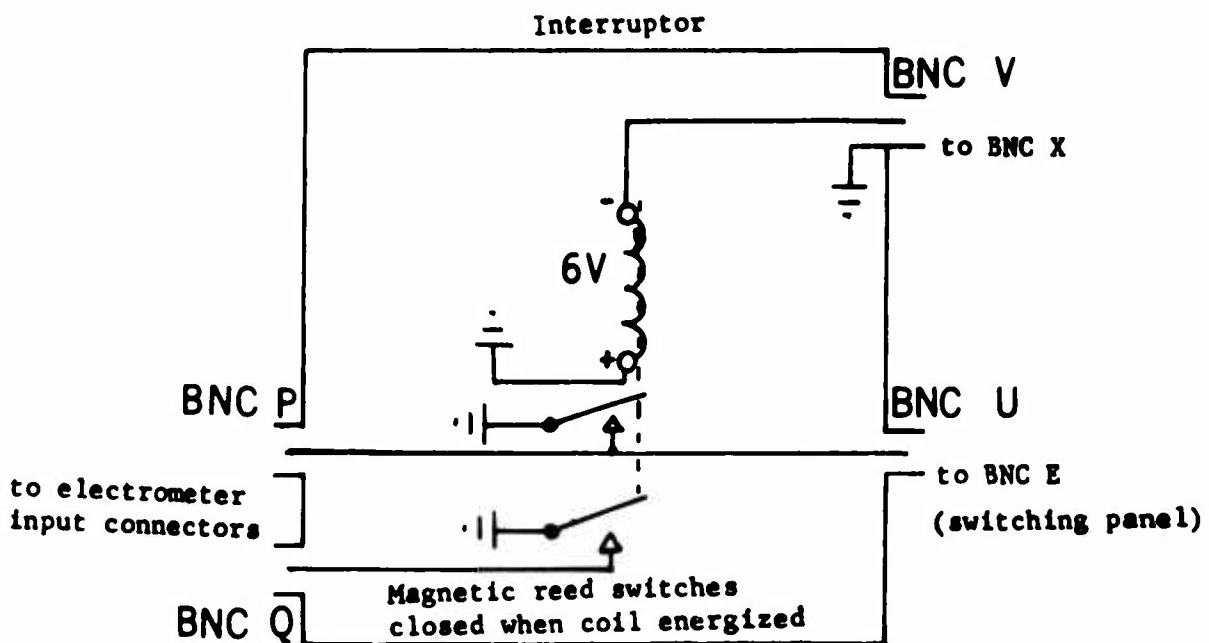
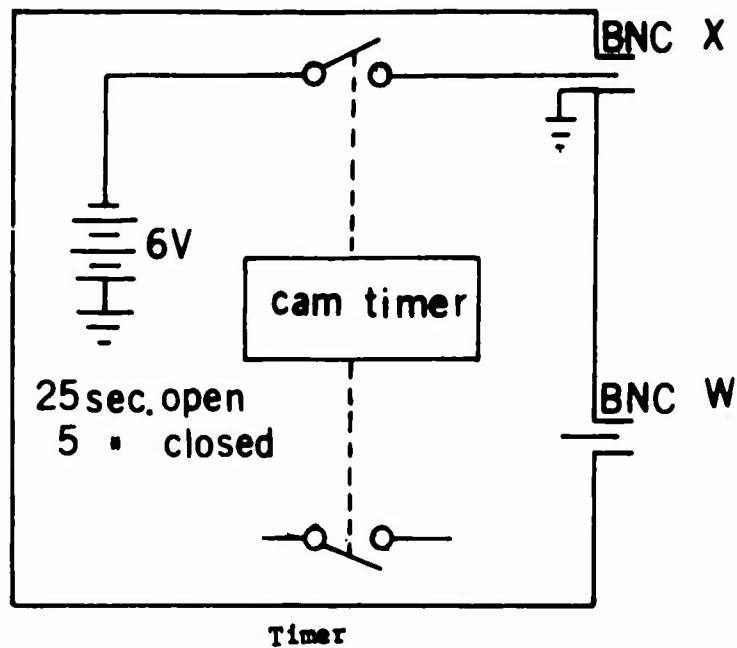
a) Basic Concept

b) Equivalent Circuit



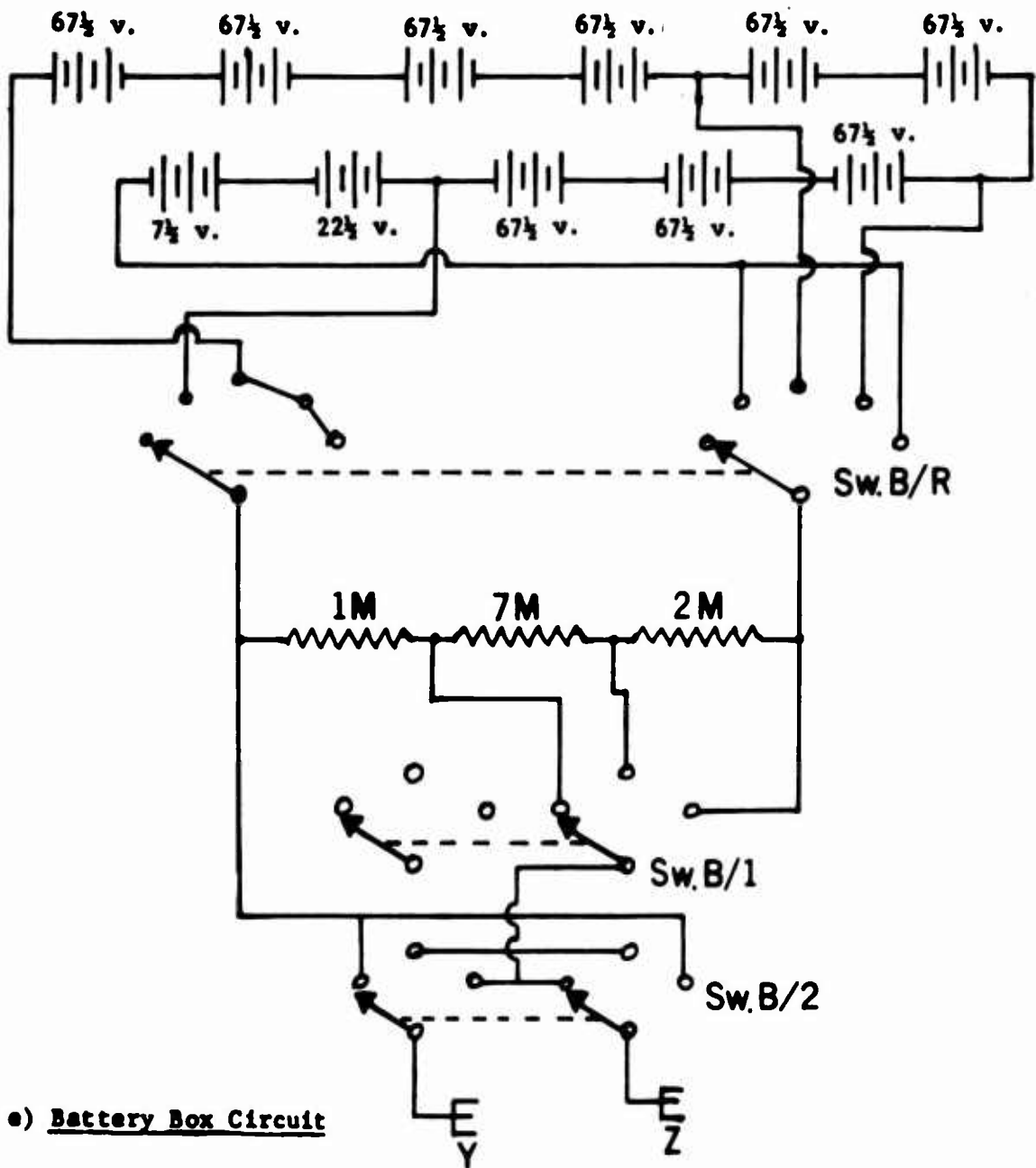
c) Block Diagram

Figure 2. Measuring Circuit Details, Steady-State Irradiation Study



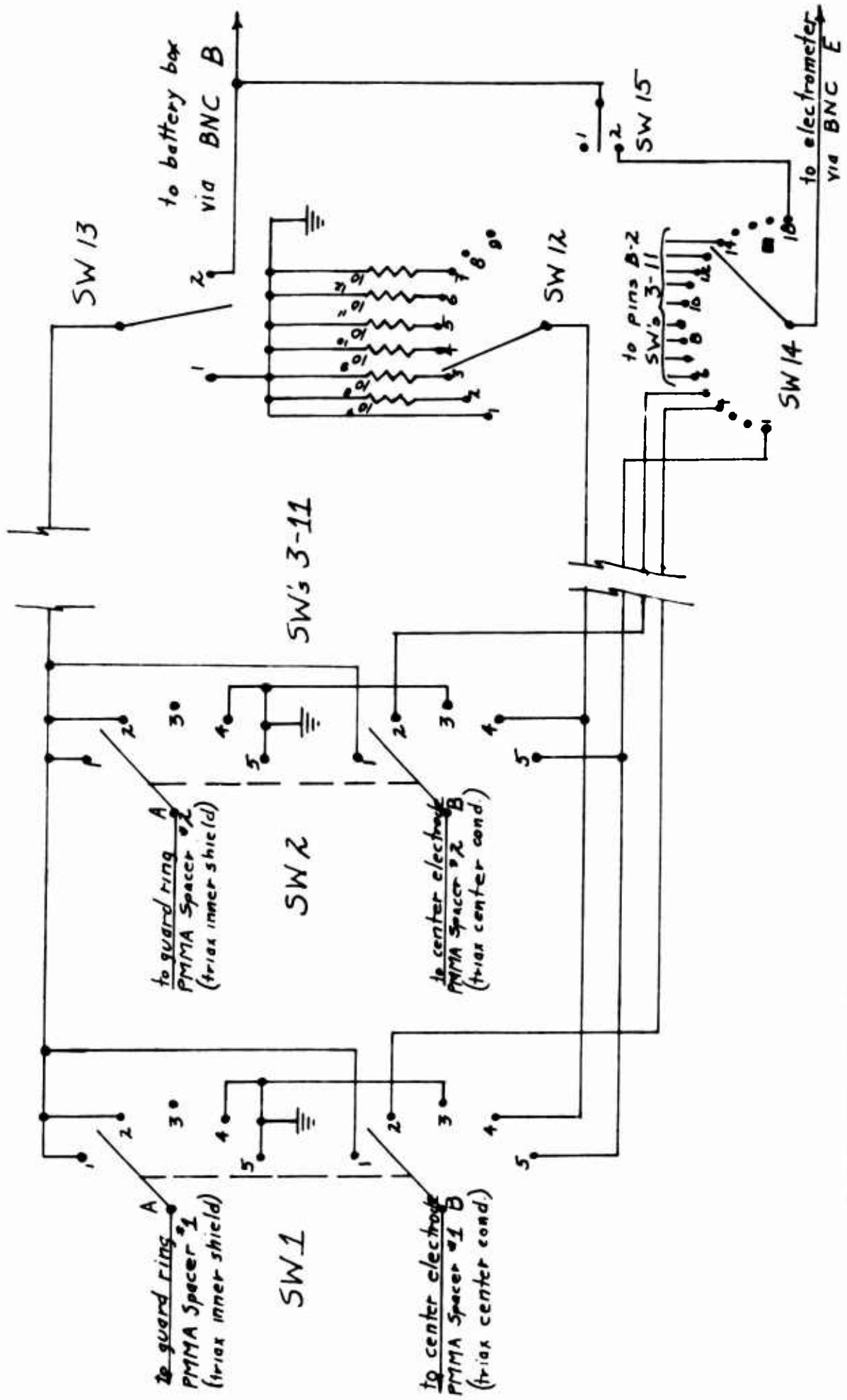
d) Electrometer Input Interruptor and Timer

Figure 2, (Cont'd). Measuring Circuit Details,
Steady-State Irradiation Study



e) Battery Box Circuit

Figure 2, (Cont'd). Measuring Circuit Details,
Steady-State Irradiation Study



f) Switching Circuit

Figure 2, (Cont'd). Measuring Circuit Details,
Steady-State Irradiation Study

of the sample, the current through the sample is given by

$$I = V_{APP}/R_M ,$$

and the sample's conductance is given quite straightforwardly as the slope of the current-voltage characteristic, i.e.,

$$G = dI/dV_{APP} .$$

The currents observed in this study were quite small (in the nano- to pico-ampere range). Consequently, a high-impedance voltage-measuring system was required, for which a commercial electrometer amplifier⁸ was used. For enradiant currents, R_M had a value of 10^8 ohms, while for the preirradiation currents it was occasionally necessary to use 10^{10} ohms. In all cases the tolerance on R_M was $\pm 1\%$.

In order to check periodically for zero-point drift in the electrometer circuit, signals were fed first into a locally designed and built input interruptor circuit. This consisted of a gas-filled, magnetic reed switch⁹ which was normally open, but when energized, closed to short across the electrometer input. This switch was housed in a small aluminum box mounted directly on the electrometer input head.

The dry cell which powered the coil of the magnetic reed switch was housed separately in another aluminum box also containing a motor-driven cam switch which automatically energized the coil for about 5 seconds, at 30-second intervals. Coaxial cables were used to connect the two boxes.

V_{APP} was provided by dry cells, housed in a battery box of local design and construction. As can be seen from the circuit diagram

(Figure 2e) a choice of several voltages was available^{*}, and provision for reversing polarity and for bypassing the batteries entirely, was incorporated into the design. As a point of minor interest, it was found necessary, in order to avoid spurious signals in some cases, to provide thorough isolation of the battery cases from ground. This was accomplished by lining the inside of the battery container with 10-mil sheets of a polyester. The mechanism(s) responsible for the spurious signals remain(s) unclear, at present.

In order to select which pair, or other combination, of electrodes was utilized at any single time, a switching panel was designed and built locally (Figure 2f). The switches used were ceramic wafer switches of high isolation resistance^{*}, and polytetrafluoroethylene (PTFE) terminal strips and wiring insulation were used throughout. A minor gap in the coverage provided by the inner shield of the connecting cables (i.e., the guard electrode) could not be avoided here. Measurements indicated, however, that surface leakage in the entire system was satisfactorily low, and no apparent damage to the experiment resulted.

Connections between sample and switching panel were made with a set of 11 triaxial cables^f. These were connected to the cables from each can in a small junction box mounted on top of the well plug, led through the wall of the hot cell, and connected at the other end to the PTFE terminal strips. The terminal strips in the plug-top junction box also were of PTFE, and of the same design as those in the switching panel. Connections between the panel, the battery box, and the electrometer input interruptor were made with coaxial cables¹¹. All cables in the system utilized polyethylene (PE) as their principal dielectric.

^{*}The battery box was modified slightly between examinations of Cans 2 and 3. Prior to the modification, fewer voltages were available, and their range extended into the tenths of volts. The results of examining Can 2 showed the low voltages to be uninteresting, and the arrangement shown in Figure 2 was installed.

4. Technique. The experimental program originally proposed for this study^a was based on the assumption that the steady-state-photoconductivity, $d\sigma$, could be determined experimentally, from measurements of the normal steady-state photocurrent, as defined previously. As pointed out, however, measurement of this component in the common organic insulators is at best an extremely difficult task. Most attempts appear to have foundered on the rock of thickness dependence, and responsible authors have either carefully pointed out that their observed conductances were not inversely proportional to sample thickness, or else confined their comments to the behavior of individual samples, drawing what conclusions they could from response to independent variables other than thickness.

As suggested by previous remarks, the measurement technique developed for this study was based upon observations made at short times, i.e., in the range of 3 to 10 minutes after applying a voltage to the sample. To cover the possibility that significant transient components might still be contributed by processes taking place in past history of the sample was devised. This technique does not provide a measure of the relative sizes of the various components contributed by the sample proper. However, it does fix their ratios, thereby permitting such interpretations as can be based upon their combined behavior.

The technique developed from this approach has three steps:

1. The voltage of interest is applied to the sample, and maintained for a fixed time,
2. Voltage polarity is reversed, and this condition is maintained for about the same time,
3. Finally, polarity is reversed once again, and the condition is maintained until sufficient data have been taken. Data are taken as functions of time

since the last polarity reversal, and comparisons are made between points taken at equal values of this time.

The key to successful use of this technique lies in choosing the "fixed time" long enough that the effects of all the voltage changes prior to the last pair can be neglected. Under this condition, all three variables (applied voltage, voltage history, and time) will be the same for all samples. Rules for making this choice have not been formulated in this study. Rather, the longest time deemed practical in terms of the time available was chosen. Judging from the results, this time appears to have been fortunately chosen, and the effects of even the next-to-last voltage change appear to be negligible. Under this condition, data can be taken during the second step, as well as the third, and two points of the current-voltage characteristic can be obtained from each cycle.

C. OBSERVATIONS

1. Variables. As indicated in the introduction to this section, the dependent variable in this study was the total current during irradiation, observed at a fixed time after changing the voltage applied to the sample's electrodes in accordance with the procedure described under Technique. Once the first half-minute or so after voltage change had passed, the observed current changed rather slowly with time. Because of this, close control of the observation time was not required. For the data given below, all measurements were made in the period between 3 and 10 minutes after application of the voltage, most of them clustering around the 6 to 7 minute region.

The independent variables investigated were largely those specified in the proposal^a: sample fabricator, to check the effects of trace impurities; dose rate; and accumulated dose. In addition

the question of volume-versus-surface effects was raised through varying sample thickness, which also provided a measure of experimental quality. And finally, the effects of structural defects were examined through preirradiation of three samples of each material in a nuclear reactor. (In all six cases the dose received in the pile was about 5 Mrads.)

2. Determination of Conductances. The currents observed in each case were examined first in the form of current-voltage characteristics. A curve typical of those found for polyethylene is given in Figure 3, and one typical of those found for polystyrene is given in Figure 4.

It will be noted that the characteristic shown for polyethylene is quite linear, with very little evidence of saturation. The only cases where any appreciable indication of saturation was seen were those of the 2- and 4-mil samples. Even here the deviation from linearity, while noticeable, was still small. None of the polystyrene characteristics showed any signs of saturation at the higher voltages.

It was necessary to curtail measurements on the 2- and 4-mil polyethylene samples at about 100 volts because catastrophic noise developed in their signals beyond this point. Later measurements at lower voltages were obtainable, so complete breakdown did not occur. However, the large noises seen were suggestive of breakdown, and probably indicated a fairly close approach to punchthrough.

It also will be noted that the characteristic shown for polystyrene exhibits the "chair" shape typical of cases where a layer of some blocking material is present at one or both electrodes. In this case the blocking apparently was overcome by the applied field somewhere in the region between plus and minus 200 volts, and the characteristic was dominated by the polystyrene in the regions outside this, i.e., throughout both regions where data were taken.

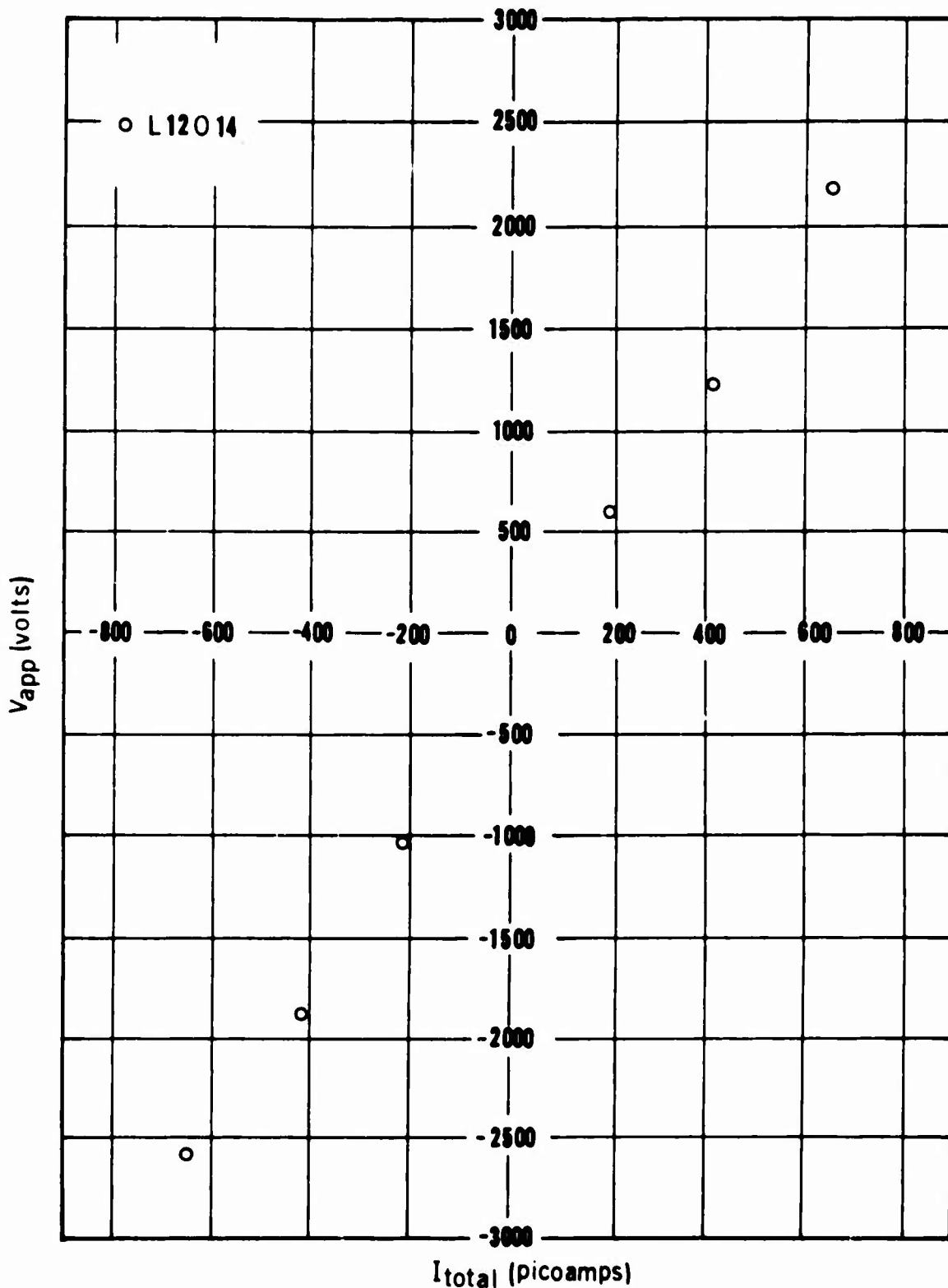


Figure 3. Total Observed Photocurrent vs. Applied Voltage for Typical Polyethylene Sample, Steady-State Irradiation Study. Currents are those observed under the controlled voltage-history procedure described in the text. Observations were made during exposure to Co^{60} gamma radiation, at an absorbed dose rate of about 63 rad/sec.

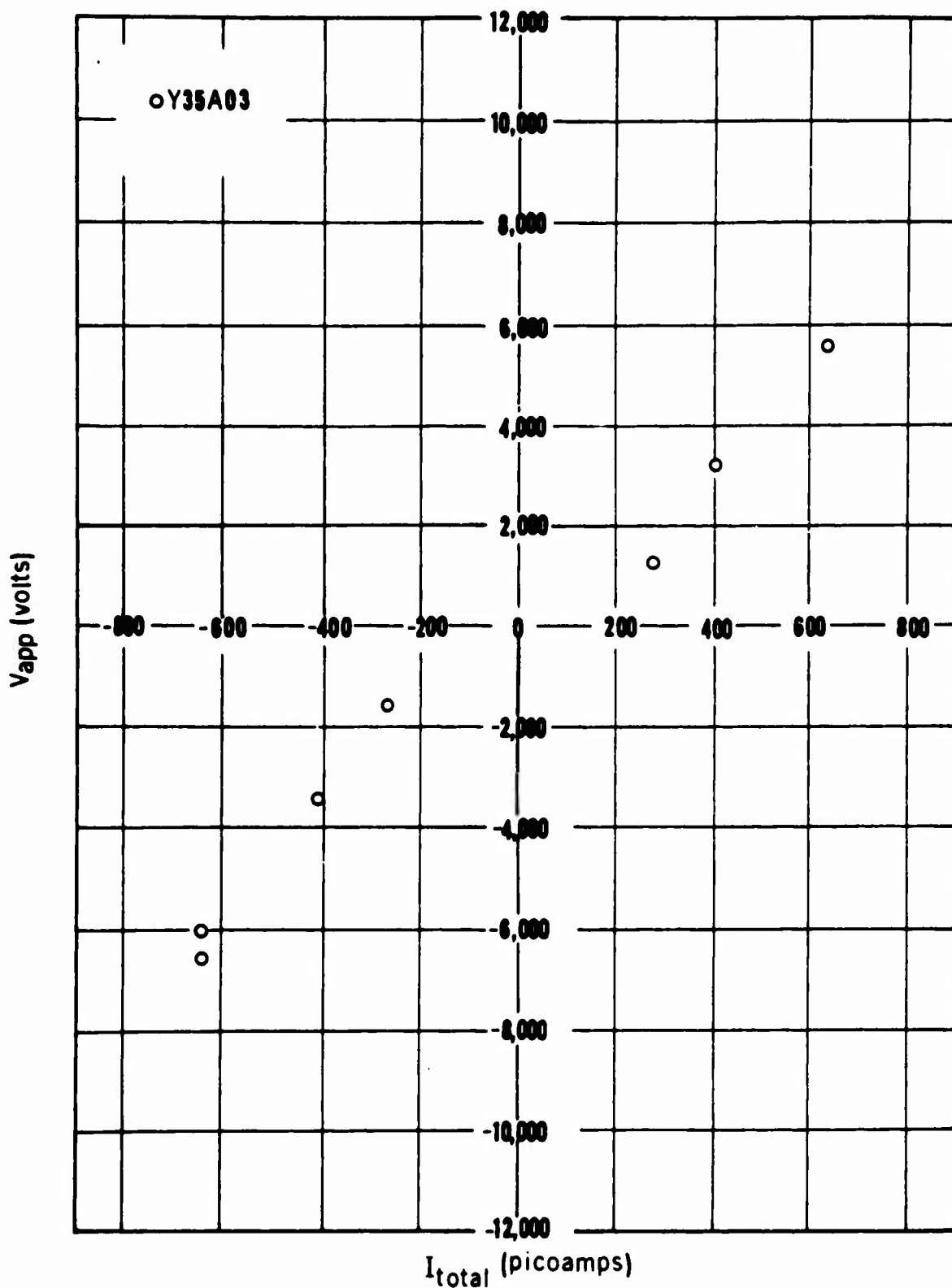


Figure 4. Total Observed Photocurrent vs. Applied Voltage for Typical Polystyrene Sample, Steady-State Irradiation Study. Currents are those observed under the controlled voltage-history procedure described in the text. Observations were made during exposure to Co^{60} gamma radiation, at an absorbed dose rate of about 59 rad/sec.

About 60% of the polystyrene characteristics displayed such effects, the remainder being as linear as the polyethylene curves. Only one polyethylene curve, that for sample L12N11 at 1.54 Mrad, displayed the chair shape, and this was to a much smaller degree than in the case of polystyrene. In all chair-shaped characteristics, the two arms formed by the data points paralleled each other quite closely.

All characteristics displayed a distinct zero-volt offset, thus providing a measure of the momentum current in each case. In all cases this offset was on the order of a few hundred picoamperes, with the median at about 200 pA. Such a low value for the momentum current is quite gratifying, particularly for single-layer samples, and is indicative of a high degree of homogeneity in the radiation field.

Each characteristic underwent a subjective visual examination for data-point consistency. Those points falling a suspicious distance from the line determined from their neighbors were recalculated from the raw data and reexamined. Of the several hundred data points taken under the technique described in this report, only three failed to pass the second examination.

All three of these points corresponded to raw data signals which displayed substantially more noise than normal. They were summarily rejected from consideration and were not included in the calculations of conductance described below.

After passing visual inspection, the points of each characteristic were fitted to a straight line by least squares techniques. In the case of the linear curves, the procedure was quite straight-forward. In the case of the chair-shaped curves, each arm was fitted separately, the two slopes thus obtained then being averaged to determine the conductance. The entire curve then was fitted to determine the most probable value for the zero-voltage offset.

Dark currents were observed prior to irradiation in about half of the samples. In all cases these were found negligible, amounting

at worst to only a few percent of the total current observed at the standard radiation field intensity. A quantitative analysis of the dark current data has not been made, so precise values cannot be cited.

The dark current was assumed to be negligible in all samples. Under this assumption, the slope derived from the least-squares fitting techniques described above, gives directly the APPARENT PHOTOCONDUCTANCE, G^* , of the sample-electrode system being observed. We insert the word apparent and use the superscript * here to acknowledge and emphasize that a sum of steady-state photocurrent and transient components is involved.

The apparent photoconductances per unit electrode area, G^*/A , for all samples observed in this study are presented, along with the corresponding sample thicknesses, t , absorbed dose rates, Γ , momentum currents, I_0 , and accumulated doses, in Tables II and III, pp 36 through 38. The value calculated for the apparent photoconductivity, σ_{calc}^* , by multiplying t by G^*/A , also is given for each case, in these tables.

It will be noted that in these tables a number of samples are designated with a'. Each of these primed samples is the same piece of material as its unprimed counterpart. The electrode connections differ between the two, however, in one case the top electrode being connected to the battery and the bottom one to the electrometer, and in the other case, vice versa.

The measurements made while investigating the dependence of polystyrene's conductance on absorbed dose rate, Γ , and while investigating the role of accumulated dose at the lower values ($>1\text{Mrad}$) in the samples of Can 5, were confined to observations made at only two applied voltages, around plus and minus 650 volts. Some question as to the reliability of conductances computed from characteristics having only two points seems justified, particularly in view of the chair effect observed in so many cases.

TABLE II. POLYETHYLENE CONDUCTIVITY DATA,
STEADY-STATE IRRADIATION STUDY

Sample	t m x 10 ⁻⁵	Γ rads/sec	Dose Mrads	G/A mpmho/cm ²	I ₀ A	ρ * calc mpU/cm	ρ * graph mpU/cm	
L12J03	27	66.5	1.70	146	-163	3.94	3.6	
L12J04	26	66.2	1.36	149	-156	3.87		
L12J04'	↓	↓	1.70	163	-191	4.24	↓	
L51J07	27	63.9	1.48	156	-925	4.21		
↓	↓	↓	3.96	150	-118	4.05		
L51J07'	↓	↓	2.26	183	+744	4.94		
L51M23	44	↓	1.48	96.3	-450	4.24		
↓	↓	↓	3.97	100	-300	4.40		
L51M23'	↓	↓	3.54	85.3	-254	3.75		
L11N22	53	64.4	2.26	73.0	-420	3.87		
L11N22'	↓	↓	3.54	95.2	-193	5.05		
L12N11	54	61.4	0.36	134	-220	7.24		
↓	↓	↓	0.84	88.9	-130	4.80		
↓	↓	↓	1.54	91.2	-182	4.92		
L12N26	52	↓	4.56	101	-222	5.45	2.4	
↓	↓	↓	pile + 0.36	43.0	-170	2.24		
↓	↓	↓	0.84	31.9	-155	1.66	↓	
↓	↓	↓	1.54	54.6	-453	2.84		
L12N36	↓	64.4	5.18	56.5	-212	2.94		
↓	↓	↓	1.48	75.0	-153	3.90		
L12N36'	↓	↓	3.96	61.6	-162	3.20		
L12N55	↓	↓	3.53	52.6	-232	2.74		
↓	↓	↓	1.48	73.5	-126	4.13		
↓	↓	↓	3.96	55.3	-187	2.88		
L11020	79	64.1	1.48	62.2	-99.2	4.91		
↓	↓	↓	3.96	64.5	-170	5.10		
L11020'	↓	↓	3.53	54.6	-201	4.31		
L12003	74	66.0	1.36	79.2	-183	5.86	↓	
L12004	75	↓	1.70	83.4	-168	6.26		
L12014	70	60.5	pile + 0.36	32.4	-160	2.27		2.4
↓	↓	↓	0.84	23.7	-160	1.66		
↓	↓	↓	1.54	36.3	-197	2.54		↓
↓	↓	↓	5.18	42.2	-206	2.95		
L12017	71	63.9	2.26	86.4	-482	6.13		
L12017'	↓	↓	3.52	52.8	-172	3.75		
L51053	78	64.4	1.48	60.7	-87.1	4.73		
↓	↓	↓	3.96	54.6	-146	4.26		
L51053'	↓	↓	2.26	83.1	-483	6.48		
L11R01	234	63.9	1.48	36.0	-212	8.42	3.6	
↓	↓	↓	3.91	38.7	-237	9.06		
L11R01'	↓	↓	2.26	45.3	-491	10.6	↓	
↓	↓	↓	3.49	29.8	-374	6.97		
L12R13	232	60.8	0.36	52.7	-235	12.2		
↓	↓	↓	0.84	26.5	-210	6.15		
↓	↓	↓	1.54	42.3	-252	9.81		
↓	↓	↓	5.18	30.0	-259	6.96		
L12R13'	↓	↓	0.57	57.0	+5	13.2		
↓	↓	↓	0.93	30.3	-180	7.03		
↓	↓	↓	1.41	30.3	-204	7.03		
↓	↓	↓	4.56	17.8	-45.0	4.13		
L12R20	228	64.1	2.26	38.1	-347	8.69	↓	
↓	↓	↓	3.50	13.0	-197	2.96		
L12R70	↓	↓	pile + 0.57	13.7	-202	3.12		2.4
↓	↓	↓	0.93	9.45	-265	2.15		
↓	↓	↓	1.41	11.0	-208	2.51	↓	
↓	↓	↓	4.56	11.2	-228	2.55		

TABLE III
POLYSTYRENE CONDUCTIVITY DATA, STEADY-STATE IRRADIATION STUDY

Sample	t	Γ	Dose Mrads	G^*/A	I_0 pA	σ^* calc	σ^* graph
	$m \times 10^{-5}$	rads/sec		mpmho/cm ²			
Y13E01	13	59.8	1.77	41.3	-164	0.537	0.50
Y41E02	12	56.6	pile +				
			0.57	28.8	-140	0.345	0.34
			0.93	25.5	-275	0.306	
			1.41	28.6	-157	0.243	
			4.56	24.1	-233	0.289	
Y41E09		60.1	1.31	39.6	-151	0.475	0.50
Y35H07	20	59.9		14.4	-152	0.288	
Y41H02		58.0	pile +				
			0.57	12.3	-218	0.246	0.34
			0.93	12.6	-114	0.252	
			1.41	13.0	-178	0.260	
			4.56	11.5	-213	0.230	
Y41H11	19		0.36	33.2	-370	0.631	0.50
			0.57	27.1	-165	0.515	
			0.84	28.6	-332	0.543	
			0.93	16.1	-734	0.306	
			1.41	11.8	-160	0.224	
			1.54	26.4	1346	0.501	
			4.56	20.0	-229	0.380	
			5.18	24.6	-372	0.467	
Y13J09	27	60.6	0.77	36.0	-209	0.972	
Y41J01	26			26.5	-431	0.689	
Y35N03	55	53.6		3.02	-517	0.166	
		59.4	1.31	2.17	-171	0.118	
Y41N01	52	58.0	0.36	8.24	-168	0.428	
			0.84	6.50	-275	0.338	
			1.54	7.35	-175	0.382	
			5.18	7.54	-196	0.392	
Y1N06	53		pile +				
			0.57	7.12	-55.5	0.377	0.34
			0.93	4.37	-231	0.231	
			1.41	4.43	-177	0.235	
			4.56	5.70	-196	0.302	
Y41N11	52	60.1	0.77	13.0	-187	0.677	0.50
			1.31	8.06	-164	0.419	

To check on this question, two-point calculations of conductance were made, using the 650-volt points, on all six-point characteristics showing the chair effect. In most cases the values computed in the two-point calculation were within 10% of those derived from the corresponding six-point calculation. The deviations thus calculated for those samples involved in the two-point measurements specified above, all fell in the range between -6% and +10%. Thus we estimate that the two-point conductances given in Tables II and III, probably lie within 10% of the values that would have been obtained had six-point characteristics been available.

3. Thickness Dependence. The apparent photoconductance per unit electrode area, G^*/A , is plotted against the inverse of sample thickness, $1/t$, for 13 samples of polyethylene, drawn from three different fabricators (Figure 5). For all of these measurements the accumulated dose was about 1-1/2 Mrad*, and absorbed dose rates were about 63 rads/sec. It will be noted that the points fall reasonably well along a straight line, and that no difference correlated with fabricator are apparent.

Values for G^*/A were calculated for one 2-mil and one 4-mil sample. These fell well below the straight line formed by the rest of the points, and presumably were substantially affected by surface conditions. They were not used in determining the straight line shown in Figure 5, which is the least-squares fit to all the data points shown. The apparent photoconductivity for these samples, given by the calculated slope of the fitted line, is 3.5 mpmho/cm.

Figure 6 presents similar data for polystyrene. The point found for a 1-mil sample fell substantially below the line obtained from the rest of the points, and has been omitted because of suspected surface effects. The points shown correspond to accumulated doses

*Throughout this report the unit "rad" specifies an absorbed dose of 100 ergs per gram of the material under discussion. Exposure doses are given in roentgens.

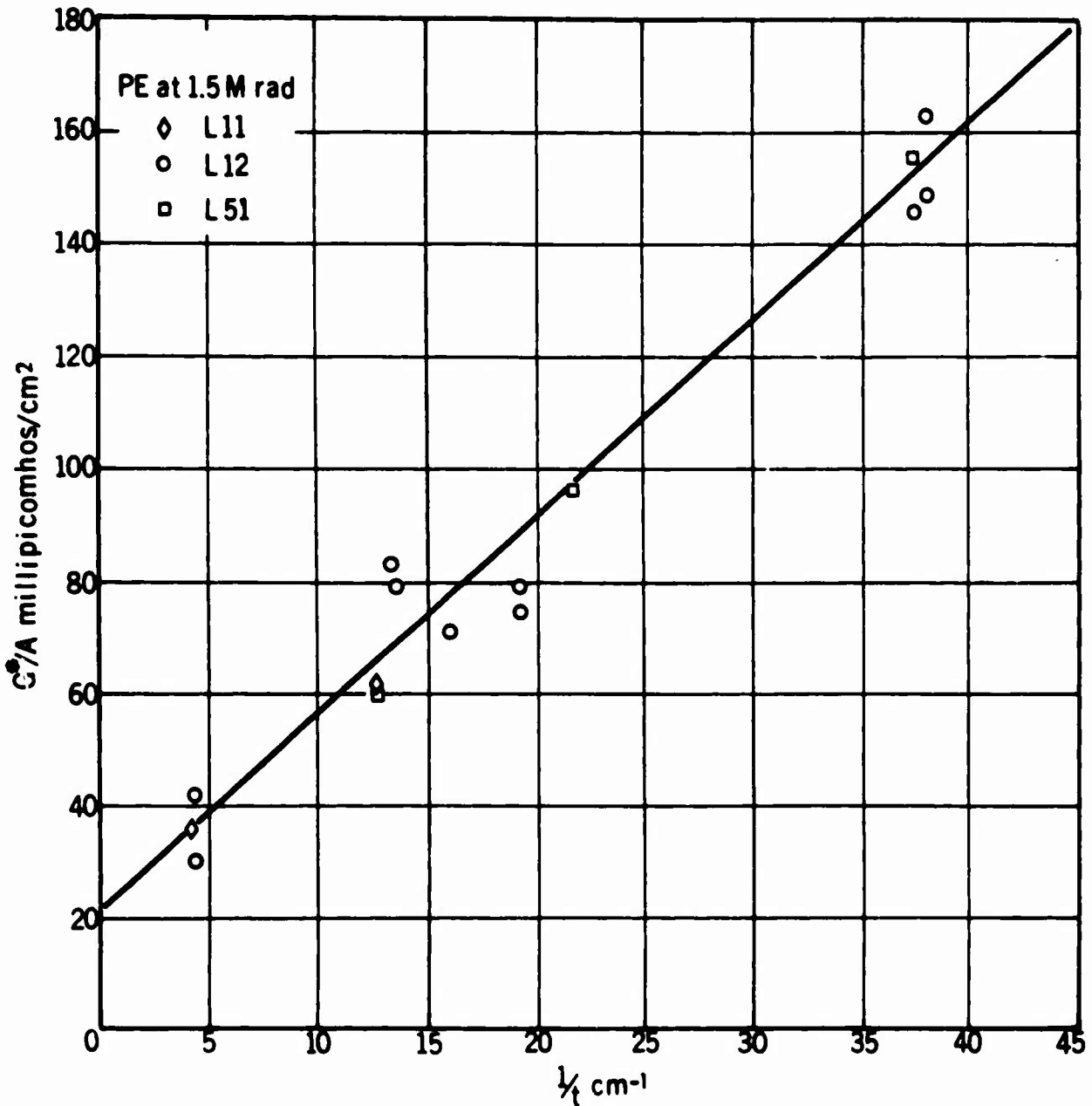


Figure 5. Total Observed Photoconductance per Unit Electrode Area vs Inverse of Sample Thickness, for Polyethylene Samples from Three Fabricators. Points are calculated from the slopes of photocurrent-voltage characteristics such as that shown in Figure 3. The line is the least-squares fit to the points shown. Absorbed dose rate approximately 63 rad/sec (Co^{60} gammas)

of about 1-1/2 Mrad, and dose rates of about 59 rads/sec. At this value of accumulated dose, data are available for sample from only two fabricators. The apparent photoconductivity calculated from the least-squares fit straight line for these data is 0.48 mpmho/cm.

4. Accumulated Dose Effects. Figure 7 presents in similar fashion the points found for the polyethylene samples of one fabricator, at the 63-rad/sec dose rate, using different symbols to indicate different accumulated doses. It will be noted that a small dependence can be seen, but that the total change found is not much more than the scatter displayed by the points observed at one dose. Further, the changes which do occur take place almost entirely in the intercept of the least-squares line, and only slightly in the slope. The slopes of the fitted lines shown are 3.4, 2.9 and 2.9 mpmho/cm for the 1-1/2 Mrad, 3-3/4 Mrad and pile-radiated samples, respectively.

The higher-accumulated-dose data for the samples obtained from the other two fabricators were too few in number to permit a reliable comparison for accumulated dose effects in each. When added to the points shown in Figure 7, however, to produce Figure 8, they are seen to fit rather closely to the line found for the first fabricator's samples at the 1-1/2 Mrad dose. Consequently we conclude that the dose accumulated from the Co^{60} gamma irradiation produced no observable change in photoconductivity, for polyethylene.

Accordingly, straight lines were fitted first, to the 44 data points listed in Table II which correspond to non-pile-bombarded material, and second, to the 12 data points in this table which correspond to pile-bombarded material. The slopes of these two lines were 3.6 mpmhos/cm and 2.4 mpmhos/cm, respectively. From these we conclude that the pile-bombardment produced about a 30% reduction in photoconductivity in polyethylene.

Figures 9 and 10 present similar displays for the polystyrene data. It will be noted in this case that accumulated dose effects, short of pile bombardment, are lost in the scatter of the data. The pile-bombarded samples, however, again display a slope which is about 70%

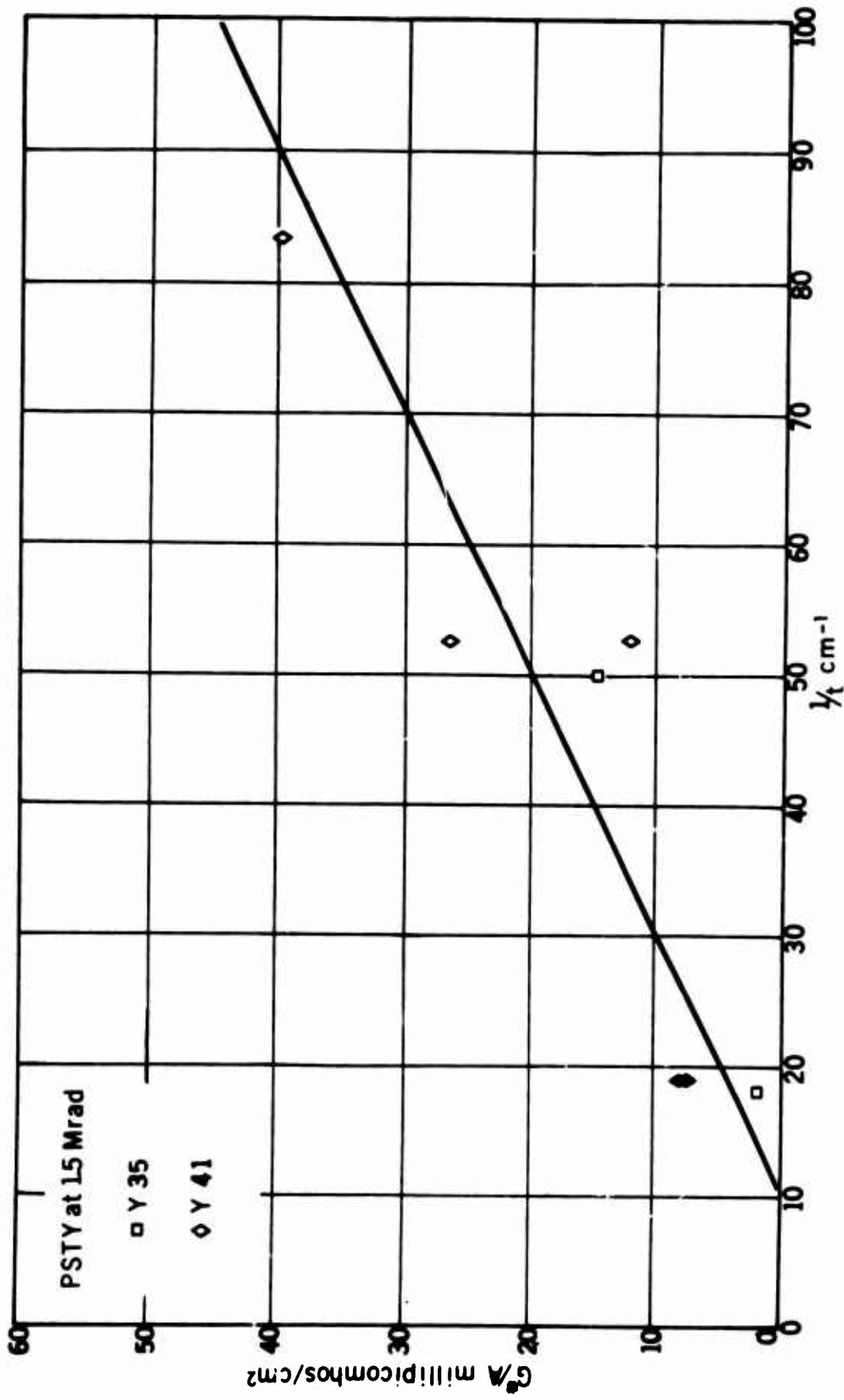


Figure 6. Total Observed Photoconductance per Unit Electrode Area vs. Inverse of Sample Thickness, for Polystyrene Samples from Two Fabricators. Points are calculated from the slopes of photocurrent-voltage characteristics such as that shown in Figure 4. The line is the least-squares fit to the points shown. Absorbed dose rate approximately 59 rad/sec (Co⁶⁰ gammas).

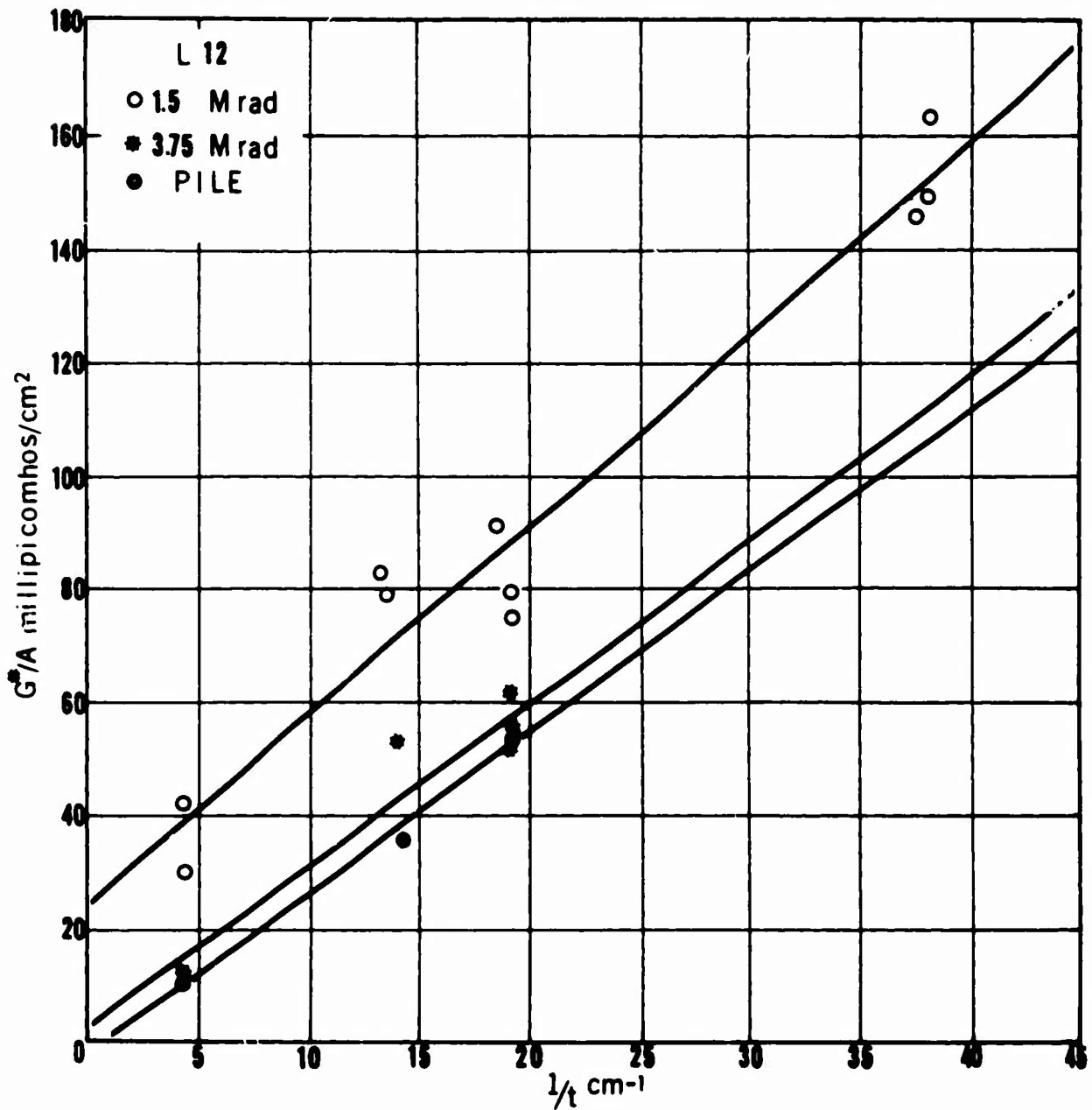


Figure 7. Total Observed Photoconductance per Unit Electrode Area vs. Inverse of Sample Thickness, for Polyethylene Samples from One Fabricator. Points are calculated from the slopes of photocurrent-voltage characteristics such as that shown in Figure 3. Lines are least-squares fits to the corresponding points. Absorbed dose rate approximately 63 rad/sec, (Co^{60} gammas). Absorbed doses range from 1-1/2 Mrad (Co^{60} gammas) to about 5 Mrad (neutrons) plus 1-1/2 Mrads (Co^{60} gammas).

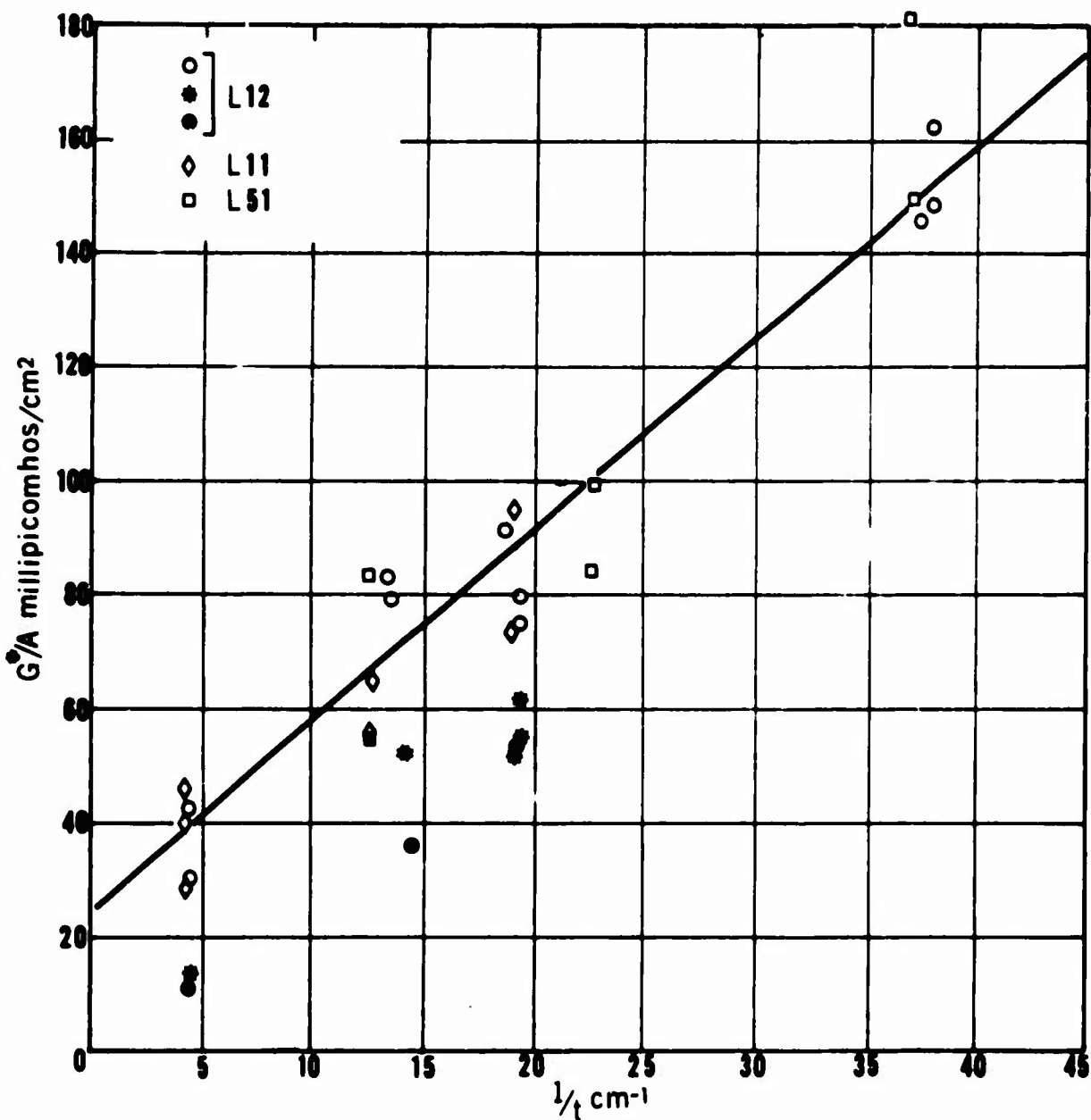


Figure 8. Total Observed Photoconductance per Unit Electrode Area vs. Inverse of Sample Thickness, for Polyethylene Samples from Three Fabricators. Points are calculated from the slopes of photocurrent-voltage characteristics such as that shown in Figure 3. The line is the least-squares fit to all the open points. Absorbed dose rate approximately 63 rad/sec. Absorbed doses range from 1-1/2 Mrad to 5 Mrad (Co^{60} gammas), for the open-point data, and from 3.8 Mrad (Co^{60} gammas) to about 5 Mrad (neutrons) plus 1-1/2 Mrad (Co^{60} gammas)

of that found for the 1-1/2 Mrad samples. Addition of the data for sample drawn from other fabricators, as can be seen in Figure 10, has very little effect on the overall picture. The slopes of the fitted lines for (i) all the samples of the first fabricator, other than the pile-bombarded ones; (ii) these plus the samples from the other two fabricators; and (iii) the pile-bombarded samples only, are 0.46, 0.50 and 0.34 mpmho/cm, respectively.

5. Dose Rate Dependence. The number of observations made at the lower dose rates was too small to permit meaningful comparisons between slopes of G^*/A versus $1/t$ plots, in view of the vertical scatter displayed by the data points. Consequently, the dose rate dependence is displayed in the form of plots of calculated apparent photoconductivity, calculated for each observation, versus dose rate (Figure 11).

The data for each sample displayed the familiar dependence

$$\sigma^* = K\Gamma^{\Delta^*_{\Gamma}}$$

where σ^* is the apparent photoconductivity, Γ is the dose rate, and Δ^*_{Γ} and K are constants. The values of Δ^*_{Γ} found for each observation are given in Table IV. The average value for all the polyethylene samples was 0.53. That for all the polystyrene samples was 0.69. We note that these values have not taken possible dark current effects into account.

6. Deferred Observations. In order to test the blocking layer hypothesis, a limited number of observations were made at times in the region of 90 minutes after application of voltage. The procedure here was the same as that used for the shorter time observations, except that the entire experimental arrangement was left undisturbed while the experimenter went out to lunch. Upon his return the last set of observations was repeated, and comparisons were made between the pre-and post-lunch readings.

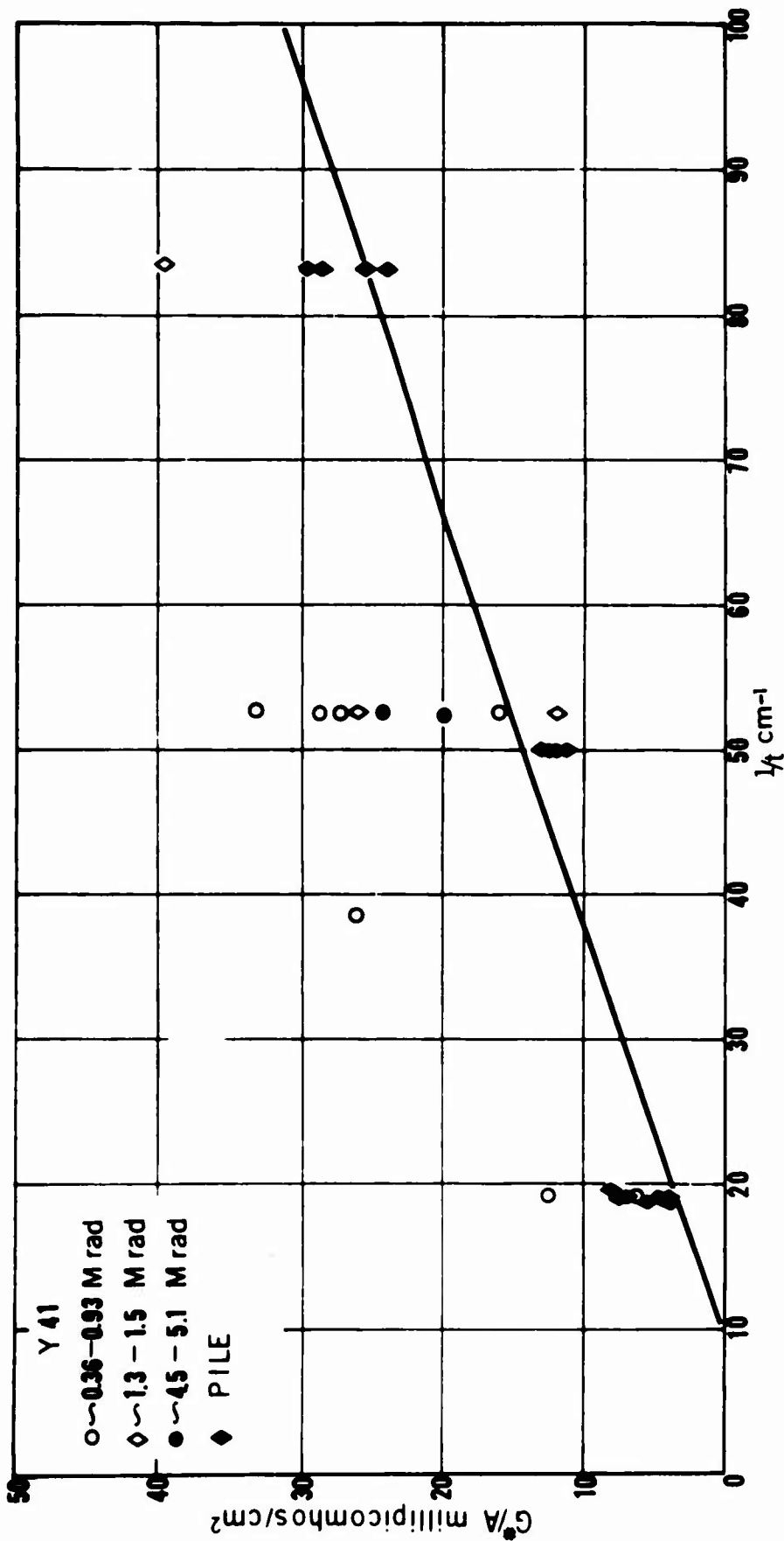


Figure 9. Total Observed Photoconductance per Unit Electrode Area vs. Inverse of Sample Thickness, for Polystyrene Samples from One Fabricator. Points are calculated from the slopes of photocurrent-voltage characteristics such as that shown in Figure 4. Lines are least-squares fits to corresponding points. Absorbed dose rate about 59 rad/sec (Co60 gammas). Absorbed doses range from 0.6 Mrad (Co60 gammas) to about 5 Mrad (neutrons) plus 4.5 Mrad (Co60 gammas).

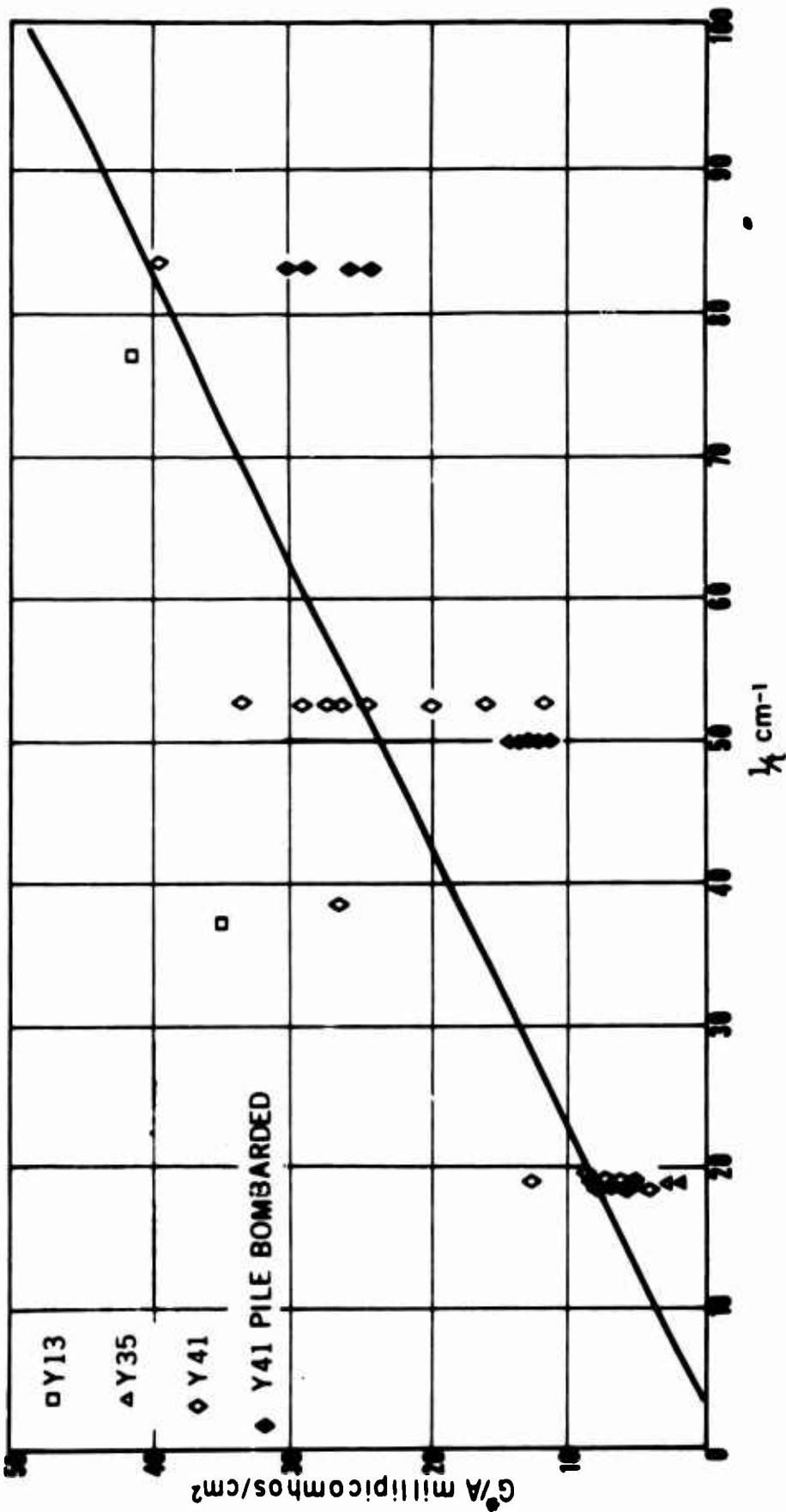


Figure 10. Total Observed Photoconductance per Unit Electrode Area vs. Inverse of Sample Thickness, for Polystyrene Samples from Three Fabricators. Points are calculated from the slopes of photocurrent-voltage characteristics such as that shown in Figure 4. The line is the least-squares fit to all the open points. Absorbed dose rate approximately 59 rad/sec. Absorbed doses range from 0.6 Mrad (Co⁶⁰ gammas) to 5 Mrad (Co⁶⁰ gammas) for the open points, and from about 5 Mrad (neutrons) plus 0.6 Mrad (Co⁶⁰ gammas) to about 5 Mrad (neutrons) plus 4.5 Mrads (Co⁶⁰ gammas), for the solid points.

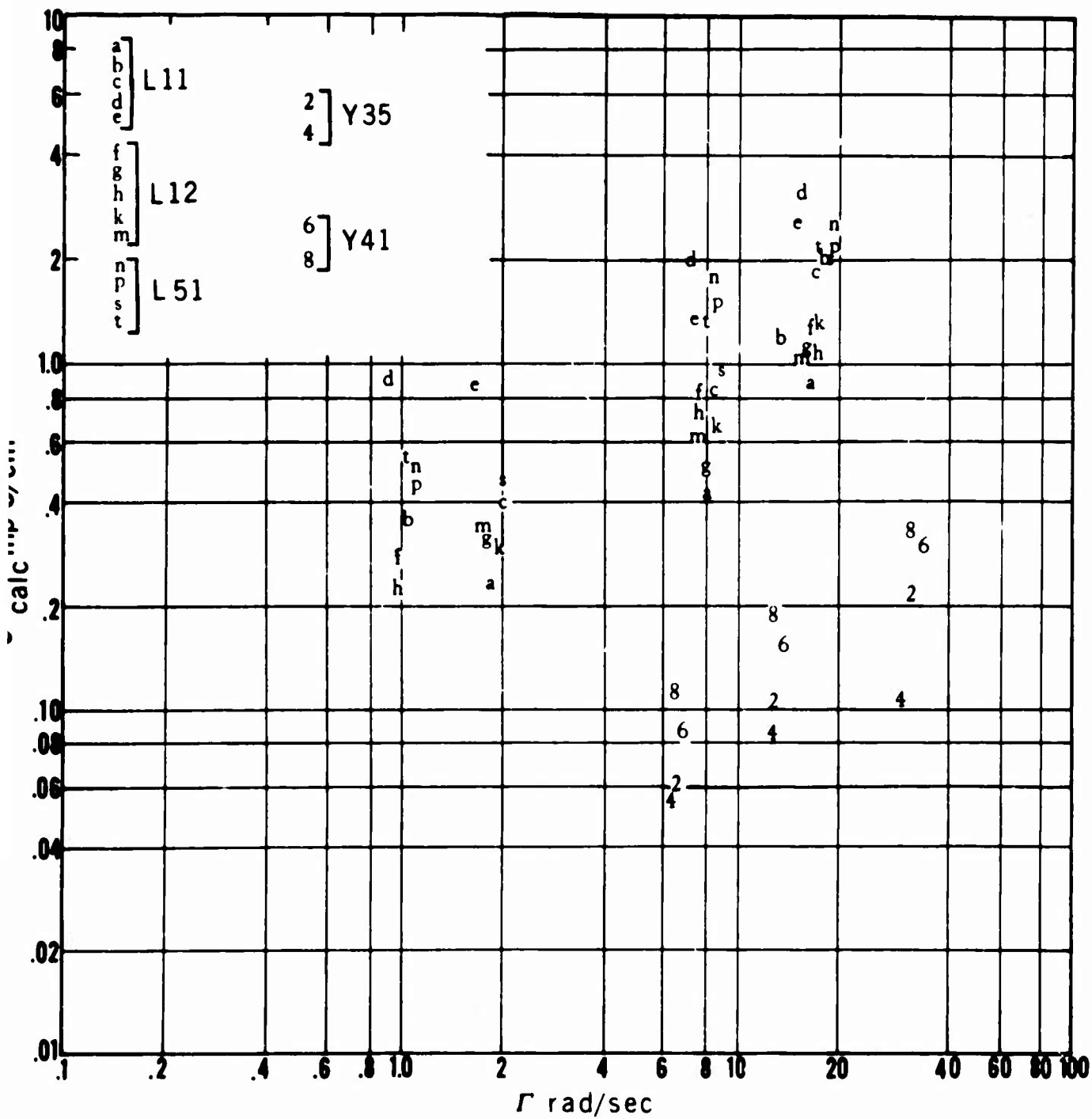


Figure 11. Total Observed Photoconductivity vs Absorbed Dose Rate for 10 Polyethylene and 4 Polystyrene Samples.

TABLE IV
POLYSTYRENE INTENSITY DATA, STEADY-STATE IRRADIATION STUDY

Sample	Γ rads/sec	Dose Mrads	G^* mpU/cm ²	I_o pA	σ^* calc. mpU/cm	Δ^* Γ
L51J07	1.08	3.05	18.6	-243	.502	0.58
↓	8.43	3.01	66.5	+44	1.80	↓
↓	19.3	2.94	94.7	+458	2.56	↓
L51M23	1.10	3.05	10.0	-163	.440	0.57
↓	8.48	3.01	33.8	+35.6	1.49	↓
↓	19.6	2.94	50.6	+64.9	2.23	↓
L51M23'	1.98	4.32	10.5	-103	.462	0.65
↓	8.74	4.22	21.9	-45.2	.964	↓
↓	18.4	4.27	47.9	-199	2.11	↓
L11N22'	1.84	4.30	4.39	-20.3	.233	0.58
↓	7.96	4.22	7.91	-24.0	.419	↓
↓	16.3	4.26	16.8	-69.5	.890	↓
L12N36	0.971	3.05	5.37	-80.2	.279	0.54
↓	7.53	3.01	16.3	-14.3	.848	↓
↓	16.6	2.94	25.1	+23.2	1.31	↓
L12N36'	1.78	4.30	5.99	-30.5	.311	0.55
↓	7.78	4.20	9.73	-14.5	.506	↓
↓	16.0	4.26	21.8	+311.	1.13	↓
L12N55	0.965	3.05	4.28	-59.2	.223	0.56
↓	7.46	3.01	13.7	+3.29	.712	↓
↓	16.4	2.94	20.8	+52.6	1.08	↓
L11020	1.03	3.05	4.40	-59.8	.348	0.57
↓	13.4	3.01	15.0	-5.34	1.19	↓
↓	18.1	2.94	26.5	+23.4	2.09	↓
L11020'	1.89	4.30	5.06	-21.8	.400	0.67
↓	8.39	4.21	10.8	-15.5	.853	↓
↓	17.2	4.26	23.4	-52.5	1.85	↓
L12017'	1.92	4.30	4.11	-9.75	.292	0.67
↓	8.43	4.20	9.52	-30.0	.676	↓
↓	17.5	4.28	18.7	-30.0	1.33	↓
L15053	1.02	3.05	6.97	-107.	.544	0.48
↓	7.64	3.01	17.1	-14.4	1.33	↓
↓	17.5	2.94	28.0	+30.2	2.18	↓
L11R01	0.916	3.05	3.84	-34.6	.899	↓
↓	7.03	3.01	8.80	-43.2	2.06	0.52
↓	15.5	2.94	13.2	-31.1	3.09	↓
L11R01'	1.66	4.24	3.71	-18.3	.868	0.47
↓	7.26	4.16	5.75	-64.5	1.35	↓
↓	14.9	4.21	11.1	-157	2.60	↓
L12R20	1.72	4.26	1.49	-1.88	.340	0.50
↓	7.46	4.18	2.73	-6.25	.622	↓
↓	15.5	4.23	4.65	-5.25	1.06	↓
Y41E09	6.73	1.73	7.01	-42.7	.0841	0.78
↓	13.3	2.48	14.1	-85.5	.169	↓
↓	35.1	2.28	25.9	-153	.311	↓
Y35H07	6.39	1.73	3.14	-35.0	.0628	0.76
↓	12.7	2.43	5.32	-52.5	.106	↓
↓	32.4	2.25	10.8	-119	.216	↓
Y35N03	6.26	1.73	0.972	-13.2	.0535	0.71
↓	12.3	2.58	1.56	-27.2	.0858	↓
↓	30.5	2.35	1.96	-71.3	.108	↓
Y41N11	6.53	1.73	2.11	-7.50	.110	0.70
↓	12.8	2.45	3.68	-28.5	.191	↓
↓	32.7	2.27	6.58	-76.5	.342	↓

This procedure provides only one point of a current-voltage characteristic. Calculation of G^* requires a second. In this case, the value of the momentum current determined from the characteristic for short-time readings was assumed to apply to the 90-minute case, to provide the second point. Values of the change of G^*/A , expressed as percentage of short-time value, are presented for 22 observations made on a total of 5 polyethylene and 9 polystyrene samples, in Figure 12.

D. Discussion. The principal accomplishment of this study is the development of a tool which, because of the linear dependence on inverse thickness shown in Figures 5 through 10, shows promise for quasi-dc investigations of the interiors of organic insulating materials. This tool is not simple to use, and much remains to be done in refining it, in establishing the underlying mechanisms, and in determining the limits of its exploitability. Nevertheless, its development is a significant event, and constitutes at least a minor breakthrough in the field of measurement technology whose development is vital to understanding this particular class of materials.

Certain features of this tool are evident from the work of this study. That some sort of surface effects exist is clear from the depressed values of conductance noted for samples in the few-mil region. These appear to be quite shallow, however, judging from the linearity observed to thicknesses as small as 10 mils in polyethylene, and 5 miles in polystyrene. These data suggest an upper limit for the surface effect layer on the order of a tenth of a mil.

The 90-minute data can shed some light on the nature of the surface layer, via negative inference based on the slow transient photocurrent. If the latter were generated by some mechanism distributed uniformly throughout the sample volume, both the 7-minute and the 90-minute conductances would be inversely proportional to sample thickness. Hence their differences also would display this dependence. If it were generated by some sort of surface leakage process, these differences would be independent of thickness. And finally,

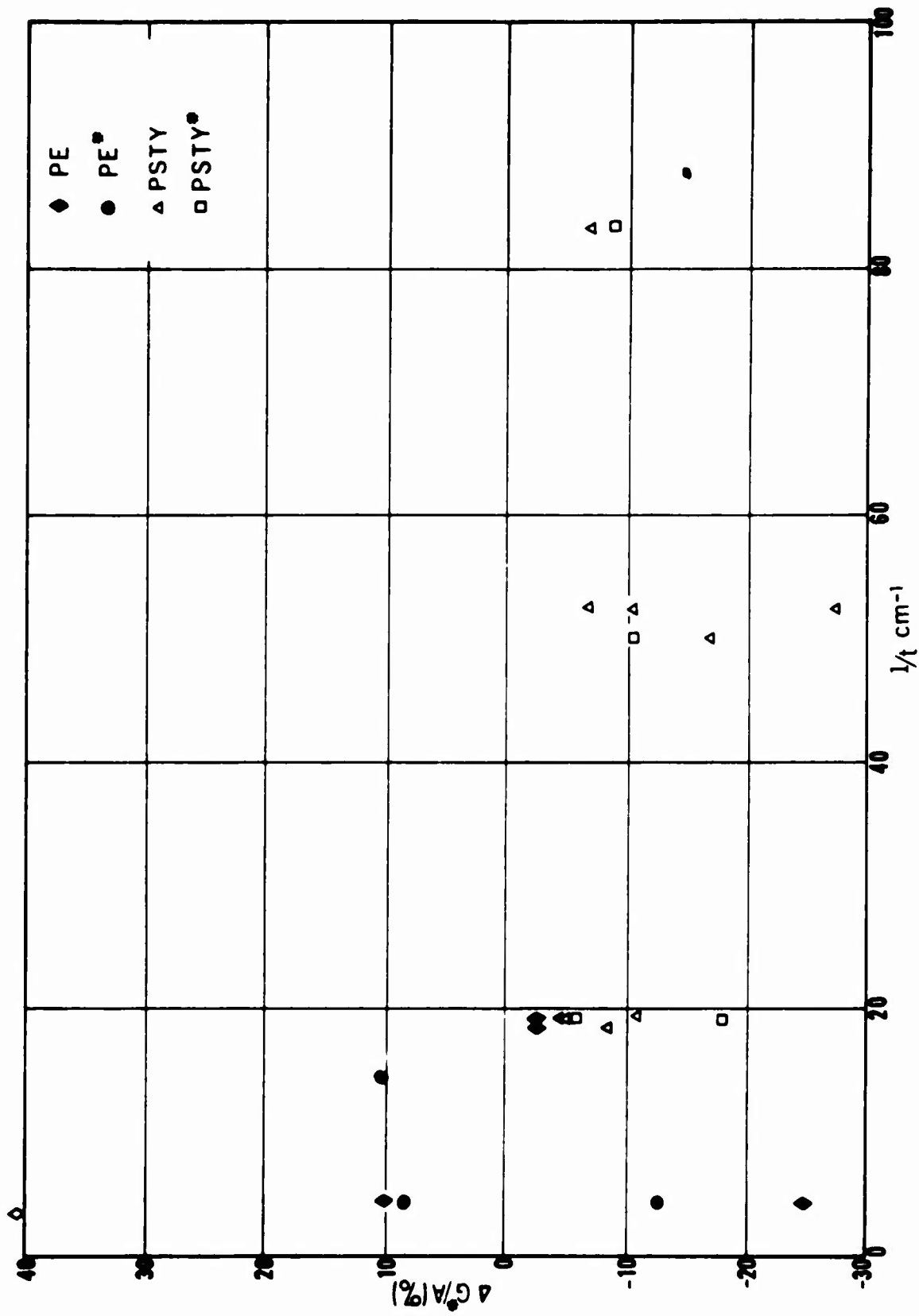


Figure 12. Percentage Change in Total Observed Photoconductance per Unit Electrode Area vs Inverse of Sample Thickness. The change is calculated as the difference between values taken from observations made 7-1 2 minutes after changing the applied voltage, and those taken from 1- to 1-1/2 hours after changing voltage.

if the slow transient corresponded to the gradual cutoff imposed by a slowly-charging blocking capacitance, the relationship between conductance and inverse sample thickness would be greater than linear.

Referring to Figure 12, the linear dependence corresponding to the volume-distributed hypothesis described above would produce a single value for percentage of conductance, constant with inverse thickness. In this case, Figure 12 should be a horizontal straight line. The surface-leakage hypothesis would correspond to a decreasing percentage change as sample thickness decreased, producing a curve which would start below the abscissa in Figure 12, and tend to rise toward it, going from left to right. The blocking layer hypothesis would produce percentage changes which would be small for thick samples and larger for thin ones, thus giving a curve in Figure 12 that sloped away from the abscissa, going from left to right.

As can be seen, the polyethylene data of Figure 12 leave much to be desired in the line of precision. The fact that half of these indicate that conductance increased with time suggests quite strongly that a significant parameter escaped adequate control during the experiment. Consequently, no firm conclusions are justified here, and the best that can be done is to note that there is no consistent evidence of any specific trend.

The precision evidenced by the polystyrene data, while no occasion for great joy, is significantly greater than that displayed by the polyethylene data, which fact hints that the variant parameter may be related to some property of the material. Unfortunately, the increase in precision is not great enough to permit a completely unambiguous assignment of behavior to one of the three hypotheses discussed above. However, the polystyrene points suggest that the surface leakage model is the most unlikely. To the author's eye, they appear to favor slightly the volume distributed hypothesis, rather than the blocking layer. It must be admitted, however, that

a downward-sloping curve could be fitted to the points with no great difficulty. Consequently, distinguishing between the blocking layer and the volume distributed hypotheses must await further data. These inferences permit a tentative conclusion that the surface layer is not likely to be a conducting layer associated with the slow transients. It may be a blocking layer having a very long time constant, or it may have negligible overall effect on the currents observed.

The inverse proportionality found between thickness and total conductance in this study suggests rather strongly that the individual mechanisms by which the major components are generated are distributed throughout the sample volume. The number and relative strengths of these significant, volume-distributed components remains to be determined. In particular, whether the normal steady-state photo-current comprises a significant portion of the observed current remains unknown. Future investigations may be able to answer this question. For the moment, however, deductions regarding conduction mechanisms must be limited to those not resting upon assumption of steady-state conditions.

Fortunately, a number of qualitative and semi-quantitative comparisons do not require the steady state, but can be made on the basis of transients, providing they are made between equivalent points along those transients. For example, the effect of impurity atoms, according to the band model, is to introduce deep trapping states into the forbidden band. If these states are deep enough, and present in sufficient concentrations, they may dominate the carrier recombination processes, thereby determining the rate at which carriers are removed from conducting states and thus influencing the instantaneous concentration of photocurrent carriers. Such a process would not necessarily require the steady state, to be detected, since the influence of the traps would be exerted throughout all time, until the concentration of conduction-state carriers became large with respect to the trap concentration.

According to this hypothesis, variations in impurity atom concentration should produce corresponding fluctuations in the concentration of conduction-state carriers, and hence in observed conductivity. If this model were to apply to the materials studied here, observed conductivity should change as impurity atom concentration changed.

In this study, materials were selected from different fabricators, located in different parts of the country, with this model in mind. In view of the number and crudity of the different materials used as plasticizers and fillers, (e.g., sawdust) which of economic necessity are obtained from local sources of supply, the probability of the products of these fabricators being equivalent in impurity atom concentrations, particularly of the nonorganic variety, approaches the vanishing point. Consequently the observed insensitivity of our conductances to fabricator provides strong evidence that the significant components of these conductances do not depend in any appreciable fashion upon the processes dominated by impurity atoms. Thus the hypothesis of impurity-dominated recombination processes apparently is not applicable to our cases.

Another model which might apply to insulators is similar to the trapping model described for impurity atoms above. In this case, however, the traps are associated with molecular irregularities rather than with impurity atoms. In this view, conduction should be sensitive to the concentration of defects.

The examination of pile-bombarded material was undertaken with this model in mind. The primary interaction between incident neutrons and target molecules displaces atoms from their original sites, rupturing intramolecular bonds and introducing structural defects into the "lattice". These new irregularities in molecular geometry, given adequate concentrations, should produce appreciable changes in conductivity. The fact that 30% reductions were seen suggests that this model may indeed apply. The fact that the reductions

seen were fairly small, suggests that the preirradiation concentration of defects was large, i.e., comparable to that produced by about 5 Mrad of neutron dose.

Unfortunately the sequence of chemical events in these materials during and after irradiation is sufficiently complicated, and our ignorance of the details is sufficiently extensive that the number of defects produced as a result of a given amount of pile bombardment cannot be calculated. Thus we have no quantitative measure of the defect concentrations involved. We note, however, that significant changes in mechanical properties begin to appear at around 10 Mrads in polyethylene, so that the concentrations of defects produced by our pile bombardment probably approached a substantial fraction of those required to change the principal "lattice" structure of this material. This implies that the original defects were not just occasional "mistakes" in the base structure of the material, but rather correspond to features of that structure which are essential in character.

In polystyrene the mechanical properties begin to show appreciable change at about 1,000 Mrads, so a similar line of semiquantitative reasoning cannot be applied on the basis of our data.

A tentative finding of some interest is the tendency of the parameter Δ_T^* toward substantially lower values than those reported previously in studies where attempts to avoid the influence of transient components were made. The extent of this tendency depends somewhat upon the unknown degree to which our data, particularly at the lowest dose rates, were influenced by the dark components. It will be noted that for polyethylene there is a distinct tendency of the lower dose-rate points in Figure 11 toward higher values than would be expected by extrapolation from the higher dose-rate points; i.e., the data for each sample tend to be concave upward. This tendency seems fairly small however, and does not appear at first glance to be large enough to account for the rather substantial difference between our observed values and the previously values of Δ_T^* .

Assuming that a quantitative investigation of this point supported our "eyeball" estimation, this observation suggests that the charge carriers responsible for the transient components are removed from their conduction states by what is essentially a so-called "bimolecular" process, and that in the case of polyethylene, where Δ_T^* approached the ideal bimolecular value of 0.5 rather closely, most of the total observed photocurrent was generated by mechanisms of this type.

Present understanding of the conductive mechanisms underlying the significant components of the observed conductivity is quite limited, as is indicated by the preceding discussion. The observed dependence on sample thickness indicates that they are distributed more or less uniformly throughout the sample volume. The fact that this dependence remains after 90 minutes of slow transient decay indicates that any blocking layer is of little influence, at least over the first half hour or so after changing the applied voltage. Hence, if such a layer exists at all, it must have a very long time constant. The fabricator comparisons indicate that impurity concentrations do not dominate the conduction processes, while the pile bombardment comparisons provide some mild evidence for defect trapping. Further illumination awaits further study.

SECTION II

TRANSIENT CONDUCTION DURING PULSED ELECTRON IRRADIATION

A. INTRODUCTION

This section of this report describes an investigation conducted with the AFCRL linear accelerator, which provided short, intense pulses of high-energy electrons, using a charge integration technique to measure the conductive properties of certain organic insulators. If one adopts the simple, one-carrier model described under background remarks in the preceding section, this type of study should be well suited to examination of the prompt component, i.e., the prompt component should be large relative to the delayed, and the charge transported through the sample by a single pulse should provide a measure of the sample's prompt conductivity. Comparison of this conductivity between various samples then should be a relatively simple matter, requiring only a single number from each sample, viz, the change of voltage across the precharged sample resulting from bombardment by a standard pulse of electrons. If leakage across the sample without radiation is small enough, and if a measuring device with high-quality insulation is used, both measurement and data analysis should be fast, simple operations, and comparisons of large numbers of samples should be feasible.

B. EXPERIMENTAL DETAILS

1. Samples. A total of 31 samples was prepared for exposure to 10-MeV electron bombardment from the AFCRL linear accelerator. The base material, supplier, and dimensions of each sample are given in Table V.

TABLE V.
SAMPLE DETAILS, PULSED ELECTRON STUDY

Sample	Mat'l	Fabricator	Nominal Thickness mils	$\frac{t}{m \times 10^{-5}}$	$\frac{A}{cm^2}$
V17N05	PVC	Union Carbide	20	52	14.1
V85N05	↓	Robeco	↓	50	↓
V95N01	↓	Scilon	↓	54	↓
V95N31	↓	↓	↓	52	↓
Y13H06 ^x	PSTY*	A&E	7½	19	↓
Y13H09	PSTY	↓	↓	↓	↓
Y13H16	PSTY*	↓	↓	↓	↓
Y13H19	PSTY	↓	↓	↓	↓
Y35H02 ^x	PSTY*	Monsanto	↓	↓	↓
Y35H05	PSTY	↓	↓	20	↓
Y35H12	PSTY*	↓	↓	19	↓
Y35H15	PSTY	↓	↓	20	↓
Y41H03	↓	Davis	↓	↓	↓
Y41H04	PSTY*	↓	↓	19	↓
Y41H13 ^h	↓	↓	↓	21	↓
Y41H23	↓	↓	↓	20	↓
Y41H24	PSTY*	↓	↓	19	↓
L11N09 ^h	PE	Alchem	20	52	↓
L11N09 ^o	↓	↓	↓	↓	↓
L11009	↓	↓	30	78	↓
L11010	PE*	↓	↓	77	↓
L11039	PE	↓	↓	78	↓
L11040	PE*	↓	↓	77	↓
L12010	↓	Allied Resinous	↓	74	↓
L12029	PE	↓	↓	70	↓
L12040	PE*	↓	↓	74	↓
L12059	PE	↓	↓	70	↓
L51036	PE*	Ethyl Visqueen	↓	79	↓
L51039	PE	↓	↓	78	↓
L51096	PE*	↓	↓	79	↓
L51099	PE	↓	↓	78	↓

x ~ samples used for Dynamic Observations

h ~ samples having very thin fore and aft plates

o ~ sample having electrodes painted directly on sample

PVC = polyvinylchloride

PSTY = polystyrene

PE = polyethylene

PSTY* = pile bombarded polystyrene

PE* = pile bombarded polyethylene

A&E = A&E Plastik Pak, Los Angeles, Calif.

Alchem = Alchem Inc., Los Angeles, Calif.

Allied Resinous = Allied Resinous Products, Conneaut, Ohio

Davis = Joseph Davis Plastic Co., Kearny, N. J.

Ethyl Visqueen = Ethyl Corp, Visqueen Div., Baton Rouge, La.

Monsanto = Monsanto Co., St. Louis, Mo.

Robeco = Robeco Chem. Inc., Japan

Seilon = Seilon, Inc., Plastics Div., Newcomerstown, Ohio

Union Carbide = Union Carbide Plastics Div., Texas City, Texas
or S. Charleston, S. C.

Sample construction is shown in Figure 13. The basic structure is that of a three-electrode, plane-parallel-plate capacitor. Two pieces of the material of interest, with an electrode and guard ring in between, are pressed together between two exterior electrodes, the array resembling a double-decker sandwich. The two exterior electrodes in turn are pressed together by two PMMA plates, which are held together by four steel screws located well outside the incident electron beam.

The irradiation location was chosen as about 6 cm from the linac exit port, where the principal beam has a cross-sectional diameter of about 2 cm. Electrodes are circular, with a diameter of 3 cm. Electrodes and guard rings all are of colloidal graphite, deposited from a hand-painted suspension. The exterior electrodes were painted directly on the PMMA front and rear plates, while the central electrode and guard ring were painted on a central spacer.

Owing to the unidirectional character of the linac beam, the PMMA spacers of the steady-state irradiation study were deemed too thick for this study, and a new design was generated. In this new design, the connecting leads for the central electrode and the guard ring are encased between two sheets of the spacer material, which are fused around the leads. Electrodes and guard rings are painted on the outer surfaces of the fused spacer, making contact with the leads via pre-drilled holes in the appropriate locations. The total thickness of the central spacer achieved by this procedure is on the order of 40 mils.

In each case the spacer was made from the same base material as the material of interest, i.e., polyethylene for a polyethylene sample, polystyrene for a polystyrene sample, and polyvinylchloride (PVC) for a PVC sample. For PVC the abutting faces of the two sheets were wet with methyl ethyl ketone and clamped until dry between two sheets of silicone rubber in a vise, at room temperature. For polystyrene the same technique sufficed, except that it was necessary to use trichloroethylene instead of MEK as the solvent. No satisfactory solvent was found for the

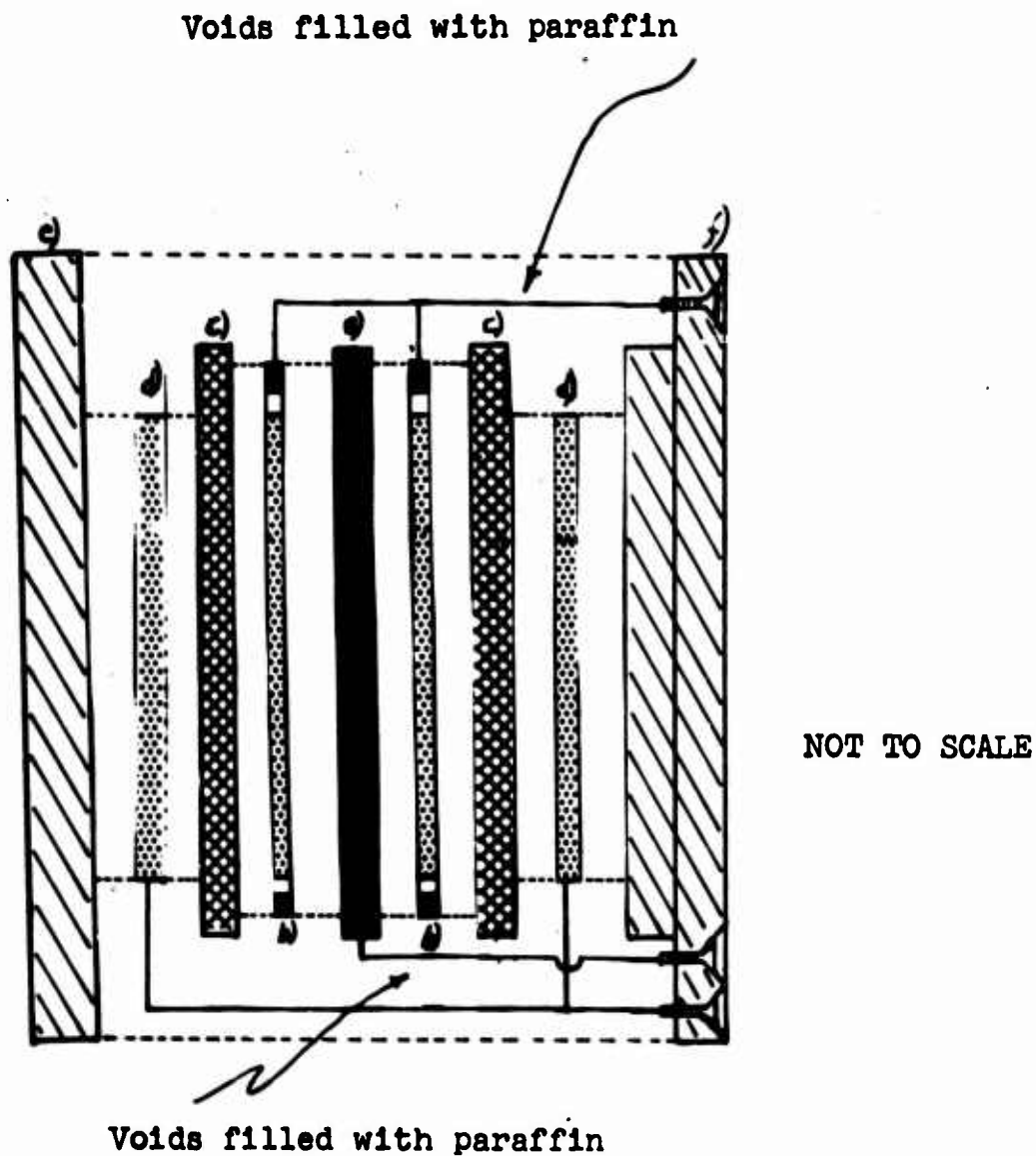


Figure 13. Pulsed Electron Study Sample Details
(Exploded View)

- a) central spacer;
- b) center electrodes and guard rings;
- c) sample;
- d) outer electrodes;
- e) front plate;
- f) back plate.

After assembly (assembly screws not shown) the regions between the dotted lines were filled with paraffin.

polyethylene case, and it was necessary to develop a heat-fusing technique.

The successful technique required the preheating of a weight and two sheets of silicone rubber to a temperature estimated to be in the range of 90°C, using a standard laboratory hot plate. The spacer components were preassembled at room temperature and placed between the rubber sheets, and the weight was placed on top. After an empirically determined time, on the order of 12 or 15 seconds, the weight was removed and the spacer assembly and the rubber sheets were transferred to a room-temperature vise, where they were clamped together until cool. After cooling, the guard ring was painted up onto the corresponding lead, to provide additional assurance of contact.

Electrical leads are brought out through three flat-headed brass screws, countersunk in the rear PMMA plate. The two exterior electrodes were connected to the same screw, by means of graphite ears painted on the PMMA plates, extending from the electrode proper to the screw holes. After assembly, and before potting, additional graphite was painted on, assuring contact to the screw. The central electrode and guard-ring wires were soldered directly to the appropriate screws.

After assembly, the samples were potted in paraffin by the same technique used in the Co⁶⁰ study. Excess paraffin was whittled away by hand, and the entire sample structure, except for the walls of the counter-sunk holes containing the electrical contacts, was coated with the commercial silver conductive paint.

During irradiation, which was performed on only one sample at a time, the sample was held on a connecting mount by two machine screws, located outside the region bombarded by the beam. Three contact pins extend beyond the front of the mount,

making electrical connection to the three flat-headed brass screws of the sample when the two mounting screws are brought up hand-snug. Two of these pins are the center pins of commercial, panel-mounted cable connectors^{13,14}, which provide cable connections to the measuring apparatus. The third pin is a set screw whose head is buried in the mount by a PMMA glue, made by dissolving PMMA scraps in trichlorethylene. This pin, which connects to the sample's guard ring, is also connected to the inner shield connection of the triaxial cable fitting via a wire, buried in a groove cut in the front face of the mount by a strip of PMMA glued in with the PMMA glue.

It should be noted that the guard electrode configuration is imperfect in the region between central spacer and the triaxial connector. Since this volume lies somewhat outside the region traversed by the principal portion of the electron beam, it is felt that this flaw is not likely to be significant. The effect of this imperfection has yet to be tested experimentally, however, and future designs might be well advised to include means for avoiding or mitigating the effects of this flaw.

The entire mount, except for the recessed areas from which the three pins protruded, was coated with the conductive paint, which also was painted up onto the outer portions of the two panel-mount connectors. Electrical contact between this paint and that on the sample was ensured by two small springs, mounted so as to be under compression while the sample was in the mounted position.

A commercial silicone stop-cock grease¹⁵ was used for potting the space around the three pin-screwhead contacts, to avoid ionized air leakage paths. This grease also was used to fill the air spaces in the commercial connectors before the cables were attached, for the same purpose. The grease surrounding the three pins provided the only surfaces which might collect and hold stray ions,

which might affect the measurements. For this experiment the danger seemed negligible because of the small area of conductor thus exposed. For a more refined experiment, however, the extra effort required to coat these surfaces with conductive paint might be justified.

A second pair of holes, threaded to accommodate machine screws, were located in the mount outside the area covered by a sample. Long screws attached here could extend forward past the sample, to permit mounting of additional components between sample and beam port. A number of unpainted sheets of PMMA, of various thicknesses, were cut and drilled for mounting on these screws, to permit selection of the part of the specific ionization curve corresponding to the sample location.

Provision for attachment of an additional capacitor, in electrical parallel with the sample but in an out-of-beam location, was made in a second mount, which resembled the first mount in all other important respects. The second mount was not used in this study, but is available for use in future studies, if desired.

During irradiation, the sample and mount were supported by a standard ring-stand and clamp, the clamp being fixed around the outside of the rather large triaxial cable connector. The weight of the array, plus the forces exerted by the cables, exerted just enough torque on the ring stand that it was advisable to weight the base of the stand down with a lead brick. With this arrangement it was possible to raise the sample well above the beam for checking cable effects with ease, and minor adjustments of position and orientation could be made easily.

2. Radiation and Dosimetry. The radiation used in this study consisted of a series of pulses of 10-MeV electrons, supplied by AFCRL linear accelerator, located at Hanscom Field, Massachusetts. The standard pulse rate for this work had a peak current of about 4 mA, and a length of about $1/2$ μ sec. Pulses were repeated at

repetition rates ranging from one each 5 seconds to about 10 per second, with a rate of one per second being used for most of the work. The central beam port was used; i.e., the electrons travelled a straight path, and were not acted upon by a beam-bending magnet.

Direct dosimetry was not attempted. Pulses were monitored with a Faraday "cup", in the form of a flat plate, located about 18 cm from the beam port, i.e., about 12 cm behind the sample location. The current from this Faraday plate was observed with an oscilloscope. Photographs of the oscilloscope trace were made prior to and after each day's run, with the sample well out of the beam path, and at least once for each sample in its in-beam position. No attempt to determine energy spectrum of the beam was made.

3. Circuitry and Technique. The basic technique upon which this study was based involved a comparison of the amounts of charge transported through various samples under identical values of environmental factors, principally applied voltage, temperature, and radiation. Given the high degree of reproducibility of radiation pulses obtainable with the linac, this can be done simply by observing the voltage on an isolated sample before and after exposure to a pulse, or a fixed number of pulses, the resulting change of voltage being a measure of the charge transported. The circuitry chosen to do this is shown in Figure 14.

In essence, this circuit consists of the capacitor sample, C_X , in series with a battery and a measuring capacitor, C_M . A charging switch, S, and a voltage-measuring device, are placed in parallel with C_M . An observation begins with S being closed long enough to charge C_X up to the battery voltage. S is then opened. Any subsequent change in V_X , e.g., a discharge during irradiation, appears as a complementary change in V_M , since the sum of V_X and V_M must equal the battery voltage*. A measured change in V_M then provides a measure of the change in V_X , and hence of the charge transported across C_X .

* Achievement of steady-state conditions is assumed throughout.

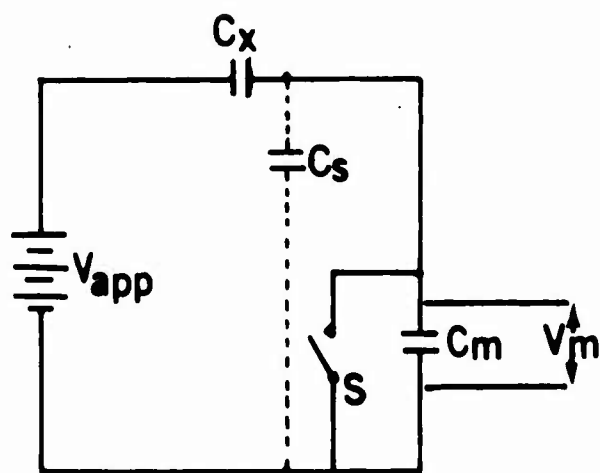


Figure 14. Measuring Circuit, Pulsed Electron Study

A commercial electrometer¹⁶, whose input circuit provided both S and C_M , was used to measure V_M . The battery box used in the Co^{60} study served as the charging battery. Connection between the battery box and the exterior electrode connector on the sample mount was provided by a coaxial cable¹⁷, while the electrometer was connected to the central electrode and guard ring through a triaxial cable¹⁸. This arrangement permitted use of the electrometer in its "fast" mode, in which the triax inner shield is driven to the same potential as the center conductor by the amplifier. This reduces to negligible size the effect of cable capacitance, which otherwise would appear as stray capacitance, C_S , paralleling C_M , thereby reducing system sensitivity. The electrometer output was recorded on a commercially available, strip-chart recorder¹⁹.

Preliminary observations indicated that transients associated with changes in applied voltage are appreciable for pulsed electron irradiation, as well as for steady-state photon bombardment. Consequently, the measurement technique developed for this study bore considerable resemblance to that of the Co^{60} study. First the sample was irradiated with the voltage of interest applied, then with the negative of that voltage applied, and finally, with the voltage of interest again applied. In some cases the frequency of pulse repetition was varied, and in others irradiation was interrupted for short periods to observe thermally activated processes. Most observations, however, were made under conditions which rather closely paralleled those of the steady-state irradiation study.

C. OBSERVATIONS

Owing to the inapplicability of the simple measurement and analysis techniques originally planned, the effort devoted to this study was expended primarily in developing more appropriate techniques.

Such a measurement technique has been developed, and a limited number of room-temperature measurements which appear suitable for quantitative analysis have been made. Data have been taken for seven polyethylene samples, six polystyrene samples, and three PVC samples.

The technique for quantitative analysis has been partially developed, but has not yet been proven out. Consequently it will not be possible to provide a quantitative analysis of data in this report. Certain qualitative and semiquantitative observations have been made, however, which are of some interest. These are now presented.

1. Momentum Transfer. We note that a "momentum transfer" component, i.e., a transfer of charge when the initial applied voltage was zero, was appreciable. In all cases save one, which was of questionable reliability on other grounds, the sense of the momentum transfer was that of accumulation of electrons on the central electrode.

In this work, the voltage induced on a standard sample by a standard pulse of 10-MeV electrons was on the order of a few tenths of a volt. In most cases repeated pulsing produced additional momentum transfers of about the same size, until a total induced voltage equal to the maximum permitted by the electrometer used (10 volts) was achieved. At this point it was necessary to close switch S, in order to protect the electrometer from over-voltages, and the observation necessarily was terminated. Reopening switch S then produced a duplicate of the preceding observations, with occasional minor variations. A tracing of a typical data record for each material, displaying the momentum transfer, is given in Figure 15.

Occasionally the first pulse produced an apparent momentum transfer which was opposite in sign to, and somewhat larger than, those described above as the normal case. The reasons for this behavior

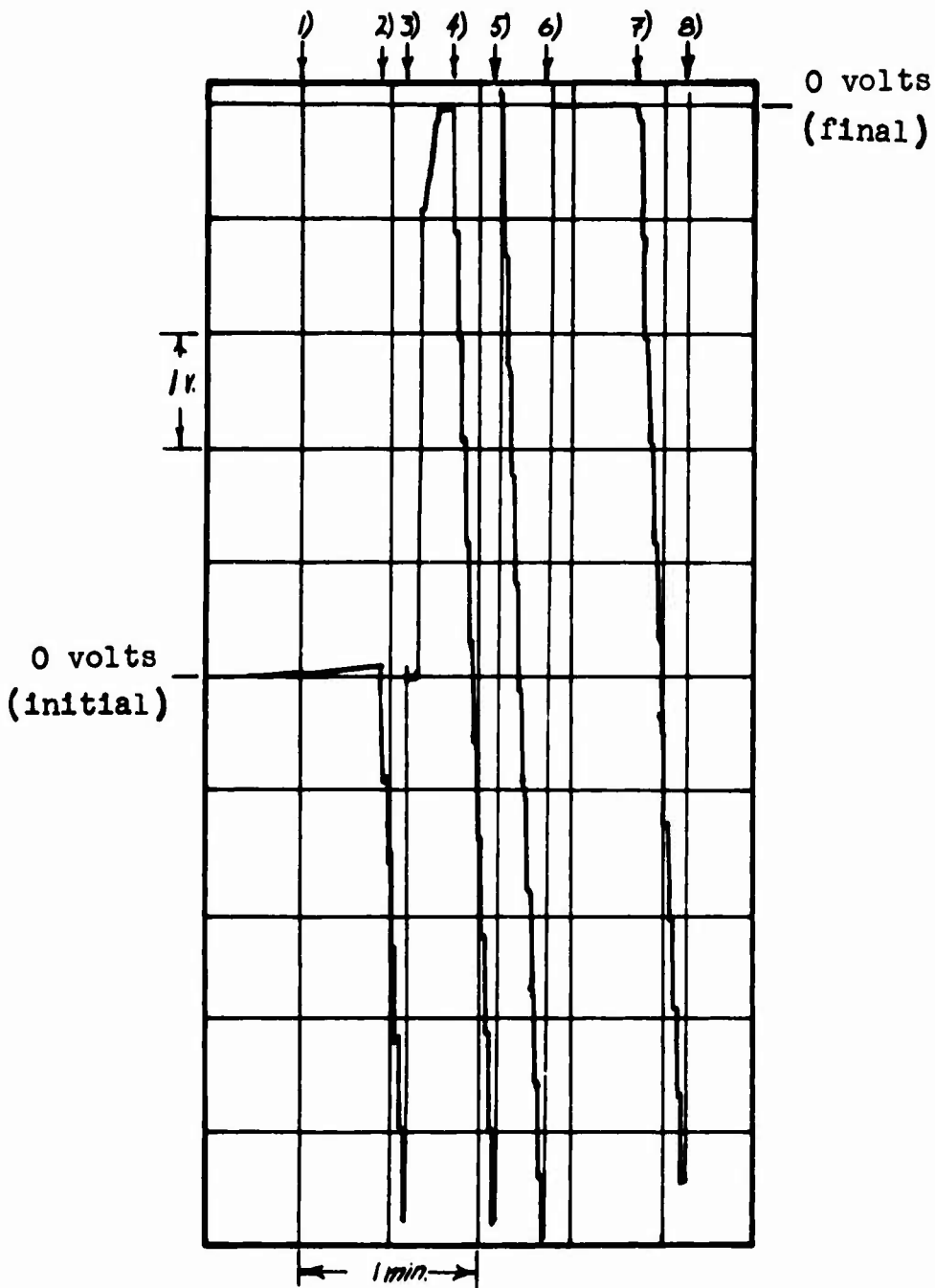
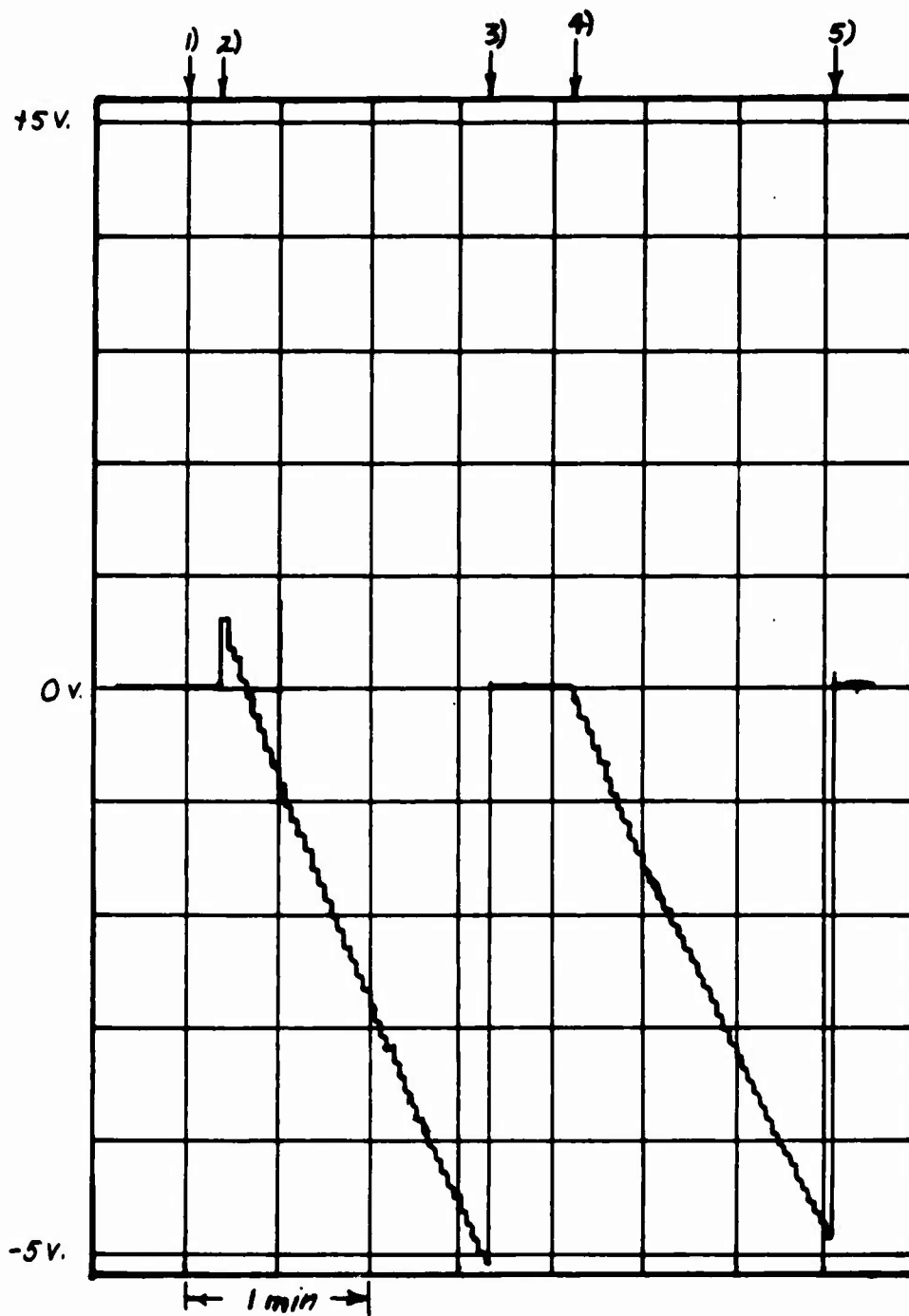


Figure 15. Pulsed Electron Study Raw Data Tracings
Displaying Momentum Transfer Component.

- a) Sample L12040 (pile-bombarded polyethylene), initial applied voltage zero volts. Event sequence:
 1) Switch S opened; 2) linac beam started; 3) S closed and vertical scale zero moved to top line of chart;
 4) S reopened; 5) S closed momentarily; 6) S closed;
 7) S reopened; 8) S closed.



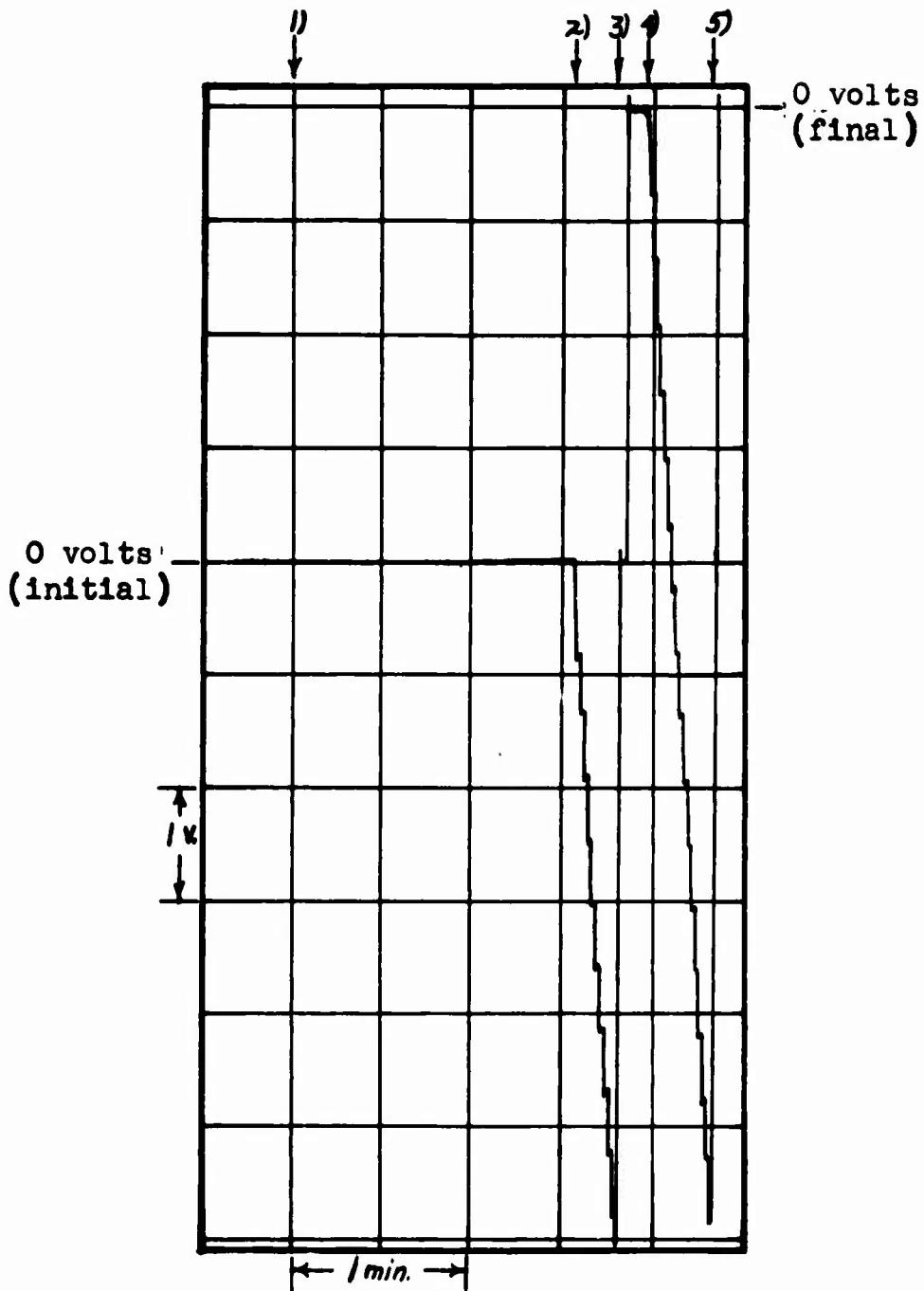
b) Sample Y35H02(PSTY*)

$V_{APP} = 0$ volts

Figure 15. Pulsed Electron Study Raw Data Tracings Displaying Momentum Transfer Component.

b) Sample Y35H02 (pile-bombarded polystyrene), initial applied voltage zero volts. Event sequence:

- 1) Switch S opened; 2) linac beam started; 3) S closed;
- 4) S reopened; 5) S closed.



c) Sample V17N05(PVC)

$V_{APP} = 0$ volts

Figure 15. Pulsed Electron Study Raw Data Tracings Displaying Momentum Transfer Component.

c) Sample V17N05 (polyvinylchloride), initial voltage zero volts. Event sequence: 1) S opened; 2) linac beam started; 3) S closed, vertical scale zero moved to top line of chart; 4) S reopened; 5) S closed.

Both of these components depended upon sample history, the prompt component displaying a considerably shorter memory than the delayed. Comparisons between two samples relying on either component require control of sample history to assure that historical differences will not invalidate the comparison.

a. Prompt Component Polarization Effects. So-called polarization effects were noted in the prompt components of all three materials, the charge per pulse transferred in the direction of the applied voltage decreasing as pulsing continued. In all three samples of PVC, and in both samples of pile-bombarded polystyrene, the prompt component decayed in a few minutes, i.e., after a few hundred pulses, to values negligible in comparison to the momentum component. In the four samples of non-pile-bombarded polystyrene, a slower decay was noted. Similar slow decay was observed in one sample each of polyethylene and pole-bombarded polyethylene. In the remaining polyethylene samples the charge transfer resulting from a single pulse was beyond the range of the electrometer, at the applied voltages used, and the presumed decay was too slow to be observed in the time available for observation.

In the case of positive applied voltage, i.e., when the exterior electrodes were made positive with respect to the central, the prompt component was opposed in direction to the momentum component. In the samples where the former became negligible with respect to the latter in a few hundred pulses, this led to the easily identified TURNAROUND POINT, where the two components were equal in magnitude and the raw data curve consequently exhibited a maximum. This point is especially convenient for comparing the performance of a single sample under various conditions, so long as the momentum transfer remains fixed, the observed parameter being the time, or perhaps the total dose required, to reach turnaround. Tracings of data records displaying the various polarization effects, including the turnaround point, are given in Figure 16.

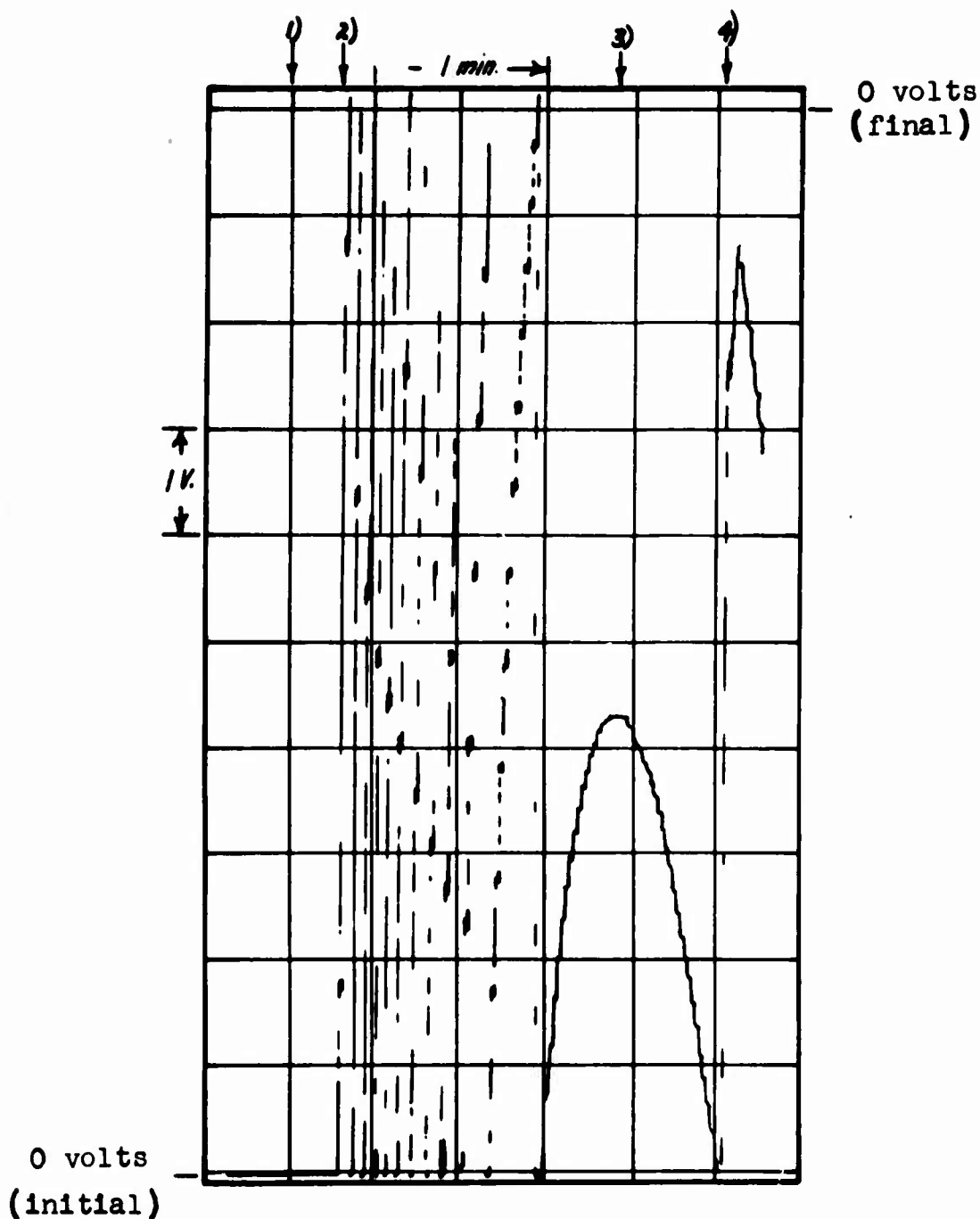


Figure 16. Pulsed Electron Study Raw Data Tracings Displaying Prompt Component, Prompt Component Polarization, and The Turnaround Point.

- a) Sample V85N05 (polyvinylchloride), initial applied voltage 465 volts. Event sequence: 1) 645 volts applied; 2) S opened and closed repeatedly to avoid off-scale voltages; 3) the turnaround point; 4) vertical scale zero moved to top line of chart.

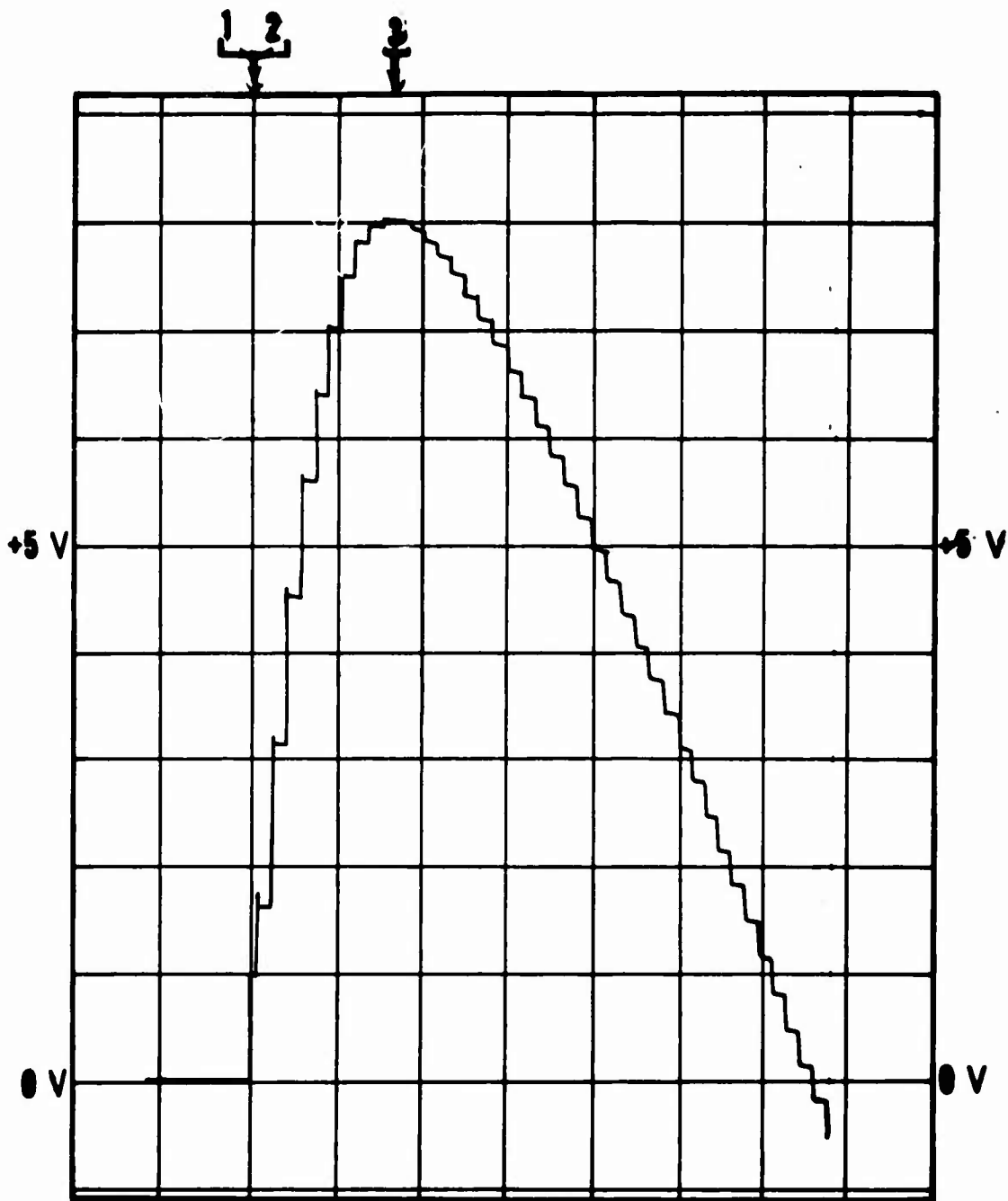


Figure 16. Pulsed Electron Study Raw Data Tracings Displaying Prompt Component, Prompt Component Polarization, and the Turnaround Point.

b) Sample Y35H02 (pile-bombarded polystyrene), initial applied voltage 23 volts. Event sequence: 1) voltage applied; 2) switch S opened; 3) turnaround point.

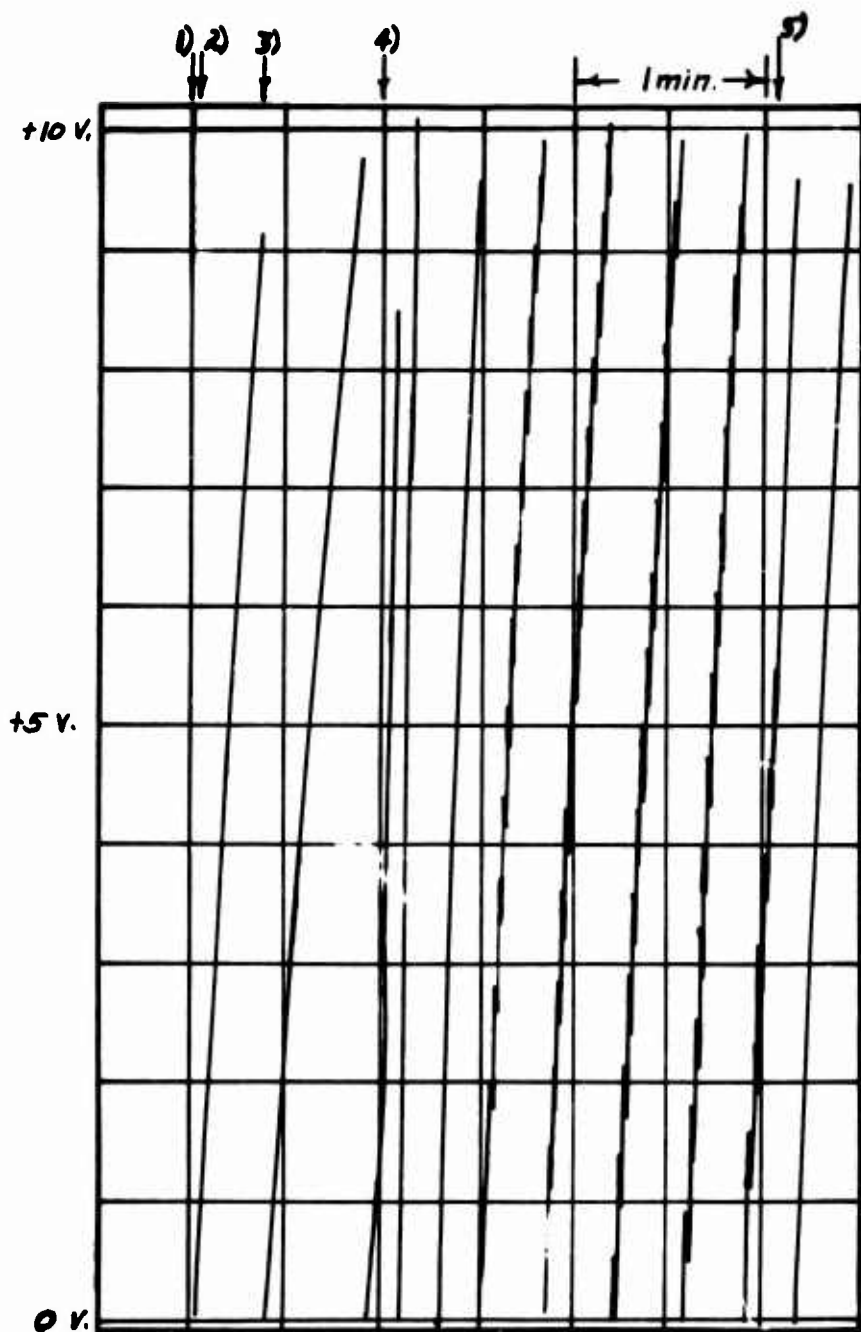


Figure 16. Pulsed Electron Study Raw Data Tracings Displaying Prompt Component, Prompt Component Polarization, and the Turnaround Point.

- c) Sample L51099 (polyethylene), initial applied voltage 233 volts. Event sequence: 1) voltage applied; 2) S opened; 3) S closed and reopened several times as needed to prevent off-scale voltages; 4) linac beam started; 5) linac beam turned off.

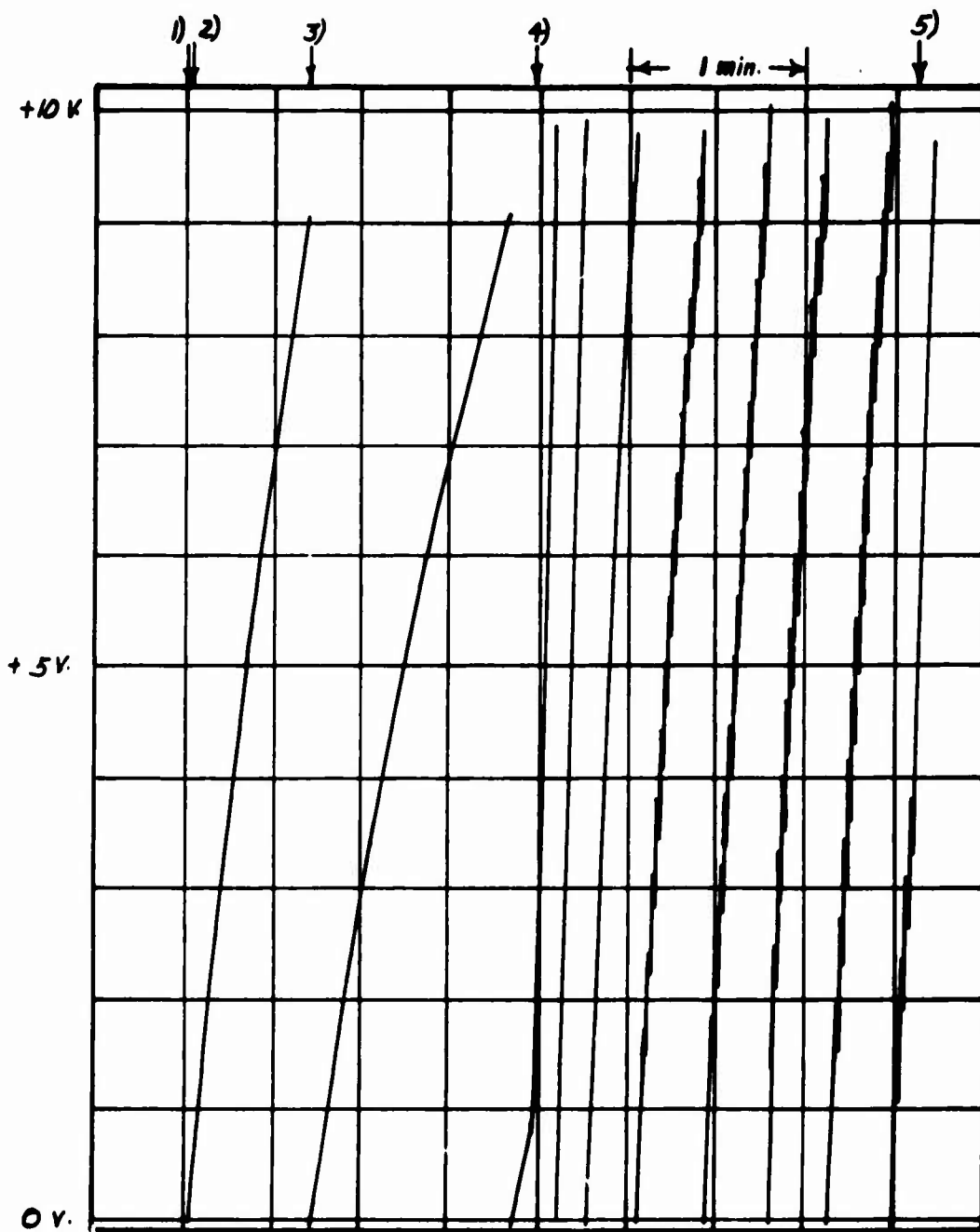


Figure 16. Pulsed Electron Study Raw Data Tracings Displaying Prompt Component, Prompt Component Polarization, and the Turnaround Point.

d) Sample L11040 (pile-bombarded polyethylene), initial applied voltage 233 volts. Event sequence: 1) voltage applied; 2) S opened; 3) S closed, reopened, as needed to avoid off-scale voltages; 4) linac beam started; 5) linac beam turned off.

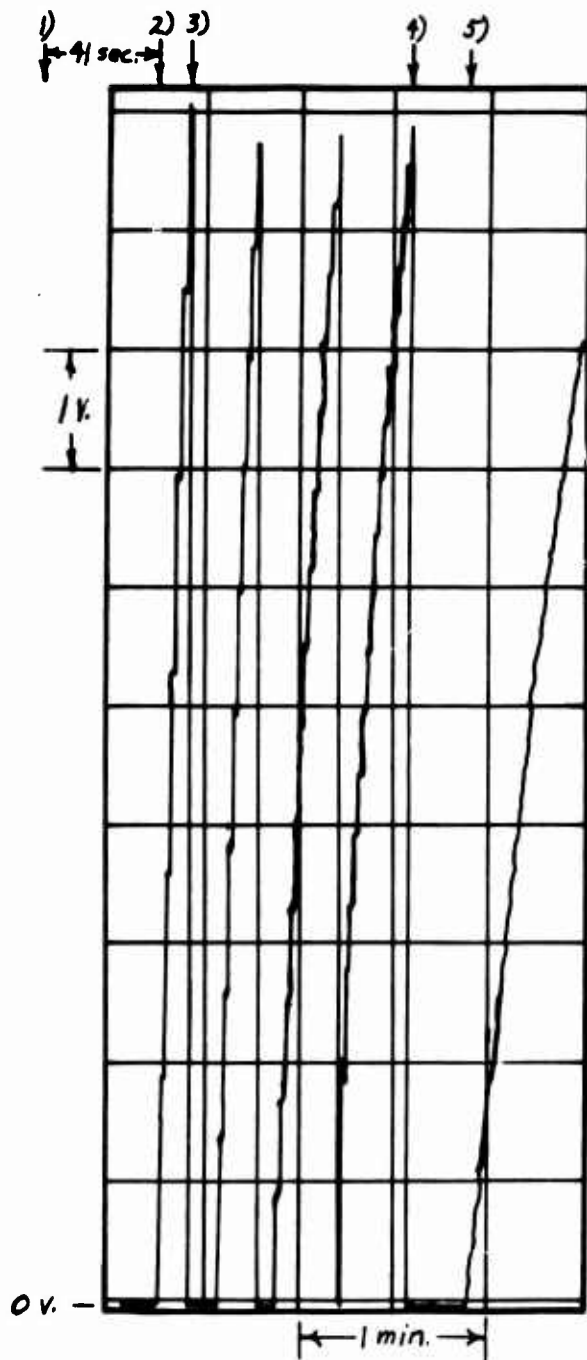


Figure 16. Pulsed Electron Study Raw Data Tracings Displaying Prompt Component, Prompt Component Polarization, and the Turnaround Point.

- e) Sample Y41H23 (polystyrene), initial applied voltage 233 volts. Event sequence: 1) voltage applied; 2) S opened; 3) S closed and reopened several times, as needed to prevent off-scale voltages; 4) S closed; 5) S reopened.

and the external conditions correlated with its appearance, have not been determined. It may well be a minor matter associated with linac operating procedures. In future work, however, some effort should be devoted to understanding this intermittent phenomenon.

The size of the momentum transfer was rather sensitive to the amount of material in the electron beam outside the electrodes. Introduction of an additional 3/16 inch of PMMA into the beam just in front of the sample increased the observed momentum transfer by a factor of about 4, while observations made on a sample whose PMMA plates were only about 20 mils thick showed the momentum transfer to be only about one-eighth that seen in a standard sample of the same material.

2. Voltage-Driven Components. Both prompt and delayed voltage-driven components were observed. According to the system described in the introduction to the first section of this report, the prompt component is that which takes place simultaneously with the pulse, while the delayed is that component observed after the pulse has passed. The response time of the recording apparatus used in this work was much larger than the pulse width, the latter being about $1/2 \mu\text{sec}$ and the former being such that the best resolution possible was on the order of a tenth of a second. To this extent, then, the prompt component discussed here differs from that of the ideal case by the contribution of the delayed component during the tenth second or so following the pulse. In most cases this difference will be small.

With this qualification in mind, we define the prompt component as that transfer of charge observed as discontinuous displacements of the recorder pen, each associated with a pulse of electrons, and each corrected by subtraction of the observed momentum component. The delayed component we define as that charge transfer observed between pulses, or following the last pulse of a series, with an applied voltage other than zero volts.

Both of these components depended upon sample history, the prompt component displaying a considerably shorter memory than the delayed. Comparisons between two samples relying on either component require control of sample history to assure that historical differences will not invalidate the comparison.

a. Prompt Component Polarization Effects. So-called polarization effects were noted in the prompt components of all three materials, the charge per pulse transferred in the direction of the applied voltage decreasing as pulsing continued. In all three samples of PVC, and in both samples of pile-bombarded polystyrene, the prompt component decayed in a few minutes, i.e., after a few hundred pulses, to values negligible in comparison to the momentum component. In the four samples of non-pile-bombarded polystyrene, a slower decay was noted. A similar slow decay was observed in one sample each of polyethylene and pile-bombarded polyethylene. In the remaining polyethylene samples the charge transfer resulting from a single pulse was beyond the range of the electrometer, at the applied voltages used, and the presumed decay was too slow to be observed in the time available for observation.

In the case of positive applied voltage, i.e. when the exterior electrodes were made positive with respect to the central, the prompt component was opposed in direction to the momentum component. In the samples where the former became negligible with respect to the latter in a few hundred pulses, this led to the easily identified TURNAROUND POINT, where the two components were equal in magnitude and the raw data curve consequently exhibited a maximum. This point is especially convenient for comparing the performances of a single sample under various conditions, so long as the momentum transfer remains fixed, the observed parameter being the time, or perhaps the total dose required, to reach turnaround. Tracings of data records displaying the various polarization effects, including the turnaround point, are given in Figure 6.

Prompt component turnaround was noted in all three samples of PVC and in both samples of pile-bombarded polystyrene. In one sample of non-pile-bombarded polystyrene, a turnaround was observed at a pulse repetition rate of 10 pps, but not at 1 pps. In all other cases other factors obscured the turnaround point.

One interesting phenomenon, namely so-called DELAYED POLARIZATION, was observed with the help of the turnaround point. It was noted in the case of the pile-bombarded polystyrene, and later in the case of PVC, that voltage changes made with the electron beam turned off produced no immediate charge transfer, the general behavior described above occurring only after the beam was turned on. Observations made first with irradiation starting about a second after changing the applied voltage, and second about 5 minutes after the voltage change, showed that the turnaround points came at equal times after the onset of irradiation; i.e., that the prompt component polarization processes did not proceed to any appreciable extent in the absence of radiation.

b. The Delayed Component. In PVC and in pile-bombarded polystyrene, the delayed component remained small with respect to the momentum component for all cases, including exposures lasting as long as 70 minutes, i.e., around 4000 pulses. In the non-pile-bombarded polystyrene samples, on the other hand, a few minutes exposure permitted the delayed component to build up to values which dominated both the prompt and the momentum components, when the pulse repetition rate was 1 pps. It seems reasonable to assume that in the latter case, the slow decay observed in the prompt component may well have reduced it to values small with respect to the momentum component, but that this was obscured by the relatively rapid growth of the delayed component.

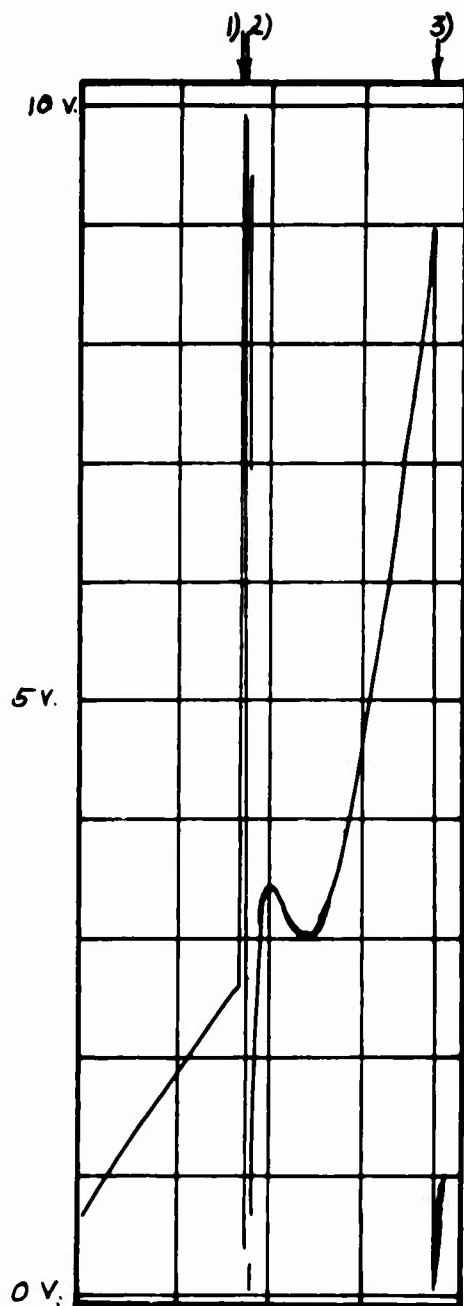
In one case a brief observation was made at 10 pps. The circumstances of this case were such that the raw data record displayed the turnaround point quite clearly. In addition, shortly after the maximum was passed, the delayed component became dominant, and

a second turnaround was recorded, this one producing a minimum point in the record. This event is shown in the tracing of Figure 17.

In the cases of polyethylene and pile-bombarded polyethylene, the dark component was comparatively large. This component was distinguishable from the delayed component only in that the former was observable prior to the first irradiation of the sample. In cases where only a few minutes elapsed between the termination of one exposure and the onset of the next, even this distinction became clouded, since the decay of the delayed component proceeded slowly.

The combined dark and delayed components became large enough to dominate the charge transfer in all polyethylene samples quite soon after irradiation started; i.e., within a few minutes. In two of the non-pile-bombarded samples, the combined components were large enough that at the small back-voltages generated during momentum transfer observations, the positive transfer between pulses was equal to the negative transfer produced by a single pulse. Thus in these two samples, a balanced condition occurred, with the data record oscillating about a value of approximately 7-1/2 volts. A third sample showed signs of approaching such a balance, but observations were terminated before the balance point was reached. Tracings of the two data records showing the balances observed are given in Figure 18.

c. Coincidental Prompt-Component Relaxation. In several cases the behavior of the delayed component was observed continuously over periods of several minutes. The procedure for doing this necessarily involved a period of continued exposure, during which the delayed component built up to an appreciable level. This was followed by the observation period, throughout which the beam was left off. The observation period generally was followed by another irradiation period, after which the delayed component decay could be observed again. In these cases the delayed component decreased rather slowly with time, the response times falling roughly in the range of minutes or tens of minutes.



Sample Y41H23 (PSTY)

$V_{APP} = +233$ volts

Figure 17. Pulsed Electron Study Raw Data Tracing Displaying Double Turnaround. Sample Y41H23 (polystyrene), initial applied voltage 233 volts, applied about 30 minutes before this observation was made. In that thirty minutes the linac beam was turned on and off several times. Event sequence: 1) Linac beam turned on, at ten pps; 2) S closed and reopened twice; 3) S closed, then reopened.

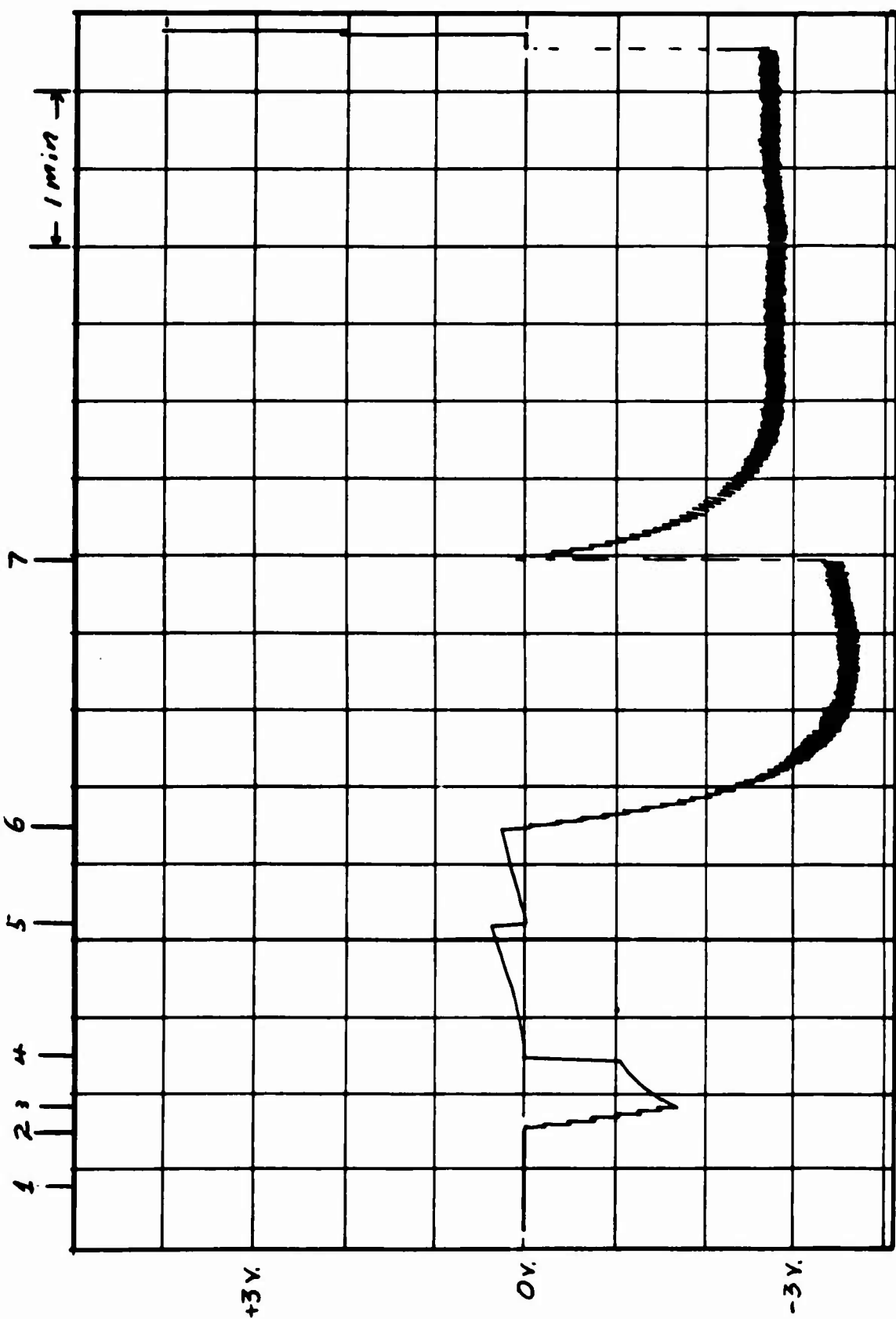


Figure 18. Pulsed Electron Study Raw Tracing Displaying Balance Between Delayed and Momentum Components.

a) Sample L11N090 (polyethylene), initial applied voltage 3 volts.
 Event sequence: 1) Switch S opened; 2) linac beam turned on; 3) linac beam turned off; 4) S closed, then opened; 5) repeat of 4); 6) linac beam turned on; 7) repeat of 4).

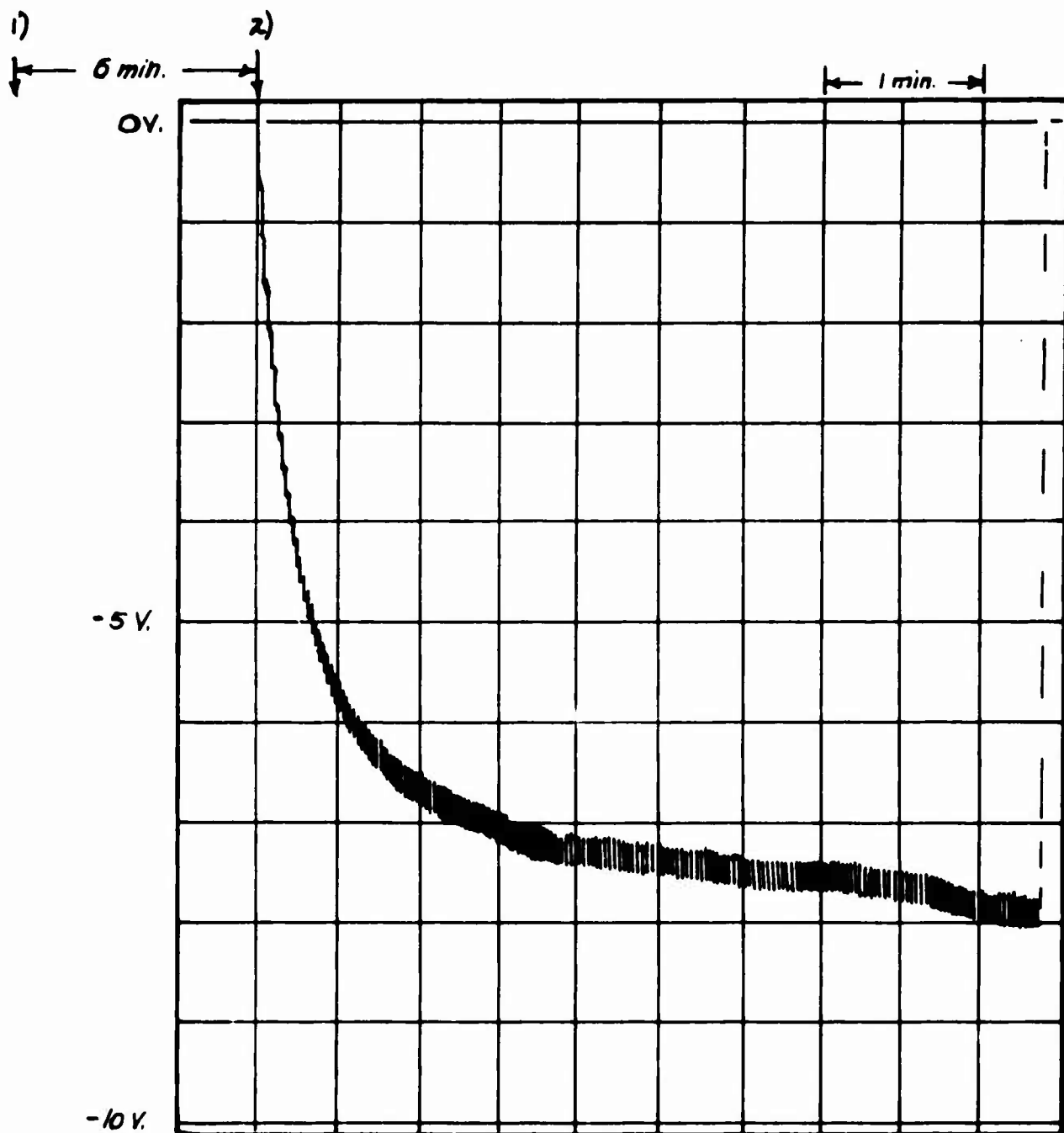


Figure 18. Pulsed Electron Study Raw Tracing Displaying Balance Between Delayed and Momentum Components.

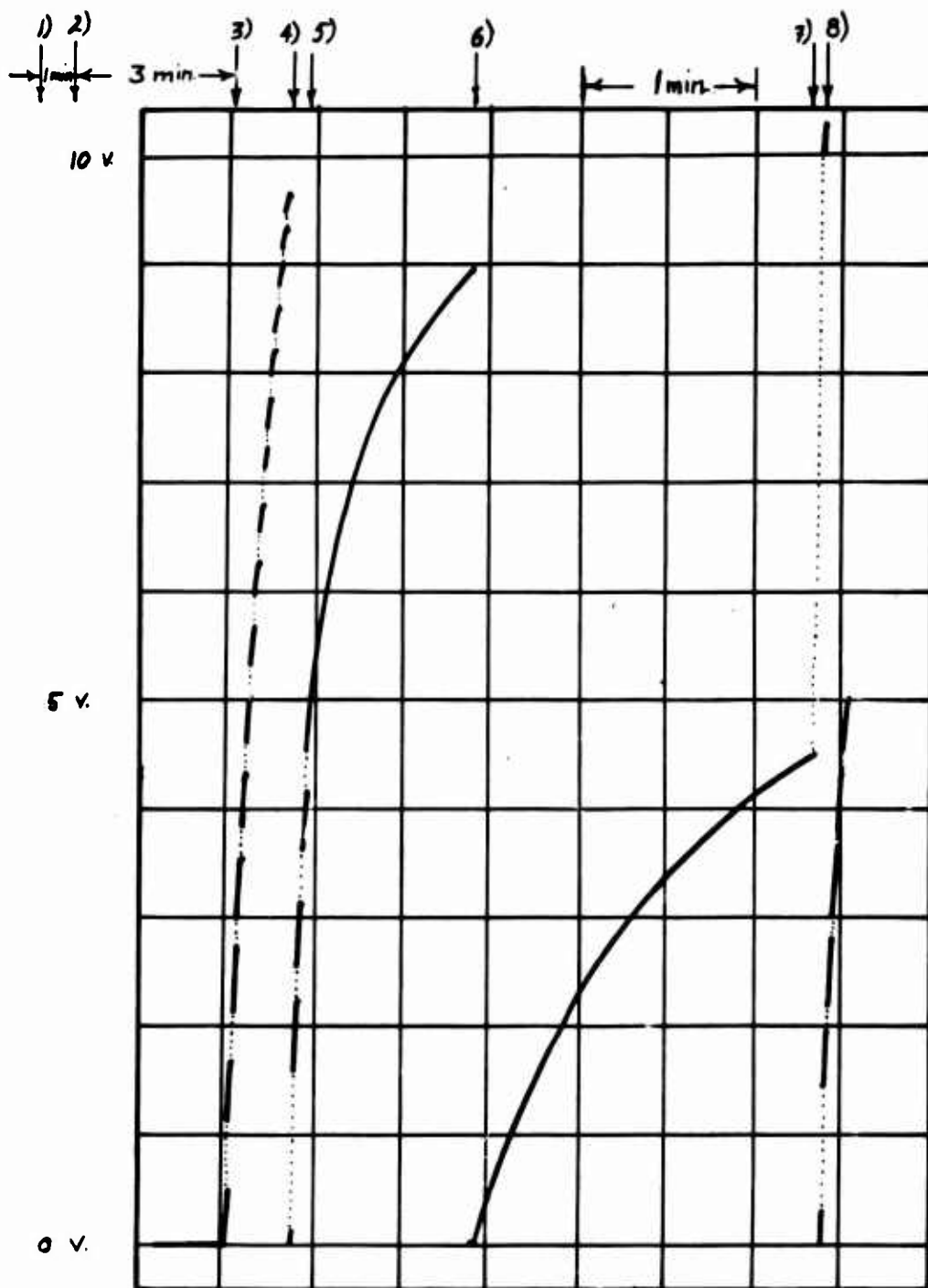
b) Sample L12059 (polyethylene), initial applied voltage zero volts, linac beam turned on about six minutes prior to figure shown. Event sequence: 1) linac beam turned on; 2) S opened.

Somewhat unexpectedly, in several cases the prompt component polarization was observed to relax during the observation period; i.e., the prompt component immediately following the observation period was markedly larger than it had been just prior to the observation period. In some cases the relaxation seemed nearly complete, and the post-observation-period prompt component was nearly as large as it had been at the onset of the first irradiation period. In all these cases, the externally applied voltage was held fixed throughout, so that the polarization relaxation observed took place with no change in applied electric field.

Relaxation of the prompt component polarization was observed in all four non-pile-bombarded polystyrene samples, and in one sample of non-pile-bombarded polyethylene. A tracing of the data records showing this behavior for one sample each of the polystyrene and the polyethylene is given in Figure 19.

3. Recharging Effect. The system of observation used permits continuous observation of the sample until a maximum potential difference of 10 volts is accumulated across the sample electrodes. Since the electrometer is rated only for input voltages up to this level, it becomes necessary at this point to close switch S, bleeding charge off the electrometer input and recharging the sample electrodes. In so doing, another phenomenon was noted; viz, that the first few pulses after S was reopened produced somewhat larger voltage changes than previously noted.

The magnitude of this perturbation bore a roughly inverse proportionality to the length of time S was closed. Whether the important parameter was time or number of pulses was not determined, the observations being made while the beam was left on continuously, with a repetition rate of about 1 pps. For the time intervals used, the magnitude of the effect was a factor of perhaps two or three, and was damped out in a matter of three or four pulses. A typical data record is shown in Figure 20.



Dotted lines correspond to electron pulses.

Figure 19. Pulsed Electron Study Raw Data Tracing Displaying Relaxation of Prompt Component Polarization.

- a) Sample L11N09^h (polyethylene), applied voltage 23 volts, applied about four minutes prior to figure shown. Linac beam started about 3 minutes prior to figure shown. Event sequence: 1) voltage applied; 2) linac beam started; 3) S opened; 4) S closed, opened; 5) linac beam turned off; 6) S closed, opened; 7) linac beam restarted; 8) S closed, reopened.

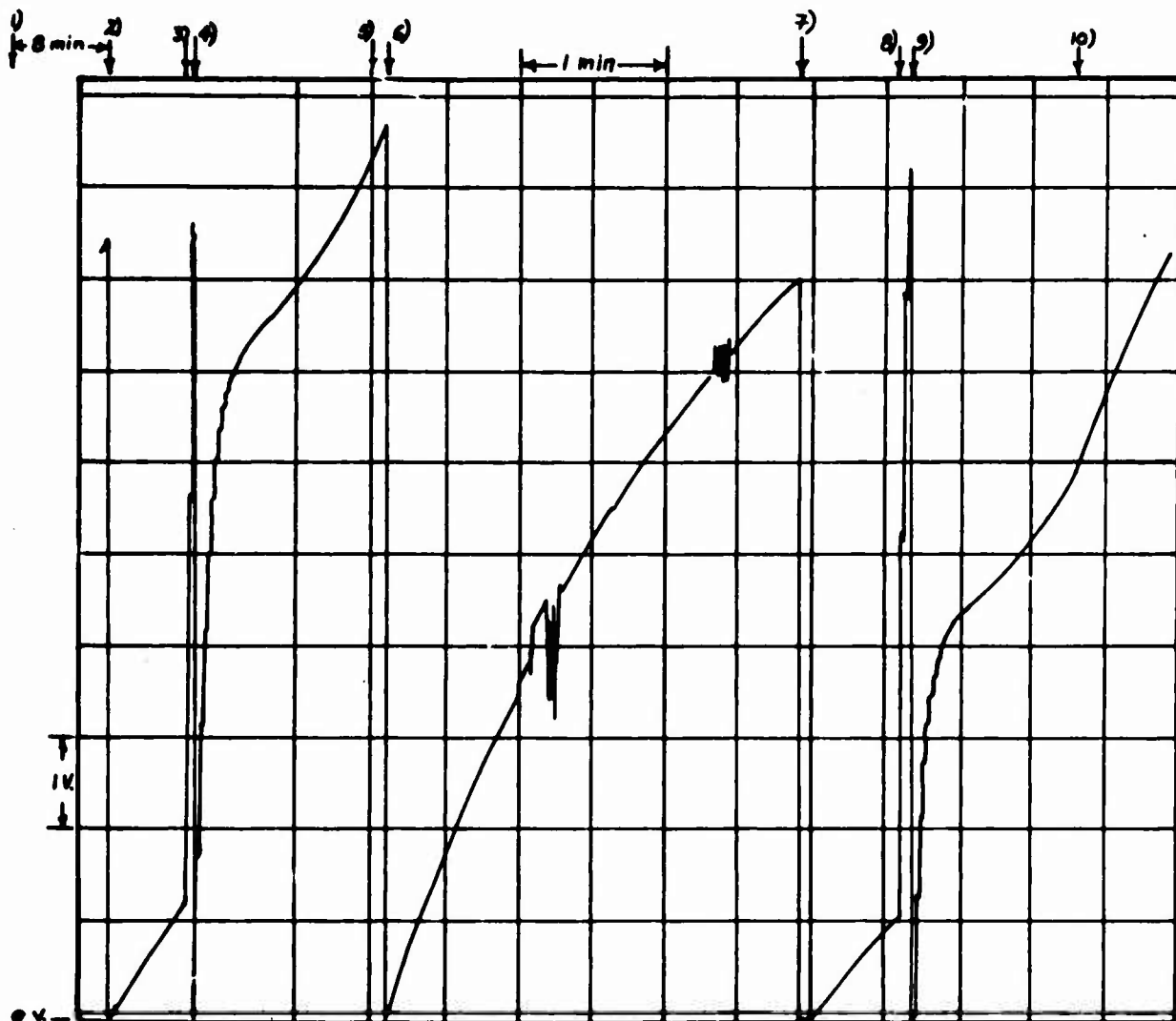


Figure 19. Pulsed Electron Study Raw Data Tracing Displaying Relaxation of Prompt Component Polarization.

b) Sample Y41H23 (polystyrene), applied voltage 233 volts, applied about 8 minutes prior to figure shown. Event sequence: 1) voltage applied; 2) S opened; 3) linac beam started; 4) S closed, opened; 5) linac beam turned off; 6) S closed, opened; 7) S closed, reopened; 8) linac beam restarted; 9) S closed, reopened; 10) linac beam turned off.

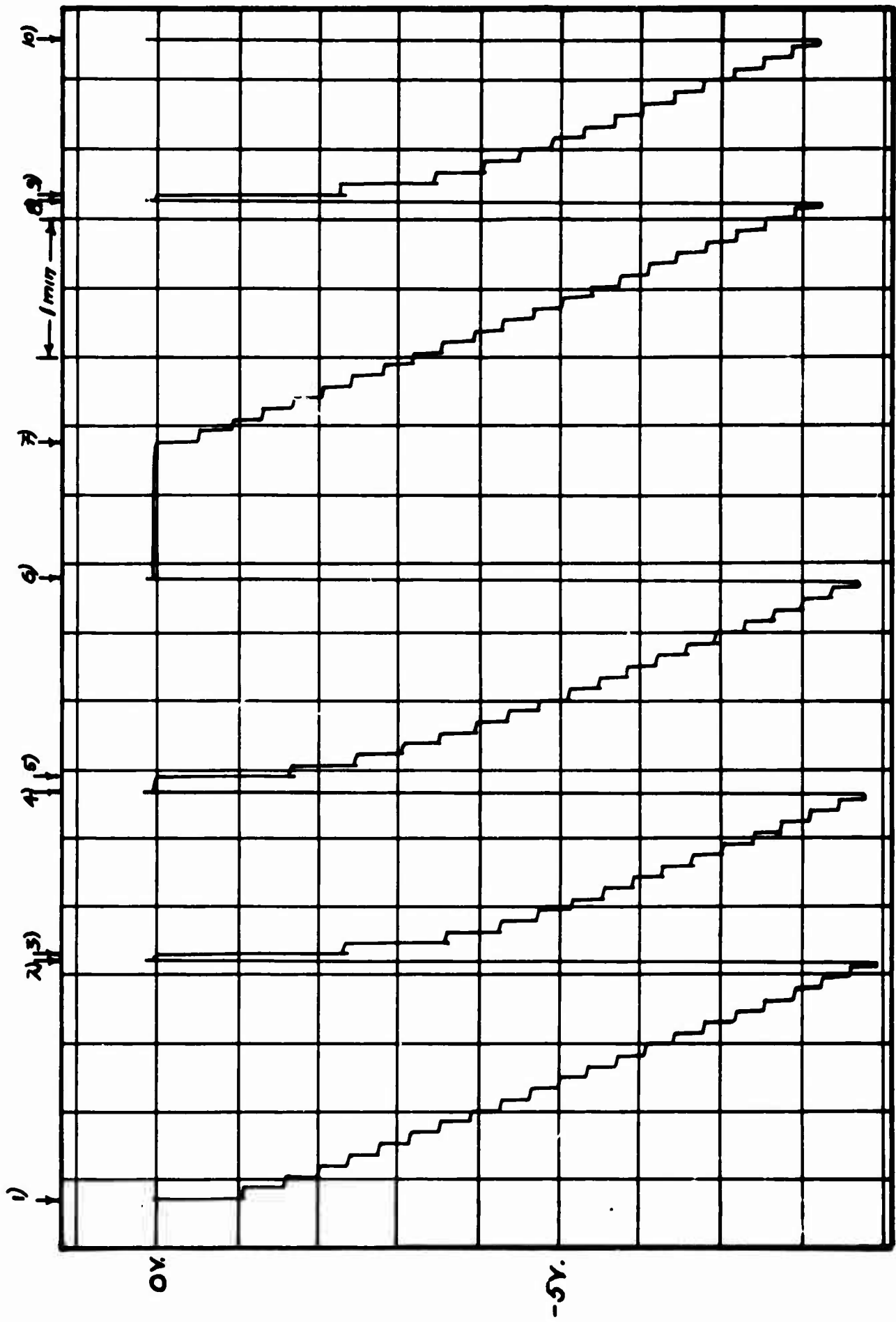


Figure 20. Pulsed Electron Study Raw Data Tracing Displaying "Recharging Effect." Sample Y35H02 (pile-bombarded polystyrene), applied voltage zero volts. Event sequence: odd numbers, S opened; even numbers, S closed.

D. DISCUSSION

1. The Momentum Component. These observations suggest a number of comments and speculations. It is obvious that the behavior observed is rather complicated, and that its study requires a fair amount of untangling of overlapping events. It is quite clear that at least three distinct conduction processes are involved, corresponding to: (i) momentum-transfer; (ii) prompt transfer; and (iii) delayed transfer. We now address ourselves to details of these processes, in turn.

We consider first the momentum component. Presumably the card carriers involved here are electrons. This primary electron undergoes a series of secondary collisions, each generating a secondary electron, which in turn undergoes further collisions. In each collision, the primary's energy and momentum are distributed further among both molecules and secondaries. This avalanching continues until each electron's energy is reduced to a value low enough that it can be removed from the conduction state by trapping or recombination. After only a few collisions the electrons will be randomized, so only a very few of the conduction state electrons found under steady state radiation, namely those with very high energies, could contribute to the momentum component.

During our observations of momentum transfer, measured counter-voltages were allowed to accumulate across the sample, up to values as large as 10 volts. If the picture described above applied, one would expect the action of the counter-voltage on the conduction-state electrons to generate a prompt component, opposed in direction to the momentum component, and increasing in size as the accumulated counter-voltage increased. This would produce an observed charge transfer per pulse that decreased as the accumulated counter-voltage increased.

As a rule, no such decrease was seen. Knowing the limits of precision of our observations, this fact permits calculation of an upper limit for the ratio of effectiveness of the "average"

conduction state electron in producing prompt current as opposed to momentum current. Further experimentation which determined the counter-voltage at which such a decrease became observable would permit the determination of this ratio, providing that components contributed by other types of charge carriers did not become dominant.

2. Prompt Currents. The nature of the charge carriers responsible for the prompt component has not yet been established. Since the primary interaction between radiation field and target material produces substantial concentrations of ionized electrons, it would be tempting to account for these by identifying them with the prompt component. Such a model would account for the short response time observed for the prompt component as well.

On the other hand, each ionized electron corresponds to an ionized molecule, which might possibly conduct either by molecular motion of some sort, or by hole transport. It would be difficult to see how the former could respond so quickly as does the prompt current, because of the relatively large masses associated with molecules or their parts, so molecular motion does not seem a likely candidate. Hole conduction, however, is not subject to this criticism, and cannot be ruled out as a possibility, on these grounds.

The previously noted absence of a prompt component, corresponding to a 10-volt counter-voltage generated during observations of the momentum component, is a little surprising in view of the response seen to externally applied voltages of the same order of magnitude. In sample Y35H02, for example, the external application of -23 volts ($\Delta V = -23$ volts, also) produced a prompt component which initially was about five times the momentum component in size. This did decay away to values negligible with respect to the momentum component, however, in about a minute or so of continued exposure.

The fact that no such prompt counter-voltage-driven component was seen suggests that the externally applied voltage and the counter-voltage differ in some fundamental respect. The most obvious

possibility for this is in the method of application, the external voltage being applied all at once, while the counter-voltage is applied in many small increments, with a pulse separating any two consecutive increments. Such a difference might be significant if the prompt component were dominated by some sort of polarization process which could go essentially to completion in one pulse when a 1/2-volt increment was applied, but could not if the increment were on the order of 20 volts. This possibility seems unlikely.

The existence of some sort of polarizing process is suggested by both the transient nature of the prompt component, and by the observed recharging effect. A complete reconciliation of the noted lack of prompt component buildup during the momentum transfer observations with such a polarizing process or processes, however, has not been achieved, nor is the route to such a reconciliation immediately obvious. Hence for the moment we merely note that the two types of voltage are somehow different, and that any comprehensive model must account for this observation.

3. The Delayed Currents. For the purpose of these comments we assume that the currents observed in the steady-state irradiation study are essentially the same as those called the delayed currents in the pulsed electron study. This identity has not been proven by experiment, however, and so to that extent must be considered only tentative. Future attention should be directed to this question.

The existence of at least three components of the delayed current seems well established. The first of these is a relatively fast-decaying transient component which disappears in the first minute or so after changing the applied voltage, and which was not involved in the calculations reported here. The second is the long-lived transient which becomes apparent after the first component has decayed away, while the third is the presumed normal steady-state photocurrent. Previous work suggests the possible existence of a fourth component in polyethylene, viz., another transient with a relaxation time on the order of 2 minutes. In this study no effort was made to observe such a transient.

The relative importance of the various components in determining the observed currents used in our calculations is not known. In addition, it must be noted that our data might conceal still other components, since the observations were not carried out to long enough times, or with enough precision, to permit a complete analysis. However, since our working current was inversely proportional to sample thickness, it is highly probable that each of the major components of that current also displays this dependence individually. From this we infer that the mechanisms by which these components are generated are each more or less uniformly distributed throughout the sample material. Other observations made in the steady-state irradiation study tell us that these mechanisms do not involve impurity-dominated recombination processes, and suggest that defects may play an important role.

At first glance, the polarization of the prompt component seems to relax much faster than does the magnitude of the delayed component. If this behavior is verified by a more detailed quantitative analysis, this observation will indicate that the prompt and delayed components also involve distinct sets of charge carriers. In this event, the model leading to a comprehensive description of charge transport properties in our materials must be a complex one.

4. A Speculative Model. One tentative model which might serve pictures the momentum component as being derived from high-energy electrons, generated either in the primary ionizing interaction between the radiation field and the target material, or perhaps in the first few secondary collisions. A large concentration of deep trapping states is required to remove these electrons from their conducting states before they lose enough energy to come under the influence of the counter-voltages developed in these experiments.

In addition to having the deep traps, the material is viewed as consisting of many small crystallites, embedded in a glassy matrix. If low-energy carriers were unable to cross crystallite boundaries, those on the inside might produce the effects noted in the prompt component, while those in the matrix might produce the behavior noted for the delayed component.

It must be emphasized that this picture is highly speculative at present, and cannot be advanced with any significant seriousness until a quantitative comparison between its implications and observed data can be made. It seems quite probable that further experimentation would be required to do so.

SECTION III

OTHER WORK

A. DYNAMIC OBSERVATIONS DURING PULSED ELECTRON IRRADIATION

A portion of the effort provided under this contract was devoted to development of a satisfactory technique for observing electrical conduction in organic insulators during, and immediately following, exposure to a high-intensity pulse of high-energy electrons. The intent of this effort was to provide a capability for studying in detail any interesting differences in behavior between samples that might be revealed by the integrated charge transfer measurements described in the preceding section of this report. The preliminary phases of this development effort have been completed, and a general capability in this area has been acquired. Details of this effort follow.

The general technique for this type of measurement has been described by others^b. The measurement circuit is the same as that shown in Figure 2b, p. 22. For this study, V_M was measured with an oscilloscope²⁴, rather than an electrometer, and R_M was in the region of 100 ohms, rather than 10^8 , thus permitting a response fast enough to observe the system during the short pulse.

The radiation for this work was provided by the AFCRL linac, operating in the single pulse mode. Beam electron energy was 10 MeV, pulse length was about 4 μ sec, and peak beam current was about 100 mA. Rough dosimetry was provided by use of the Faraday plate described in the preceding section of this report. The current from this plate was observed for each pulse on the dual trace oscilloscope used to measure sample current, the Faraday plate response being given by the lower trace, and the sample response being given in the upper trace.

The samples used for this work were taken from the group of 31 described in the preceding section of this report. A total of 150 observations, utilizing 2 samples of pile-bombarded polystyrene, was made. The samples used are indicated in Table VI.

Data were recorded photographically. Typical observations are given in Figures 21 and 22.

It will be noted (Figures 21 and 22) that all three components, prompt, delayed, and momentum are significant. It also will be noted (Figure 22) that the ubiquitous polarization effects can be seen in the prompt component. Similar effects were seen in both samples.

B. TEMPERATURE DEPENDENCE OF TRAPPING

Another part of the effort provided under this contract was directed toward determining the temperature dependence of radiation-induced conduction in organic insulators, utilizing an existing 150-kV flash x-ray machine already on hand at Northrop. Approximately 2000 pulses were fired in attempts to observe such effects in several samples, using this apparatus at room temperature. The search was pursued to signal levels approaching the Johnson noise limit, with no signals other than those associated with electromagnetic pickup from the x-ray machine being observed. These results cast considerable doubt on the value previously tabulated by others for the prompt component coefficient in polyethylene. The salient details of this effort follow.

1. Samples. The samples for this effort resembled rather closely those of the pulsed electron study, with the same double-decker geometry being used to reduce the momentum currents. Graphite electrodes were hand-painted on a central divider plate made of the same material as the sample, and having the same general

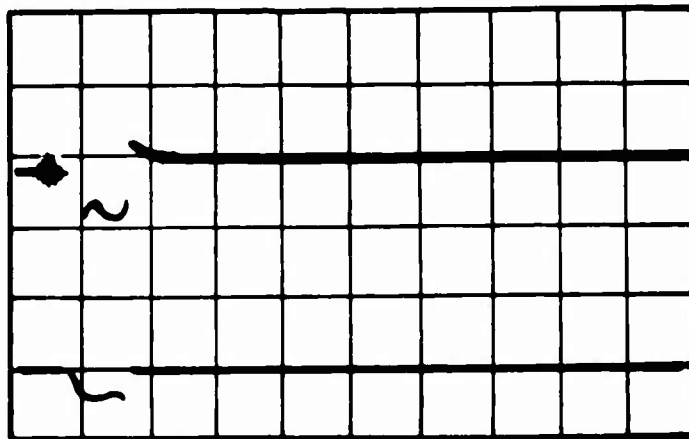
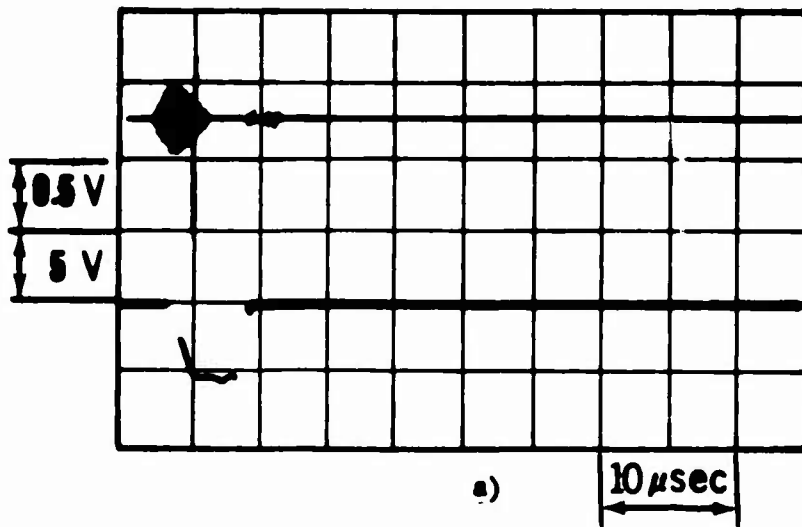


Figure 21. Dynamic Study Raw Data Tracings Displaying Momentum Component. Lower traces give shape of pulse of 10 Mev electrons as measured with a Faraday plate located behind the sample. (Input resistor 50 ohms) Upper traces give response of sample Y35H02 to these pulses. (Input resistor 100 ohms) Tracing a) shows response with sample located about 5" above the beam path. Tracing b) corresponds to sample centered in beam path. In both cases applied voltage was zero volts, i.e., the sample electrodes were connected directly together by the 100 ohm input resistor. Sweep speeds were 5 microsec/cm. Vertical sensitivities: Upper trace, 0.5 v/cm; lower trace, 5 v/cm.



Figure 22. Dynamic Study Raw Data Tracings Displaying Prompt Component Polarization. Lower traces give shapes of successive pulses of 10 Mev electrons, as measured with a Faraday plate located behind the sample. (Input resistor 50 ohms.) Upper traces give responses of sample Y35H02 to these pulses. (Input resistor 100 ohms.) Quantities t give the times elapsed since the applied voltages listed at the tops of the columns were applied.

structure as those of the pulsed electron samples. In this case a 4-mil-diameter copper-constantan thermocouple was strung through the middle of the central spacer, since measurements as a function of temperature were anticipated. Construction techniques for the spacers were as described previously. Electrodes were 1 inch in diameter, rather than 3 cm.

In the first sample the fore and aft electrodes were painted on plates of polytetrafluoroethylene (PTFE) rather than PMMA, since temperatures above the softening point of PMMA were anticipated. When no signals were found using this sample, the fit of these PTFE plates was examined more closely, and found questionable. It appeared that the PTFE plates had "crept" after sample assembly, introducing irregular gaps between sample dielectric and electrodes on the order of $1/64$ inch wide. The remaining samples were made using PMMA fore and aft plates, which did not exhibit this difficulty.

The sample mounting parts also were made of PTFE, and differed in geometry from those of the pulsed electron study in order to accommodate the different mounting facilities available in the existing exposure chamber. Silicone stopcock grease¹⁵ was used as a potting material in the regions near the x-ray beam path. In other regions the vacuum provided by the existing chamber (on the order of 5 microns) was relied upon to isolate leads and feedthroughs.

Most of the effort was spent on two polyethylene samples, with a limited number of attempts made on one sample each of polystyrene and PVC, and a few on a commercially available polyester capacitor²⁰. The last of these had tubular geometry featuring an outside diameter on the order of an inch, so that absorption of the x-rays was severe, and the average dose rate was significantly smaller than in the case of the double-decker samples.

2. Radiation and Dosimetry. Radiation was provided by the Northrop 150-kV flash x-ray apparatus, which features a commercially available, tungsten-target x-ray tube²¹. The beam was filtered by a 5-mil covar window, plus approximately 1/8 inch of aluminum which comprised the walls of the double-jacketed vacuum chamber.

This apparatus was operated in the single pulse mode, with a pulse width of about 50 nsec. A measurement of dose per pulse was made using small ionization chambers placed outside the vacuum jacket. Assuming a simple inverse square dependence on distance from the x-ray tube target, and allowing 10% for absorption by the jacket, this measurement indicated a delivered dose per pulse at the sample location of about 0.41 rad, in polyethylene, or a dose rate during the pulse of about 9 Mrad/sec.

3. Measuring Circuit and Observations. The measuring circuit design was essentially that used in the dynamic measurements described above (see Figure 23). The sensing unit differed in including a switch, for convenience in changing the value of the measuring resistor, and the voltage measuring device was a single-trace oscilloscope, rather than dual. This scope also had a memory storage feature²², so that observations could be made directly, rather than requiring an intermediate photographic step. In some cases the signal was put into a second preamplifier, to obtain maximum sensitivity, and since the x-ray shielding problem was much less severe than in the pulsed electron case, shorter cables, and hence larger measuring resistors, could be used, without loss of time resolution.

Observations were made with the sample chamber evacuated to pressures on the order of 5 microns, using various applied voltages up to 700 volts and measuring resistors at various values in the range of 50 to 5000 ohms. A number of signals were seen, but these exhibited poor reproducibility and did not depend in any simple fashion on the value of the applied voltage or the measuring resistor, or the interposition of a 1/4-inch lead plate

between the x-ray tube and the sample chamber. The measuring system parameters for these observations were such that consistent signals on the order of $0.01 \mu\text{A}$ should have been clearly discernable with time resolution on the order of 20 nsec.

Reproducible signals which were qualitatively well-behaved with respect to applied voltage and measuring resistance, and roughly linear with respect to chamber pressure, were observed when the chamber was back-filled with helium, at pressures ranging from about 100 microns to some two atmospheres. These signals were in the micro- to milli-ampere region, with rise times on the order of 100 nsec and decay time-constants in the neighborhood of $0.4 \mu\text{sec}$. Insertion of a 1/4-inch thick sheet of lead between x-ray tube and sample chamber caused these signals to disappear. They also disappeared when chamber pressure was reduced again to the 5-micron region.

4. Discussion. The well-behaved signals observed at higher pressures presumably resulted from ionized gas conduction between exposed portions of the electrical leads. These were of unknown area and were located some 1 or 2 inches off the beam axis, i.e., well away from the main portion of the beam. Quantitative calculations of the currents to be expected in this situation are precluded by our ignorance of both the effective geometric factors and the appropriate beam intensity. However, both of these factors probably were at least two orders of magnitude smaller than the corresponding factors for the samples. Thus we conclude that the measuring apparatus was functioning properly, and should have been able to detect currents in the microampere range with no difficulty.

Rough values to be expected for prompt currents in our measurements were calculated from proportionality constants reported by others^h. These ranged from 0.7 to $13 \mu\text{A}$ for polystyrene, and from 2 to $28 \mu\text{A}$ for polyethylene, values falling within the range

measurable by our system. The constants reported were based upon observations made under steady-state irradiation, and rest upon the assumption that the prompt component cominates the total current observed under those conditions. This is a questionable assumption, at best, so the failure to find an observable signal in our measurements simply may indicate that it is not valid.

We note that these samples had an electrode area of about 10 cm^2 and were exposed to a radiation field with an intensity on the order of 8 Mrad/sec , while the corresponding samples in the Co^{60} study had electrode areas of about 1000 cm^2 and were exposed at the rate of about 60 rad/sec . Given our negative results in this study, i.e., prompt currents less than 10 nA , the maximum prompt current that could have been expected in the Co^{60} study polyethylene samples, at equivalent applied electric fields, was 300 pA . For polystyrene the corresponding figure is about 30 pA^* . The currents actually observed in the Co^{60} study were 1000 to 5000 pA and about 400 pA , respectively. Thus these negative observations tend to confirm the assumption made in the Co^{60} study that in that study the currents observed were predominantly of the delayed component variety.

*The difference between the two materials hinges on their different values for Δ in the expression $I \propto \Delta$. In these calculations the minimum values observed, namely 0.5 for polyethylene and 0.7 for polystyrene, were used. Larger values would produce even smaller values for the maximum prompt current, thus strengthening the conclusions presented here.

SECTION IV

GENERAL SUMMARY OF RESULTS AND RECOMMENDATIONS

A. SPECIFIC RESULTS OF THE CURRENT WORK

The principal result of the current work is the development of a technique for measurement of quasi-dc, bulk photoconductivity in polyethylene and polystyrene, during steady-state irradiation. This technique utilizes the sum of two or more component currents: the normal steady-state photocurrent; and at least one slow transient photocurrent having a relaxation time on the order of minutes. This total photocurrent is shown to be linear with applied voltage up to fields approaching 10% of breakdown strength, and to vary in inverse proportion to sample thickness.

Comparisons of various samples utilizing this technique show both polyethylene and polystyrene to be insensitive to minor fabrication differences, thus suggesting strongly that their conduction processes during irradiation of the strength and type used in this work are not dominated by impurity-controlled recombination mechanisms. Similar comparisons suggest that these processes may fundamentally involve structural irregularities which are present in very large concentrations in the unirradiated material.

The pulsed irradiation studies display the presence of at least three, experimentally distinguishable, component currents, namely the prompt component; the delayed component; and the momentum component; in electron-irradiated polyethylene, polystyrene, and polyvinylchloride. Negative observations suggested that the total photocurrent observed in the steady-state case, described above, probably was dominated by the delayed component. In addition, a number of observations permitting speculations on various aspects of the conduction mechanisms involved in photoconduction in these materials, were made.

B. CURRENT STATE OF THE ART

1. Design Problems and Semantic Difficulties. It is readily apparent from the observations reported here that the general question of electrical conduction in enradient organic insulators is quite complicated, there being at least three distinct components, responsive to different sets of independent variables. The fact that these three sets exhibit a certain amount of overlapping contributes to the confusion, and it is not particularly surprising that different investigators report apparently conflicting results.

Discussions of such situations are particularly vulnerable to semantic confusion, and considerable care must be taken to ensure that the ideas actually conveyed by a discussion bear a reasonably close resemblance to those it was intended to convey. Care must be taken to define terminology adequately, and particular care must be taken to recognize the limits of applicability of concepts carried over from other fields, e.g., the term "conductivity" itself, which can mean quite different things to those occupying different viewpoints.

The designer of a microcircuit, for example, may want to know how much leakage to expect across a planar isolation layer as a function of radiation intensity. In general one expects this to be dominated by what we have designated as the momentum current, since most radiation fields that a microcircuit might be exposed to will be asymmetric with regard to the isolation layer's plane. Consequently the "conductivity" requested by this designer may depend primarily upon radiation field parameters such as momentum and energy spectra, and the atomic numbers of the isolation layer and the surrounding materials, and rather less upon the potential drop across the layer, the layer's thickness or the molecular structure of the layer.

The designer of an ionization chamber may want to know how much leakage to expect in a cylindrical capacitor when his chamber is used in a hot cell. The cylindrical geometry will reduce the momentum current drastically, and the radiation intensity will be relatively low, leading to a small prompt component. Thus the leakage in this case will be dominated by the delayed component, and this man's "conductivity" may well be a function of how long an exposure to the field is required in order to take a reading, as well as a function of radiation intensity.

The designer of a guidance system for a rocket, on the other hand, may want to know how much current to expect in the same cylindrical capacitor, under a particular pulsed radiation environment. This most probably will be dominated by the prompt component, since the cylindrical geometry of the capacitor will reduce the momentum current drastically, and the delayed component should not have enough time to build up to a significant level. Here, our present knowledge suggests that the principal parameter will be radiation intensity, although the polarization effects observed indicate that the capacitor's recent history may be significant, too.

The concept of conductivity was originally developed for the case of essentially free carriers, and as such carries an implications of a constant value at all points within the material in question. From a practical point of view it is a scalar property whose usefulness hinges upon its ability, when multiplied by the electric field in the material, to predict the element of electric current that will be contributed by each element of the material. The dangers inherent in carrying over the concept of a single-valued conductivity to the field of enradiant insulators are as obvious as the penalties attendant upon inadequate designs in any of the cases cited.

At the present time, the assistance that can be offered to our three hypothetical designers is somewhat limited, both by lack of data for specific materials, and by the as yet incomplete understanding of the current-generating mechanisms involved. The present work constitutes a significant advance of the art beyond its previous state, through providing the first reliable volume quasi-dc conductivity data for two popular materials. Much more remains to be done, however, before the field can be reduced to a handbook status.

2. Future Outlook. Since there appears to be a set of three different conduction processes, any one of which may be dominant, it follows that there are three investigative lines to be followed. The relative priority to be attached to these lines depends, of course, upon the relative urgencies associated with the types of design problems corresponding to these lines. From the experimenter's viewpoint the most efficient procedure would be to pursue all three lines simultaneously, since a relatively small percentage increase in the time devoted to data taking would provide raw data appropriate to all three lines from a single series of experiments. As the lines proceeded through data reduction to model formation, of course, one would expect a decreasing amount of overlap. It would not be entirely surprising, however, to find an appreciable overlap even in the final stages.

With regard to the future, a general pattern does seem to be emerging from the gradually accumulating knowledge in this field. Three important components are experimentally identifiable, and their general behavior is being mapped out, bit by bit. There is every reason to expect that further work will identify the parameters controlling these components, and that knowledge of these will suggest the limits to which they can be controlled, and suitable means for controlling them, within such limits.

Once an adequate understanding of the controlling parameters is achieved, it will become possible to define those quantities which will be of use to designers in their various fields. Then, and not until then, will it become possible to tabulate numerical values of these quantities for the various materials available to the designers, and to determine the feasibility of something approaching a handbook table.

C. SPECIFIC RECOMMENDATIONS FOR FUTURE WORK

The recommendations for future work fall into two classes: those designed to improve our understanding of the mechanisms underlying radiation-induced conduction; and those designed to provide as much immediate help to the designer of radiation-hardened components as present basic knowledge permits.

Recommendations of both classes are now given for each of the three subareas of radiation-induced conduction discussed in this report.

1. Momentum Components.

a. For Improved Understanding. The previous speculations on momentum current mechanisms are open to question on the basis of another observation; namely, that the size of the pulsed electron momentum transfer is sensitive to the amount of PMMA in the beam upstream of the sample. In order to be certain that the transfers observed are indeed generated in the sample material and not by some mechanism external to the sample, this sensitivity should be studied rather thoroughly.

An additional problem is raised by certain previous work^f, which suggests that the momentum component is not linearly proportional to radiation intensity. The extent to which this is true, and the circumstances surrounding such behavior, requires some attention, for the simple model described above rather implies a linear dependence here.

b. For Immediate Use. From a practical point of view, we note that there exists a class of radiation-hardening design problems in which the radiation-induced conduction is dominated by specific information to assist the designer in meeting these problems, and virtually none available in a form convenient for his use. If he is to be given any assistance in this area, a considerable amount of work remains to be done both in the region of predictive calculations, and determination of critical constants in specific materials.

2. Prompt Components.

a. For Improved Understanding. One obvious question concerning the prompt component is whether it is volume distributed. To answer this question will require further experimentation, using the techniques developed during this contract to examine the relationship between charge transfer across samples having the same history, and sample thickness.

One line of analysis which may prove useful, in the event that the polarization effects prove to be volume distributed, is the response time of polarization, and of its relaxation, and their dependence upon various independent variables, e.g., dose rate and temperature.

Other workers^b have reported that special electrode deposition techniques have eliminated polarization effects in the prompt component. This suggests that the polarization effects result from electrode interface problems. Thus the thickness dependence question becomes especially interesting, from a fundamental point of view.

Two questions which may be answerable from the data already on hand are whether the conduction processes responsible for the prompt component are sensitive to trace impurities and/or defect concentrations. This will require further data analysis, however.

Another question, inspired by the speculative model described earlier, is whether the prompt component depends upon sample crystallinity.

A related question is the effect of sample rigidity. Both of these should be susceptible to attack using the same controlled history approach, although the latter would require measurements at temperatures other than room temperature.

b. For Immediate Use. Rather little immediately useful data pertaining to the prompt component can be gathered until the behavior has been mapped out in more detail. One area of immediate practical interest can be identified, namely, that of the influence of electrode materials and means of application. If the observed polarization is a surface phenomenon, the road to controlled reproducibility for those cases in which the prompt component dominates turns toward electrode attachment processes, while if it is a volume phenomenon, other procedures must be developed.

3. The Delayed Components

a. For Improved Understanding. A number of possibilities for further study suggest themselves. The most obvious of these would be a study of the decay behavior of the transients, attempting to identify the various components according to relaxation time. A natural extension of this line of investigation would be to study the effects of temperature on these times, and to characterize the various components by their dependences on sample thickness, radiation intensity, and material crystallinity. An extension of the neutron-bombardment study to higher doses also seems quite obvious. Also in line for similar examination should be the postirradiation time dependence of delayed component decay. All of these approaches should provide relevant information, which, taken en masse, should be quite helpful in assigning specific carriers and mechanisms to the various components.

A somewhat less obvious approach to further understanding would involve clarification of the importance of the voltage change, ΔV . In the present study, V and ΔV were proportional to each other, thus making the current-voltage characteristics displays of I vs

V, and vs ΔV , simultaneously. If the roles of V and ΔV could be separated, a comparison of the relative strengths of the transient and steady-state components could be deduced from the relative importances of V and ΔV in determining I. If V dominated, the observed conductances would be dominated by the normal steady-state photocurrent, and further analyses along the lines of the lifetime calculations suggested in this contract's proposal, would be meaningful. Should ΔV dominate, on the other hand, one would conclude that the transient processes dominated the observed conductances, and that the utility of lifetime analyses would depend upon further establishment of conductive mechanism details.

With one exception, studies based upon controlled addition of dopants or other impurities do not seem promising, in view of the negative results of the fabricator comparison reported here. The exception would be an attempt to map out the electric field distribution inside a slab of dielectric material via the Mossbauer effect. Given that a suitable Mossbauer absorber could be dissolved into the dielectric, the shift due to the Stark effect might be large enough to be observable. In this case, the amount of the shift would be a measure of the local electric field strength.

One other approach which might be worth developing is that of subjecting samples to controlled thermal treatment. Other workers have reported substantial changes in mobility for two organic dielectric liquids, after repeated passes through a zone-refining process. If confirmed, such results would have definite implications regarding procedures by which conduction in dielectric materials could be controlled.

b. For Immediate Use. From a practical point of view it should now be possible, thanks to the technique developed in this work, to accumulate tables of parameters characterizing both polyethylene and polystyrene with respect to the delayed component. This will require a number of experiments at various radiation

intensities, using several thicknesses of material, and should be extended to include several types of radiation field. Other materials should be established, and the corresponding data compiled. If the range of materials is found sufficiently broad, some effort should be directed toward refining the technique.

For the most part, refinement of the technique will depend upon improved understanding of the underlying mechanisms. One improvement that might be possible directly, however, would be to provide better control of possible leakage paths paralleling the sample. The substantial variations noted for the same sample at different times, and with reversed orientation with respect to the measuring circuit, suggests that this parallel leakage was not completely under control. In view of the small quantities involved, e.g., the variations noted corresponded to parallel leakages in the picomho range, such a conclusion seems not unreasonable. Accordingly, attention to those places in the measuring circuit where small interruptions in the guarding configuration were permitted, might provide considerable improvement in measurement precision.

A certain amount of attention to the effects of various electrode materials and electrode application techniques also would seem well directed. Reports by others of sharp reduction of transient effects in studying the prompt component, through various electrode application techniques, raise the question of whether similar reductions might be found also in the delayed component. In view of the thickness relationship found in this study, such a reduction would at first glance seem contradictory, but might be explicable on the assumption that the electrode application technique permitted substantial diffusion of the electrode material into the bulk of the sample, thus changing the basic bulk properties of the material. Some practical interest should attach to experimental studies of the influences of various electrode materials and electrode application techniques, particularly those involving metallic electrodes, since these are quite commonly encountered.

REFERENCES

- a. Nortronics Staff, "Investigation of Radiation Effects in Electronic Materials," Nortronics Applied Research Department, 65-34p, Hawthorne, California, December 1965.
- b. Compton, D. M. J., Cheney, G. T. and Poll, R. A., J. App. Phys. 36, 2434(1965).
- c. Frankovsky, F. A. and Shatakes, M., "Reactor and Linear Accelerator Induced Effects in Dielectrics," IBM Federal Systems Division, Owego, N. Y., IBM Document 66-825-1944 March 1966.
- d. Silverman, J., Trans. Am. Nuc. Soc. F, 442(1964)
- e. Winslow, J. W. and Jenkins, R. J., "Evaluation of Delayed Transient Phenomena in Polyethylene as Basis for X-ray Detectors," USNRWL-LR-109, USNRDL, San Francisco, Calif., July 1965.
- f. Winslow, J. W. and Alger, R. S., "Radiation-Induced Currents in Solid Organic Insulators, USNRDL-TR-325, USNRDL, San Francisco, Calif., 21 May 1959.
- g. Harrison, S. E., Coppage, F. N., and Snyder, A. W., IEEE Trans. Nuclear Sci., 118 (1963)
- h. Wicklein, H. W., Nutley, H. and Ferry, J. M., ibid., p. 131.

EQUIPMENT

1. Model DW-1 Deadweight Micrometer, dial M. E. J. Cody & Co., Melrose Park, Ill.
2. 'dag' dispersion #154, Acheson Colloids Co.
3. Sylgard #184 Potting & Encapsulating Resin, Dow-Corning Co.
4. Embedding Paraffin M7352-4, Scientific Products Co.
5. RG-59/U triaxial cable
6. RG-58/U coaxial cable
7. Miuiuoise triaxial cable #250-3833, Microdot Inc.
8. Model 603 Electrometer, Leithley Instruments, Inc.
9. General Electric Co. #CR120M900B01 magnetic reed switch
10. Shallcross #12435, #12212, and #12407 ceramic wafer switches.
11. RG/58U coaxial cable
12. E-Kote 40, Epoxy Products Co.
13. BNC Bulkhead Receptacle
14. Amphenol FXR #34450 Bulkhead Receptacle
15. Dow-Corning High-vacuum grease silicone lubricant
16. Model 601 electrometer, Keithley Instruments, Inc.
17. Amphenol #21-204 triaxial cable
18. RG62A/U coaxial cable
19. Leeds & Northrop Speedowax H
20. WMF 4P68, Cornell-Dubilier Electronics
21. Fexitron 150 kv x-ray tube, Field Emission Corp.
22. Tektronix Model 549, Type L preamplifier
23. Eastman 910 Adhesive, Tennessee Eastman Co.
24. Tektronix Type 551 dual-beam oscilloscope, type L preamplifiers.

Unclassified

Security Classification

DOCUMENT CONTROL DATA - R&D		
<i>(Security classification of title, body of abstract and indexing annotation must be entered when the overall report is classified)</i>		
1. ORIGINATING ACTIVITY (Corporate author) Northrop Corporate Laboratories 3401 West Broadway Hawthorne, California 90250		2a. REPORT SECURITY CLASSIFICATION Unclassified
		2b. GROUP
3. REPORT TITLE TRANSIENT CONDUCTIVITY IN ORGANIC INSULATORS		
4. DESCRIPTIVE NOTES (Type of report and inclusive dates) Scientific. Final. June 1966 - June 1967		Approved 29 Sept. 1967
5. AUTHOR(S) (Last name, first name, initial) Winslow, John W.		
6. REPORT DATE September 1967	7a. TOTAL NO OF PAGES 131	7b. NO OF REFS 8
8a. CONTRACT OR GRANT NO AF 19(628)-6047	9a. ORIGINATOR'S REPORT NUMBER(S) NCL 67-35R	
b. PROJECT NO., Task, Work Unit Nos. 4608-01 - 01		
c. DoD Element 62405274	9b. OTHER REPORT NO(S) (Any other numbers that may be assigned this report)	
d. DoD Subelement 634608	AFCRL-67-0515	
10. AVAILABILITY/LIMITATION NOTICES Distribution of this document is unlimited. It may be released to the Clearinghouse, Department of Commerce, for sale to the general public.		
11. SUPPLEMENTARY NOTES TECH, OTHER	12. SPONSORING MILITARY ACTIVITY Air Force Cambridge Research Laboratories (CRW) L. G. Hanscom Field Bedford, Massachusetts 01730	
13. ABSTRACT - A technique for measuring quasi-dc photoconductance in amorphous polymers during steady-state irradiation has been developed. This technique, which involves control of the sample's history prior to making measurements, has been applied to 21 polyethylene and 14 polystyrene samples, during exposure to Co ⁶⁰ gamma fields with intensities up to 2×10^5 r/hr. Conductances observed using this technique were inversely proportional to sample thickness, thus permitting calculation of the bulk, quasi-dc photoconductivities. Preliminary observations were made of polyethylene, polystyrene and polyvinylchloride under pulsed irradiation. These observations verified three components of radiation-induced conductance: the momentum transfer, the prompt and the delayed. These observations suggest: 1) that the prompt components in all three materials exhibit so-called polarization effects; 2) that the technique developed for the steady-state irradiation case appears promising for study of the pulsed-irradiation case; 3) that the three components may well involve distinct sets of charge carriers; and 4) that the prompt component in the steady-state case was negligible, so that the observations there reflected primarily the behavior of the delayed component. To date, analyses of the data from these observations indicate the following: 1) that both these materials are essentially ohmic, at least up to applied electric fields on the order of 10% of breakdown; 2) that trace impurities do not play important roles in the conduction mechanisms involved in either material; 3) that structural defects may play such a role, but if they do, they are present in very large concentrations-in polyethylene at least so large they are considered essential structural features; and 4) that in both materials, dependence on radiation intensity is weaker than reported. -		

KEY WORDS	LINK A		LINK B		LINK C	
	ROLE	WT	ROLE	WT	ROLE	WT
Experimental Technique	8	3	8	3	8	
Radiation Induced Conductivity	8	3	8	3	8	
Amorphous Polymers	1,8	3	1,8	3	1,8	3
Dielectrics	1	3	1	3	1	3
Polyethylene	1	2			1	1
Polystyrene	1	2			1	1
Polyvinylchloride					1	1
Steady-state Irradiation	5,6	3	5,6	3		
Pulsed Irradiation					5,6	3
Structural Defects	6	1	6	1		
Trace Impurities	3	0	3	0		
Sample Thickness	10	3				
Radiation Intensity Dependence	5	1				
Prompt Component					7	2
Delayed Component	7		7		7	2
Momentum Component	7		7		7	2
Polarization Effects						
INSTRUCTIONS						
	3		3		3	2

<p>1. ORIGINATING ACTIVITY: Enter the name and address of the contractor, subcontractor, grantee, Department of Defense activity or other organization (<i>corporate author</i>) issuing the report.</p> <p>2a. REPORT SECURITY CLASSIFICATION: Enter the overall security classification of the report. Indicate whether "Restricted Data" is included. Marking is to be in accordance with appropriate security regulations.</p> <p>2b. GROUP: Automatic downgrading is specified in DoD Directive 5200.10 and Armed Forces Industrial Manual. Enter the group number. Also, when applicable, show that optional markings have been used for Group 3 and Group 4 as authorized.</p> <p>3. REPORT TITLE: Enter the complete report title in all capital letters. Titles in all cases should be unclassified. If a meaningful title cannot be selected without classification, show title classification in all capitals in parenthesis immediately following the title.</p> <p>4. DESCRIPTIVE NOTES: If appropriate, enter the type of report, e.g., interim, progress, summary, annual, or final. Give the inclusive dates when a specific reporting period is covered.</p> <p>5. AUTHOR(S): Enter the name(s) of author(s) as shown on or in the report. Enter last name, first name, middle initial. If military, show rank and branch of service. The name of the principal author is an absolute minimum requirement.</p> <p>6. REPORT DATE: Enter the date of the report as day, month, year; or month, year. If more than one date appears on the report, use date of publication.</p> <p>7a. TOTAL NUMBER OF PAGES: The total page count should follow normal pagination procedures, i.e., enter the number of pages containing information.</p> <p>7b. NUMBER OF REFERENCES: Enter the total number of references cited in the report.</p> <p>8a. CONTRACT OR GRANT NUMBER: If appropriate, enter the applicable number of the contract or grant under which the report was written.</p> <p>8b, 8c, & 8d. PROJECT NUMBER: Enter the appropriate military department identification, such as project number, subproject number, system numbers, task number, etc.</p> <p>9a. ORIGINATOR'S REPORT NUMBER(S): Enter the official report number by which the document will be identified and controlled by the originating activity. This number must be unique to this report.</p> <p>9b. OTHER REPORT NUMBER(S): If the report has been assigned any other report numbers (<i>either by the originator or by the sponsor</i>), also enter this number(s).</p>	<p>10. AVAILABILITY/LIMITATION NOTICES: Enter any limitations on further dissemination of the report, other than those imposed by security classification, using standard statements such as:</p> <p>(1) "Qualified requesters may obtain copies of this report from DDC."</p> <p>(2) "Foreign announcement and dissemination of this report by DDC is not authorized."</p> <p>(3) "U. S. Government agencies may obtain copies of this report directly from DDC. Other qualified DDC users shall request through _____."</p> <p>(4) "U. S. military agencies may obtain copies of this report directly from DDC. Other qualified users shall request through _____."</p> <p>(5) "All distribution of this report is controlled. Qualified DDC users shall request through _____."</p> <p>If the report has been furnished to the Office of Technical Services, Department of Commerce, for sale to the public, indicate this fact and enter the price, if known.</p> <p>11. SUPPLEMENTARY NOTES: Use for additional explanatory notes.</p> <p>12. SPONSORING MILITARY ACTIVITY: Enter the name of the departmental project office or laboratory sponsoring (<i>paying for</i>) the research and development. Include address.</p> <p>13. ABSTRACT: Enter an abstract giving a brief and factual summary of the document indicative of the report, even though it may also appear elsewhere in the body of the technical report. If additional space is required, a continuation sheet shall be attached.</p> <p>It is highly desirable that the abstract of classified reports be unclassified. Each paragraph of the abstract shall end with an indication of the military security classification of the information in the paragraph, represented as (TS), (S), (C), or (U).</p> <p>There is no limitation on the length of the abstract. However, the suggested length is from 150 to 225 words.</p> <p>14. KEY WORDS: Key words are technically meaningful terms or short phrases that characterize a report and may be used as index entries for cataloging the report. Key words must be selected so that no security classification is required. Identifiers, such as equipment model designation, trade name, military project code name, geographic location, may be used as key words but will be followed by an indication of technical context. The assignment of links, rules, and weights is optional.</p>
--	---